

AD-781 885

NONLINEAR HELICOPTER ROTOR LIFTING
SURFACE THEORY. PART I

Thomas A. Csencsitz, et al

West Virginia University

Prepared for:

Office of Naval Research

September 1973

DISTRIBUTED BY:

NTIS

National Technical Information Service
U. S. DEPARTMENT OF COMMERCE
5285 Port Royal Road, Springfield Va. 22151

Unclassified

Security Classification

AD. 781885

DOCUMENT CONTROL DATA - R & D

Report classification of title, body of abstract and indexing information. Do not enter 1 when the overall report is classified.

1. ORIGINATING AGENCY (If appropriate, author)		22. REPORT SECURITY CLASSIFICATION	
West Virginia University Department of Aerospace Engineering Morgantown, West Virginia 26506		Unclassified	
2. REPORT TITLE		23. GROUP	
Nonlinear Helicopter Rotor Lifting Surface Theory (Part I)		-	
4. DESCRIPTOR NOTES (Type of report and inclusive dates)			
Scientific			
5. AUTHOR(S) (First name, middle initial, last name)			
Thomas A. Csencsitz, Jerome B. Fanucci, and Hsi F. Chou			
6. REPORT DATE	10. TOTAL NO. OF PAGES	11. NO. OF ILLUS.	
September, 1973	209	21	
8a. CONTRACT OR GRANT NO.	9a. ORIGINATOR'S REPORT NUMBER(S)		
N00014-68-A-0512	Aerospace Engineering TR-35		
b. PROJECT NO.	9b. OTHER REPORT NUMBER(S) (Any other numbers that may be assigned this report)		
NR 215-163	-		
c.	Project Navy V/STOL Aerodynamics		
d.			
10. DISTRIBUTION STATEMENT			
Approved for Public Release; Distribution Unlimited			
11. SUPPLEMENTARY NOTES		12. SPONSORING MILITARY AGENCY	
		Office of Naval Research Aeronautics, Code 461 Arlington, Virginia 22217	
13. ABSTRACT			
<p>A numerical method is developed based on potential flow nonlinear lifting surface theory for predicting the surface velocities and pressures on a rotor blade of an arbitrary helicopter rotor system which is executing a constant rotational and constant axial translational motion including, specifically, the hover flight mode. The formulation of the problem is exact in the sense that the normal surface boundary condition is satisfied on the surface of the rotor blade. The problem is governed by a Fredholm integral equation of the first kind which relates a singular velocity doublet potential surface distribution applied on the rotor blades and wakes to the normal relative velocity on the rotor blade surface. The wake model is assumed to be of a prescribed shape.</p> <p>The solution of the integral is obtained in a numerical fashion by approximating the actual rotor blade upper and lower surfaces and wake surfaces by a finite number of elemental surfaces on which the doublet strength is assumed constant and then satisfying the resulting set of numerical normal surface boundary conditions at the centroid of each of the blade elemental surfaces.</p> <p>A computer program was developed for the lifting surface theory which depends on a given geometry of the wake. This program lends itself to an iterative procedure for a future force free wake lifting surface theory analysis. The computer results for two case studies is also presented. The program listing is available from West Virginia University.</p>			

14 KEY WORDS	LINK A		LINK B		LINK C	
	ROLE	WT	ROLE	WT	ROLE	WT
Helicopter Rotors Hover Axial Flight Potential Flow Theory Nonlinear Lifting Surface Doublets.						

ia

WEST VIRGINIA UNIVERSITY
College of Engineering

Aerospace
Engineering
TR-35

PART I
NONLINEAR HELICOPTER ROTOR LIFTING
SURFACE THEORY

by

Thomas A. Csencsitz, Jerome B. Fanucci, and Hsi F. Chou

September, 1973

Prepared Under Contract
N00014-68-A-0512

for the

Office of Naval Research
Aeronautics, Code 461
(NR 215-163)

Reproduction in whole or in part is permitted for
any purpose of the United States Government.

Approved for public release; distribution unlimited.

West Virginia University
Department of Aerospace Engineering
Morgantown, West Virginia

jt

ABSTRACT

A numerical method is developed based on potential flow non-linear lifting surface theory for predicting the surface velocities and pressures on a rotor blade of an arbitrary helicopter rotor system which is executing a constant rotational and constant axial translational motion including, specifically, the hover flight mode. The formulation of the problem is exact in the sense that the normal surface boundary condition is satisfied on the surface of the rotor blade. The problem is governed by a Fredholm integral equation of the first kind which relates a singular velocity doublet potential surface distribution applied on the rotor blades and wakes to the normal relative velocity on the rotor blade surface. The wake model is assumed to be of a prescribed shape.

The solution of the integral is obtained in a numerical fashion by approximating the actual rotor blade upper and lower surfaces and wake surfaces by a finite number of elemental surfaces on which the doublet strength is assumed constant and then satisfying the resulting set of numerical normal surface boundary conditions at the centroid of each of the blade elemental surfaces.

A computer program was developed for the lifting surface theory which depends on a given geometry of the wake. This program lends itself to an iterative procedure for a future force free wake lifting surface theory analysis. The computer results for two case studies is also presented.

ACKNOWLEDGMENTS

This report contains a portion of the dissertation of the first author submitted to the Graduate School of West Virginia University in partial fulfillment of the requirements for the degree of Doctor of Philosophy.

The first author should like to extend his appreciation to Dr. A. I. van de Vooren, who during the formulation phase of the problem, was a Visiting Professor in the Department of Aerospace Engineering. In particular the first author wishes to acknowledge the assistance given him by his dissertation advisor, the second author, Dr. Jerome B. Fanucci.

The authors should also like to extend their appreciation to Mrs. Donna Moore and Mrs. Carolyn Swecker for typing the report.

This report was developed as part of the WVU Navy V/STOL Aerodynamics ONR Contract N00014-68-A-0512. Mr. Tom Wilson, Aeronautics Branch, Office of Naval Research, was the project monitor.

TABLE OF CONTENTS

	Page
TITLE PAGE	i
ABSTRACT	ii
ACKNOWLEDGMENTS	iii
TABLE OF CONTENTS	iv
LIST OF FIGURES	vi
LIST OF TABLES	ix
SYMBOLS	x
BODY OF THE REPORT	1
I. INTRODUCTION	1
1.1 Scope	1
1.2 Literature Review	2
1.3 Report Layout	6
2. DISCUSSION OF THE BASIC PROBLEM	7
2.1 Formulation of the Governing Equations	7
2.2 Doublet Potential Discussion	15
2.3 Evaluation of the Doublet Wake Strength	17
2.4 Numerical Reduction of the Integral Expressions for the Doublet Potential and its Derivative	19
2.5 Numerical Reduction of the Integral Surface Boundary Condition	23
2.6 Influence Coefficient Evaluation	28
2.7 Pressure Coefficient Evaluation	32
3. DISCUSSION OF THE SOLUTION SCHEME	34
3.1 Method of Presentation	34
3.2 Rotor Planform Description	34
3.3 Elemental Planar Surface Description	38
3.4 Blade Influence Calculations	43
3.5 Wake Influence Calculations	49
3.6 Generation of the Set of Surface Boundary Conditions and the Numerical Solution	53
3.7 Determination of Velocities, Pressures and Forces	57

4.	DISCUSSION OF THE COMPUTER PROGRAM	59
4.1	General Description	59
4.2	Specific Program Description	61
5.	RESULTS AND CONCLUSIONS	63
6.	EXTENSIONS	69
	REFERENCES	71
	BIBLIOGRAPHY	73
	FIGURES	74
	TABLES	103
	APPENDICES OF THE REPORT	108
A.	SUMMARY OF THE TRANSFORMATION EQUATIONS	109
B.	RELATIONS BETWEEN DOUBLET'S AND VORTICES AND EXTENSION OF HELMHOLTZ CONDITION	114
C.	ANALYTIC EXPRESSION FOR φ AND $\bar{\nabla} \varphi$	122
D.	DETAILED DISCUSSION OF THE COMPUTER PROGRAM	137
D.1	INTRODUCTION	138
D.2	MAIN - INFLUENCE CALCULATIONS PROGRAM	139
D.3	MAIN - CREATE SOLUTION FILE PROGRAM	170
D.4	MAIN - SOLVE BY ELIMINATION PROGRAM	175
D.5	MAIN - SOLVE BY ITERATION PROGRAM	180
D.6	MAIN - TRANSFER SOLUTION FILE PROGRAM	184
D.7	MAIN - VELOCITY CALCULATIONS PROGRAM	185
D.8	MAIN - PRINT PROGRAM	188
D.9	CONCLUDING REMARKS	192

LIST OF FIGURES

FIGURE NO.	PAGE
MAIN BODY OF REPORT	
1. Axis Convention Relating the Potential at a Field Point Induced by a Doublet Surface Distribution	75
2. Rotor System Axis Convention	76
3. Rotor Blade Axis Convention	77
4. Computer Program Flow Diagram	78
5. Control Surface Density Plot (Case 1)	80
6. Pressure Coefficient vs. Chord Station (Span Station 1, Case 1)	81
7. Pressure Coefficient vs. Chord Station (Span Station 2, Case 1)	82
8. Pressure Coefficient vs. Chord Station (Span Station 3, Case 1)	83
9. Pressure Coefficient vs. Chord Station (Span Station 4, Case 1)	84
10. Surface Velocity vs. Chord Station	85
11. Control Surface Density Plot (Case 2)	86
12. $C_{P_{UPPER}} - C_{P_{LOWER}}$ vs. Chord Station (Span Station 1, Case 2)	87
13. $C_{P_{UPPER}} - C_{P_{LOWER}}$ vs. Chord Station (Span Station 2, Case 2)	88
14. $C_{P_{UPPER}} - C_{P_{LOWER}}$ vs. Chord Station (Span Station 3, Case 2)	89
15. $C_{P_{UPPER}} - C_{P_{LOWER}}$ vs. Chord Station (Span Station 5, Case 2)	90
16. $C_{P_{UPPER}} - C_{P_{LOWER}}$ vs. Chord Station (Span Station 7, Case 2)	91

17.	$C_{P_{UPPER}} - C_{P_{LOWER}}$ vs. Chord Station (Span Station 8, Case 2)	92
18.	$C_{P_{UPPER}} - C_{P_{LOWER}}$ vs. Chord Station (Span Station 9, Case 2)	93
19.	$C_{P_{UPPER}} - C_{P_{LOWER}}$ vs. Chord Station (Span Station 11, Case 2)	94
20.	$C_{P_{UPPER}} - C_{P_{LOWER}}$ vs. Chord Station (Span Station 13, Case 2)	95
21.	$C_{P_{UPPER}} - C_{P_{LOWER}}$ vs. Chord Station (Span Station 14, Case 2)	96
22.	$C_{P_{UPPER}} - C_{P_{LOWER}}$ vs. Chord Station (Span Station 15, Case 2)	97
23.	Pressure Difference vs. Chord Station Composite Plot for Selected Span Station of Case 2	98
24.	Experimentally Determined Pressure Difference vs. Chord Station (Redrawn from NACA TN 2953)	99
25.	Experimentally Determined Section Normal Force Component with the Present Result	100
26.	Upper Rotor Surface Velocity Direction Plot for Case 2	101
27.	Lower Rotor Surface Velocity Direction Plot for Case 2	102

APPENDIX SECTIONS

B.1	Surface Axis Convention	116
B.2	Line Integral Path for Evaluation of the Circulation	119
C.1	Axis Convention Relating the Potential at a Point Induced by a Source Plus Sink	124
C.2	Axis Convention Relating the Planar N=4 Sided Doublet Surface Distribution to some Field Point	127

C.3a	Indexing Convention for the Planar $N=4$ Sided Surface . . .	129
C.3b	Subdivision of Region S into Regions R_{ij}	129
D.1	Main - Influence Calculations Detailed Flow Diagram . . .	150

LIST OF TABLES

TABLE NO.	PAGE
1. Rotor Input Summary for Case 1	104
2. Computer Execution Time Summary for Case 1	105
3. Rotor Input Summary for Case 2	106
4. Computer Execution Time Summary for Case 2	107

SYMBOLS

The following is an abridged list of symbols used in the report. Only those symbols of select importance which are used repeatedly throughout the report are listed here. All symbols are defined in the body of the report at the time of their initial use. The same symbols may refer to dimensional or non-dimensional quantities depending upon the context of the immediate section of the report in which they are used. The physical units of any parameter may always be assigned as follows:

- a) All lengths are in units of feet.
- b) All forces are in units of pounds.
- c) All masses are in units of slugs.
- d) All times are in units of seconds.
- e) All angles are in units of radians.

The non-dimensionalized parameters are obtained by dividing all lengths by the rotor radius and dividing all velocities by the rotor rotational tip speed. In those sections where it becomes necessary to distinguish dimensional quantities from the non-dimensional quantities we have underlined the dimensional quantity, eg. \underline{R} implies units of length and R implies a non-dimensionalized length.

English

A	Area
B1	Hub radius taken to be the distance along the span axis from the axis of rotation to the root section.
B2	True span length taken to be the rotor radius less the hub radius.

B3	Chord station along which the blade span axis lies.
CG	Chord grid station expressed in terms of percent chord length.
C_p	Pressure Coefficient defined on the basis of the tip speed squared.
C_{p1}	Used in the program and is the same as C_p above.
C_{p2}	Used in the program to define a pressure coefficient based on the local relative free stream velocity squared.
C_Q	Rotor Torque Coefficient (refer to equation 3.7.5)
C_T	Rotor Thrust Coefficient (refer to equation 3.7.4)
DT	Angular measure that two adjacent rotor blade span axes are displaced from each other.
F	Force
I	Integral as defined by equation (2.4.7)
I_S	Partial derivative with respect to S of the integral I. S is a dummy variable.
P	Pressure
Q	Torque
R	Rotor radius
\bar{R}	Position vector from the origin to some field point.
$ \bar{R} $	Absolute length of vector R.
\bar{R}_S	Position vector from the origin to some point on the body or wake surface.
\bar{R}_{SP}	Position vector from some point on the body or wake surface to some field point.
S	Function which defines body surface or span station depending on context.
SG	Span grid station expressed in terms of percent true span length.
THETA	Geometric pitch at a span section.

T_0	Geometric pitch at the root section.
T_T	Linear twist of the rotor blade. Defined as the geometric pitch at the tip less that at the root.
\bar{V}	Vector velocity with respect to the (X,Y,Z,t) reference frame.
\bar{V}_T	Vector translational velocity of the body with respect to the (X,Y,Z,t) reference frame.
W	Function which defines wake surface.
m	Refer to equation (2.6.7)
\bar{n}	Vector surface unit normal positive out from the surface.
t	Time
w_{av}	Average downwash at the rotor blade trailing edge derived from momentum considerations.

Greek

α	Refer to equation (2.6.8)
β	Refer to equation (2.6.9)
λ	Rotor free stream inflow ratio and given by the rotor axial climb velocity divided by the tip speed.
μ	Doublet strength per unit area
ρ	Density
ϕ	Doublet potential function
ω	Rotor rotational rate ($\omega = \bar{\omega} $)
$\bar{\omega}$	Vector rotation of the body with respect to the (x,y,z,t) reference frame

Operators

$\frac{\partial}{\partial s}$	Partial derivative with respect to some dummy variable S
-------------------------------	--

$\frac{D}{Dt}$	Substantial derivative
$\bar{\nabla}$	Vector gradient operator

Subscripts

∞	Condition existing in the free stream environment
avg.	Average
ind	Potential induced parameter
b	body
w	wake
U	Upper surface
L	Lower surface
P	Specific point P
S	Dummy directional axis or parameter
TE	Trailing edge

Superscripts

'	Parameter referenced to the (x',y',z',t') reference frame
-	Vector parameter
^	Unit vector parameter

Indices

I	Indexed blade elemental surface. The elemental surfaces are indexed consecutively from the leading edge to the trailing edge by proceeding from the inboard span segment to the outboard span segment first on the upper blade surface then on the lower blade surface
---	--

I_{\max}	Maximum number of indexed blade elemental surfaces per blade.
J	Same as I above and used in terms of a dummy summation.
J_{\max}	Same as I_{\max} above.
K	Indexed wake elemental surface. The wake elemental surfaces are indexed consecutively from the trailing edge segment in a streamlinewise sense.
K_{\max}	Maximum number of indexed wake elemental surfaces which streamlinewise trail a particular trailing edge span segment.
L	Indexed blade number. The blades are numbered consecutively in the direction of rotation.
L_{\max}	Number of rotor blades.
M	Indexed span station or span segment. $M=1$ is at or near the root section respectively.
M_{\max}	Maximum number of indexed span stations.
MM	Maximum number of indexed span segments. ($MM = M_{\max} - 1$)
N	Indexed chord station or chord segment. $N = 1$ is at or near the leading edge respectively.
N_{\max}	Maximum number of indexed chord stations.
NN	Maximum number of indexed chord segments. ($NN = N_{\max} - 1$)
i	Indexed corner points of the elemental surfaces. The corner points are indexed consecutively in a clockwise manner when viewing the surface along the negative surface unit normal direction. Also used to index the segment of the elemental surface lying between corner points i and i+1.
J	Indexed corner point immediately adjacent clockwise to some i indexed elemental surface corner point. Used in the same sense as i above.
n	Maximum number of i indexed corner points which define an elemental surface (usually $n = 4$)

Reference Coordinate System

- (X,Y,Z) Inertial fixed coordinate system in general. Used also as a dummy reference system coincident with the (ξ, η, ζ) systems below
- (X',Y',Z') Non-inertial body fixed coordinate system
- (ξ, η, ζ) Element fixed coordinate system
- (X₁,Y₁,Z₁) Blade one body fixed coordinate system coincident with (X',Y',Z')
- (r, θ, z') Non-inertial body fixed cylindrical coordinate system defined in the usual sense within (X',Y',Z')

CHAPTER 1. INTRODUCTION

1.1 Scope and Objectives

There is a need for a more rigorous approach to the treatment of complex three-dimensional flows for geometries of certain V/STOL aircraft. In the case of rotors in quasi-hover, the downwash velocity associated with the generation of lift is large when compared to the axial flight velocity. In this situation the classical assumptions of lifting potential flow aerodynamic theory such as linearized boundary conditions, lifting lines and rigid non-force free wakes do not lead to accurate predictions. Without accurate inviscid flow predictions the even more complicated viscous flow analysis cannot even be begun.

The progress in high speed digital computer technology now allows one to formulate the flow problem more realistically. Although the formulations necessitate the approximation of the integral and differential equations they may be considered exact in the sense that the solution is attained uniformly as the computational network is refined.

The present work is specifically concerned with developing a potential flow lifting surface theory applicable to rotors in the axial flight mode specifically including the hover mode. The theory is an exact numerical analysis and its major objective is to predict the local three dimensional blade surface velocities and pressures. The theory necessarily incorporates a prescribed wake model because of the complex nature of the problem. The force free wake analysis is

to be achieved by successive iterations on the wake geometry by incorporating a wake prediction method into the analysis. In addition to developing the actual theory, the feasibility of applying the theory is also demonstrated since a computer program was also developed and is presented herein. The theory and program developed are applicable to any arbitrary shaped rotor blade having a finite non-zero hub radius and a pointed trailing edge. It is specifically not necessary for the rotor blades to be thin as the surface boundary conditions are satisfied on a surface network described on the wetted blade surface area. Furthermore, perturbation velocities are not required to be small. These last two constraints are associated with the so-called linearized lifting surface theory and small disturbance theory respectively.

1.2 Literature Review

In the discussion of any lifting surface theory one must first distinguish between two basic classes of problems. One class of problems is concerned with the prediction of local surface loadings by assuming a loading function which is expressed as a series of assumed modes with unknown coefficients. These unknown coefficients are then obtained by satisfying the normal velocity condition either directly or indirectly at a set of points whose number equals the number of unknown coefficients. In certain cases the set of points may exceed the number of unknown coefficients in which case the normal velocity condition is satisfied approximately at the set of points by appropriately weighting the set of points. Multhopp's collocation

method (reference 1) for calculating the lift distribution of wings in subsonic flows exemplifies this method. A very elegant analysis by Verbaugh (reference 2) concerning unsteady lifting surface theory for ship screws employs the acceleration potential in solving this class of lifting surface theory problem.

The second class of lifting surface theory problems is concerned with the prediction of local surface loadings by assuming a distribution of surface elements on which the loadings are unknown but on which a set of influence coefficients can be defined. Perhaps the most complete authoritative discussion of this method is that presented by Hess and Smith (reference 3). In this method the integral equation resulting from the application of the normal surface boundary condition is reduced to a sum of integrations to be performed over a finite set of surface elements such that the surface boundary condition is satisfied locally at one point on each surface element. The loading function is some velocity potential function of unknown strength which may, however, be analytically integrated over the surface element region. A linear set of equations results such that the unknowns are the potential function strengths on each surface element and the coefficients represent the elemental integration results. The results obtained by this method are excellent as documented by Hess and Smith (reference 3) for nonlifting bodies.

The lifting surface theory method presented in this report relies heavily on the excellent work of Hess and Smith (reference 3). The presented problem differs fundamentally in that this theory is concerned with a rotating lifting body behind which trails a wake region.

Various authors have noted the complexity of the calculations required when one attempts to use this lifting surface theory method for a lifting body. As late as 1971 Johnson (reference 4) noted in substance that the extent of the calculations involved in these methods prohibited the direct application of the conventional lifting surface theory technique to the calculation of rotary wing air loads. Many authors have ingeniously attempted to simplify the exact lifting surface theory method in order to attain valid results. Erickson (reference 5) reduced (after Prandtl) the lifting blade surface model to a lifting line model. As such, his lifting line theory was based on a bound vortex line and a continuous wake vortex sheet which he allowed to distort on successive iterative steps. The contraction pattern was fixed according to actuator disc theory. Landgrebe (reference 6) also showed that the realistic self-induced distorted wake geometries could be computed by application of the classical Biot-Savart law applied over wake vortex filaments.

Erikson and Hough (reference 7) showed that the applicability of the lifting line model for hover prediction was questionable as blade surface induced velocities vary rapidly along the chord direction which, of course, would invalidate a lifting line model. The reason for this rapid variation lies in the fact that the wake has a pronounced influence on the rotor blade because of its near proximity in hover.

At Sikorsky Aircraft Rorke and Wells (reference 8) have described another unique variation on the true rotor lifting surface theory. They have coupled a prescribed wake-momentum analysis to the conventional

strip-momentum theory in order to predict the rotor hover performance. The prescribed wake geometry in this method is determined in part by a theoretical analysis, the details of which were presented by Clark and Leiper (reference 9). This analysis is a true engineering design analysis and has been optimized so as to require very little computer time. This technique does, of course, require airfoil sectional aerodynamic coefficients.

There are other variations of the rotor lifting surface theory presented in the literature but to this author's knowledge none of the so called rotor lifting surface theories presented are in fact true applications of the ideal lifting surface model. Furthermore, it appears that no single reported rotor prediction method is capable of predicting local surface velocities or pressures on some arbitrary rotor geometry surface. Thus it appears that design studies of new rotor blade shapes differing significantly from existing blade shapes cannot be performed at the present time with any level of confidence. Because of this technological deficit (see references 10 and 11) it was decided to attempt to develop a true rotor lifting surface theory and actually apply this theory in terms of an exact numerical sense. This work is concerned with the initial phase of the development, that is, for a prescribed wake trailing an arbitrary shaped body develop a lifting surface theory which will predict for the axial flight mode local surface velocities and loadings. The succeeding phase will be to use the theory and program of the initial phase and modify them so as to include a wake iterative scheme in order to include a force free wake analysis into the lifting surface theory.

We have not attempted to review here the subject of lifting surface theory in its entirety but have rather restricted the review to selected current rotor lifting surface theories indicative of the general development trends. For an additional literature review concerned mainly with lifting surface theory applied to planar flows refer to Djodjodihardjo (reference 12). Djodjodihardjo and Widnall (reference 13) in a paper which summarizes the previous reference presents, in part, a discussion of the doublet velocity potential which we have used to verify the derived integrated doublet velocity potential used herein.

In addition to the explicit references above we have included a list of references which we have used for obtaining fundamental information and for obtaining information related to general rotor performance prediction methods.

1.3 Report Layout

We have presented in Chapter 2 the formulation of the problem in terms of the governing equations. Chapter 3 presents a step by step discussion of the overall problem solution. Chapter 4 discusses the computer program in a general manner. The results of two computer run cases are presented in Chapter 5. In Chapter 6 we have discussed extensions to the present problem. We have relegated all discussion material not actually essential to the main problem discussion to Appendices A, B and C so as not to interrupt the overall problem discussion. Appendix D describes the computer program in detail as to its options and input/output.

CHAPTER 2. DISCUSSION OF THE BASIC PROBLEM

2.1 Formulation of the Governing Equations

As a lifting rotor moves into the air it disturbs the air in such a manner as to derive its lift. This problem is concerned with the prediction of the local surface pressure acting on the rotor blades in hover or axial flight through an analysis of the rotor induced velocities. We shall formulate in this section the equations governing the fluid motion.

Let us consider the lifting rotor system to consist of:

- a) a three dimensional body of arbitrary shape which is executing a constant rotatory and translatory motion, and
- b) a wake which trails the lifting body. The surface of the body may be represented by

$$S(\bar{R}, t) = 0 \quad (2.1.1)$$

and the wake following the body may be defined by a surface of velocity discontinuity given by

$$W(\bar{R}, t) = 0 \quad (2.1.2)$$

In the above equations \bar{R} is the position vector with respect to some fixed inertial reference frame. The external flow field is assumed to be an incompressible flow field which is inviscid and initially irrotational and at rest. The wake is further assumed to be composed of two surfaces coincident with each other. Each wake surface is

assumed to have its origin at some infinitesimal region located on the body upper and lower surfaces at the trailing edge. These trailing edge regions as such represent the lines along which the viscous boundary layer smoothly leaves the trailing edge. It is assumed in the analysis to follow that there exists no flow separation from the body except at the trailing edge, thus the body must have a sharp trailing edge.

It follows now from the condition of irrotationality and the continuity equation that a velocity potential $\phi(\bar{R}, t)$ can be defined such that it must satisfy Laplace's equation

$$\nabla^2 \phi(\bar{R}, t) = 0 \quad (2.1.3)$$

The velocity potential at an exterior field point can be given by an integral equation which incorporates a distribution of singularities over the lifting body and wake surface. In this analysis we will take as our distributed surface singularities the doublet or dipole which is itself composed of two more basic singularities, namely the source and sink. In Appendix C is presented a discussion of the doublet potential and its axis convention. The resulting integral equation for the doublet velocity potential is given by

$$\phi(\bar{R}, t) = -\frac{1}{4\pi} \iint_{S+W} \gamma(\bar{R}_s, t) \frac{\bar{n}(\bar{R}_s, t) \cdot \bar{R}_{sp}(\bar{R}; \bar{R}_s, t)}{|\bar{R}_{sp}(\bar{R}; \bar{R}_s, t)|^3} dS \quad (2.1.4)$$

where

\bar{R} is the position vector to some field point, P.

\bar{R}_S is the position vector to some surface point.

\bar{n} is the unit outward surface normal.

$\bar{R}_{Sp} = \bar{R} - \bar{R}_S$, which is the vector from the surface point to the field point.

μ is the doublet strength per unit area at some surface point.

The potential as given satisfies Laplace's equation identically. The above velocity potential is subject to the following boundary conditions:

- a) In the far region away from the doublet surface distribution the fluid velocity (\bar{V}) given by

$$\bar{V} = \bar{\nabla} \phi \quad (2.1.5)$$

should approach zero. Thus the far boundary condition becomes

$$\lim_{R_{Sp} \rightarrow \infty} \nabla \phi(\bar{R}, t) \rightarrow 0. \quad (2.1.6)$$

This boundary condition is inherently satisfied by the doublet velocity potential.

- b) In the region of the body surface the normal velocity at the surface must be zero. This kinematic normal boundary condition may be expressed as

$$\frac{DS}{Dt} = \frac{\partial S}{\partial t} + \bar{v} \cdot \bar{\nabla} S = 0$$

$$\text{ON } S(\bar{R}, t) = 0.$$

(2.1.7)

- c) In the region of the wake surface, since the wake cannot maintain a pressure discontinuity, the pressure across the wake surface must be continuous. Thus

$$P_u - P_l = 0$$

(2.1.8)

$$\text{on } W(\bar{R}, t) = 0$$

where P_u and P_l are the pressures on the local wake upper and lower surfaces.

- d) In the region of the trailing edge the fluid velocity must be directed smoothly from the body surface to the wake surface. This is the Kutta-Joukowski condition.

The pressure P anywhere in the flow field is given by the equation of motion

$$\frac{D\bar{v}}{Dt} = -\frac{1}{\rho} \bar{\nabla} P$$

(2.1.9)

which is uncoupled from the governing kinematic equation given by Laplace's equation. It is, however, coupled into the overall problem through the boundary condition (c) above.

For convenience we will now transform the above equations which are expressed with respect to a fixed inertial reference frame to a

non-inertial body reference frame designated by primed coordinates. Let us assume that the body is translating and rotating about the translational axis with respect to the inertial reference frame at a constant translational velocity given by \vec{V}_T and constant rotational velocity given by $\vec{\omega}$. In Appendix A is presented a summary of the transformation relations. The body surface and wake surface equations given by equations (2.1.1) and (2.1.2) transform respectively to

$$S(\vec{R}') = 0 \quad (2.1.10)$$

$$W(\vec{R}') = 0 \quad (2.1.11)$$

The velocity potential in the body fixed reference frame becomes independent of time and is given by

$$\phi = \phi(\vec{R}') \quad (2.1.12)$$

Laplace's equation transforms directly to

$$\nabla'^2 \phi(\vec{R}') = 0 \quad (2.1.13)$$

Whereas before, however, $\nabla \phi(\vec{R}, t)$ was the total fluid velocity \vec{v} , $\nabla \phi(\vec{R}')$, in the body fixed system becomes the velocity induced about a relative free stream velocity. If we define

\vec{v}'_{ind} as

$$\vec{v}'_{ind} = \nabla' \phi(\vec{R}') \quad (2.1.14)$$

and \bar{V}'_{∞} as the relative free stream velocity given by

$$\bar{V}'_{\infty} = - [\bar{\omega} \times \bar{R}' + \bar{V}_T] \quad (2.1.15)$$

then the inertial and body fixed velocities are related as follows

$$\bar{V} = \bar{V}' + \bar{\omega} \times \bar{R}' + \bar{V}_T \quad (2.1.16)$$

where

$$\bar{V}' = \bar{V}'_{ind} + \bar{V}'_{\infty} . \quad (2.1.17)$$

The integral equation for the doublet velocity potential becomes

$$\phi(\bar{R}') = -\frac{1}{4\pi} \iint_{S+W} \gamma(\bar{R}'_s) \frac{\bar{R}(\bar{R}'_s) \cdot \bar{R}'_{sp}(\bar{R}'_s; \bar{R}'_s)}{|\bar{R}'_{sp}(\bar{R}'_s; \bar{R}'_s)|^3} dS \quad (2.1.18)$$

where the symbols are the same as before except the reference coordinate system is now the primed body fixed reference system. The boundary conditions in the new reference plane become:

a) In the far region

$$\lim_{R'_{sp} \rightarrow \infty} \bar{\nabla}' \phi(\bar{R}') \rightarrow 0 \quad (2.1.19)$$

which remains inherently satisfied.

b) On the body surface since

$$\frac{D}{Dt} = \frac{\partial}{\partial t} \quad (2.1.20)$$

and since $\frac{\partial S(\vec{R}')}{\partial t} = 0$ we must satisfy the following relation

$$\vec{v}'_{ind} \cdot \vec{\nabla}' S = - \vec{v}'_{\infty} \cdot \vec{\nabla}' S$$

ON $S(\vec{R}') = 0$.

(2.1.21)

c) On the wake surface,

$$p_u - p_k = 0$$

(2.1.22)

ON $W(\vec{R}') = 0$.

The Kutta condition (boundary condition d) may be applied as stated earlier. The pressure anywhere in the flow field may be determined from the transformed equation of motion which will be discussed later.

Since the velocity potential is a solution to Laplace's equation and since it also inherently satisfies the far boundary condition we no longer need consider these two equations. Let us consider now the near boundary condition. If we define \vec{n} to be the outward surface unit normal vector, then we may write

$$\vec{n} = \pm \frac{\vec{\nabla}' S}{|\vec{\nabla}' S|} \quad (2.1.23)$$

Furthermore, using this result and equation (2.1.14) we may rewrite the near boundary condition given by equation (2.1.21) as follows:

$$\bar{\nabla}' \phi \cdot \bar{n} = - \bar{V}'_{\alpha} \cdot \bar{n} \quad (2.1.24)$$

$$\text{on } S(\bar{R}') = 0 .$$

Written in this form we see now that the solution to the given problem requires solving in the body fixed reference system an integral equation given by the near boundary condition expressed by equation (2.1.24) where ϕ is defined by equation (2.1.18) subject to explicit boundary conditions (c) and (d). Note that the solution does not necessarily involve the potential ϕ but rather involves the vector gradient of ϕ , that is $\bar{\nabla}' \phi$. In essence then the formulation of the basic governing equations is complete.

Before proceeding into the detailed formulation we shall first discuss the doublet potential in order to further clarify its use.

2.2 Doublet Potential Discussion

We have taken as our potential function a potential derived on the basis of a surface doublet (dipole) distribution. In particular we note using Figure 1 that the potential induced at a point P by a surface doublet distribution given by $\mu(\vec{R}_s')$ whose axis is everywhere normal to the local surface, that is

$$-\vec{\psi}(\vec{R}_s') = \mu(\vec{R}_s') \vec{n} \quad (2.2.1)$$

is given by

$$\phi(P) = -\frac{1}{4\pi} \iint_{\text{Surface}} \mu(\vec{R}_s') \frac{\vec{n} \cdot \vec{R}_{sp}'}{|\vec{R}_{sp}'|^3} dS \quad (2.2.2)$$

In Appendix C we have derived this doublet potential as presented in terms of its more basic source plus sink potentials in order to clarify the axis convention of the doublet.

We have chosen to model the rotor and wake surfaces with a doublet distribution rather than a vorticity distribution, which could also have been used, for a number of reasons. The main reason stems from the fact that a vorticity model does require the specification of two functions lying along the surface in two vector directions mutually perpendicular to each other. This aspect of vorticity in light of the doublet model would unnecessarily complicate the geometry of the problem. The two models are of course mathematically related (refer to Appendix B) and both inherently satisfy Laplace's equation and the boundary condition at infinity.

The application of the doublet model involves a doublet distribution applied on the wetted areas of all rotor blades. Furthermore, trailing continuously from the upper and lower blade surfaces are two sheets upon which are also applied doublets. These two sheets are taken to be coincident with each other thus allowing for vector sums of the doublet strengths.

It should be noted at this point that the doublets are distributed on the blade surfaces. This method is to be distinguished from the so called linearized method which through linearization of the surface boundary condition would allow doublets to be distributed on a mean camber plane. The blade surface distribution although more complex is of course exact and does not impose the planform restrictions of the linearized method.

2.3 Evaluation of the Doublet Wake Strength

Let us consider now the doublet velocity potential in more detail. Suppose we first separate the wake region integration from the blade region integration such that we may write

$$\begin{aligned} \phi(\bar{R}') = & -\frac{1}{4\pi} \iint_S \gamma_b(\bar{R}'_s) \frac{\bar{R}(\bar{R}'_s) \cdot \bar{R}'_{SP}(\bar{R}'_s, \bar{R}'_s)}{|\bar{R}'_{SP}|^3} dS + 2 \\ & - \frac{1}{4\pi} \iint_W \gamma_w(\bar{R}'_s) \frac{\bar{R}(\bar{R}'_s) \cdot \bar{R}'_{SP}(\bar{R}'_s, \bar{R}'_s)}{|\bar{R}'_{SP}|^3} dS \end{aligned} \quad (2.3.1)$$

where now $\gamma_b(\bar{R}'_s)$ and $\gamma_w(\bar{R}'_s)$ represent the doublet strengths on the body and wake regions respectively. As was pointed out earlier the wake is actually composed of two coincident sheets on each of which the doublet strength is given as an upper doublet strength γ_{wU} and a lower doublet strength γ_{wL} . If we account for the opposite direction of the doublet axis and take as a net axis direction the outward normal of the upper wake surface then in effect the net doublet strength on the wake surface is given locally by

$$\gamma_w = \gamma_{wU} - \gamma_{wL} \quad (2.3.2)$$

In Appendix B it is shown that Helmholtz's theorem on conservation of vorticity logically extends to the conservation of wake doublet strength. In this problem the blade loadings are independent of the rotational azimuth body position and as such the wake doublet strength remains

constant along a wake streamline. Following along a wake streamline up to the trailing edge by utilizing the Kutta condition we find that along any wake streamline that originates at trailing edge span station S_{TE} the doublet wake strength is constant and is given by the difference in value of the blade doublet upper and lower trailing edge surface doublet strength, that is

$$\mu_w(S_{TE}) = \mu_b(S_{TE_U}) - \mu_b(S_{TE_L}) \quad (2.3.3)$$

Thus the wake doublet strength varies with span station, is constant along a streamline and is given in terms of the body trailing edge doublet strengths. The velocity potential may now be written as

$$\begin{aligned} \phi(\vec{R}') = & -\frac{1}{4\pi} \iint_S \mu_b(\vec{R}_s') \frac{\vec{n}(\vec{R}_s') \cdot \vec{R}_{sp}'}{|\vec{R}_{sp}'|^3} dS + \mu_w \\ & -\frac{1}{4\pi} \iint_W [\mu_b(S_{TE_U}) - \mu_b(S_{TE_L})] \frac{\vec{n}(\vec{R}_s') \cdot \vec{R}_{sp}'}{|\vec{R}_{sp}'|^3} dS \end{aligned} \quad (2.3.4)$$

2.4 Numerical Reduction of the Integral Expression for the Doublet Potential and its Derivative

We may now reduce this integral expression for the doublet potential to a numerical relation. In order to do this we first assume that there are L_{\max} equally spaced, identical rotor blade bodies whose surface equations are given by

$$S_L(\bar{R}') = 0 \quad L=1, L_{\max} \quad (2.4.1)$$

Similarly we assume that there are L_{\max} equally spaced, identical wake surfaces whose surface equations are given by

$$W_L(\bar{R}') = 0 \quad L=1, L_{\max} \quad (2.4.2)$$

Thus equation (2.3.4) may now be written as

$$\begin{aligned} \phi(\bar{R}') = & -\frac{1}{4\pi} \sum_{L=1}^{L_{\max}} \iint_{S_L} M_b(\bar{R}'_{S_L}) \frac{\bar{n}(\bar{R}'_{S_L}) \cdot \bar{R}'_{S_L P}}{|\bar{R}'_{S_L P}|^3} dS + \bar{z} \\ & - \frac{1}{4\pi} \sum_{L=1}^{L_{\max}} \iint_{W_L} [M_b(S_{TE_{L_2}}) - M_b(S_{TE_{L_1}})] \otimes \bar{z} \\ & \times \frac{\bar{n}(\bar{R}'_{S_L}) \cdot \bar{R}'_{S_L P}}{|\bar{R}'_{S_L P}|^3} dS \end{aligned} \quad (2.4.3)$$

Let us assume now that rotor blade body one and wake surface one can be subdivided into $M = 1, M_{max}$ span segments. Furthermore we shall assume that along blade segment M there are $N = 1, N_{UJ}$ and N_{LJ} upper and lower surface planar areas respectively. In the wake one region we assume that along wake span station M there are $K = 1, K_{max}$ streamline defined planar wake surface areas. We assume further that on blade bodies $L = 2, L_{max}$ and wake surfaces $L = 2, L_{max}$ there are similarly defined elements which are determined from blade body one and wake surface one by simple element rotation. If in addition we assume that the doublet strength on any element is a constant we may rewrite the doublet potential given by equation (2.4.3) as follows

$$\begin{aligned}
 \Phi(\bar{R}') &= -\frac{1}{4\pi} \sum_{L=1}^{L_{max}} \sum_{M=1}^{M_{max}} \sum_{N=1}^{N_{UJ}} M_{B(L,M)U} \iint_{S_{(L,M)U}} \frac{\bar{x}(\bar{R}'_{S(L,M)U}) \cdot \bar{R}'_{SP}}{|\bar{R}'_{SP}|^3} dS \quad (1) \\
 &\quad - \frac{1}{4\pi} \sum_{L=1}^{L_{max}} \sum_{M=1}^{M_{max}} \sum_{N=1}^{N_{LJ}} M_{B(L,M)L} \iint_{S_{(L,M)L}} \frac{\bar{x}(\bar{R}'_{S(L,M)L}) \cdot \bar{R}'_{SP}}{|\bar{R}'_{SP}|^3} dS \quad (2) \\
 &\quad - \frac{1}{4\pi} \sum_{L=1}^{L_{max}} \sum_{M=1}^{M_{max}} \sum_{K=1}^{K_{max}} [M_{B(L,M)U} - M_{B(L,M)L}] \iint_{S_{(L,M)L}} \frac{\bar{x}(\bar{R}'_{S(L,M)L}) \cdot \bar{R}'_{SP}}{|\bar{R}'_{SP}|^3} dS \quad (3)
 \end{aligned}$$

(2.4.4)

Noting now that the blade loadings and thus the doublet strengths are independent of blade azimuth position in this problem we may identify

$$M_{B(L,M)U} = M_{B(L,M)U_{L12}} = M_{B(L,M)U} \quad (2.4.5)$$

That is the doublet strength on blade L upper surface element (N,M) has the same value of doublet strength on blade L+1 upper surface element (N,M). Applying this condition also to the lower blade surface elements and to the wake elements we find that the velocity potential may now be written as

$$\begin{aligned}
 \phi(\bar{R}') &= -\frac{1}{4\pi} \sum_{M=1}^{M_{1L}} \sum_{N=1}^{N_{1L}} A_{D(N,M)_L} \sum_{L=1}^{L_{max}} I(\bar{R}')_{(N,M)_L} + \int \\
 &- \frac{1}{4\pi} \sum_{M=1}^{M_{1L}} \sum_{N=1}^{N_{1L}} A_{D(N,M)_L} \sum_{L=1}^{L_{max}} I(\bar{R}')_{(N,M)_L} + \int \\
 &- \frac{1}{4\pi} \sum_{M=1}^{M_{1L}} [A_{D(M)_L} - A_{D(M)_L}] \sum_{K=1}^{K_{max}} \sum_{L=1}^{L_{max}} I(\bar{R}')_{(K,M)_L} ,
 \end{aligned}
 \tag{2.4.6}$$

where for ease in writing we have defined for a dummy element surface (I,J),

$$I(\bar{R}')_{(I,J)_L} = \iint_{S_{(I,J)_L}} \frac{\bar{n}(\bar{R}'_{(I,J)_L}) \cdot \bar{R}'_{sr}}{|\bar{R}'_{sr}|^3} dS .
 \tag{2.4.7}$$

In effect $I(\bar{R}')_{(I,J)_L}$ is a potential influence coefficient which represents the geometric influence of some surface element (I,J) of blade or wake L on the potential at some point \bar{R}' .

The induced velocity at some field point along a direction \hat{s} may be written as

$$V_{ind_s} = \frac{\partial \phi}{\partial s}, \quad (2.4.8)$$

where the derivative with respect to s of the potential follows directly from equation (2.4.6) and is given by

$$\begin{aligned} \frac{\partial \phi}{\partial s}(\bar{R}') &= -\frac{1}{4\pi} \sum_{M=1}^{M1} \sum_{N=1}^{N1} A_{0(M,N)} \sum_{L=1}^{Lmax} I_s(\bar{R}')_{(M,N)_L} + \bar{v} \\ &- \frac{1}{4\pi} \sum_{M=1}^{M1} \sum_{N=1}^{N1} A_{0(M,N)} \sum_{L=1}^{Lmax} I_s(\bar{R}')_{(M,N)_L} + \bar{v} \\ &- \frac{1}{4\pi} \sum_{M=1}^{M1} [A_{0(M,1)} - A_{0(M,2)}] \sum_{K=1}^{Kmax} \sum_{L=1}^{Lmax} I_s(\bar{R}')_{(M,1)_L} \end{aligned} \quad (2.4.9)$$

where we have defined

$$I_s(\bar{R}')_{(I,J)_L} = \frac{\partial}{\partial s} I(\bar{R}')_{(I,J)_L}. \quad (2.4.10)$$

Here $I_s(\bar{R}')_{(I,J)_L}$ is a velocity influence coefficient in the \hat{s} direction which represents the geometric influence of some surface element (I,J) of blade or wake L on some point \bar{R}' .

2.5 Numerical Reduction of the Integral Surface Boundary Condition

Let us summarize at this point the major results of the previous discussions. First it has been shown that the equation to be solved is the near boundary condition given by equation (2.1.24) and repeated here is

$$\vec{\nabla} \phi \cdot \vec{n} = -V_{\infty}' \cdot \vec{n} \quad (2.5.1)$$

ON SCB' = 0

This equation states that the normal fluid velocity on the body must be zero. In addition this equation is subject to the following additional constraints:

- A) The fluid flow must leave the trailing edge smoothly.
- B) The pressure must be continuous across the wake. This ensures the existence of a, so called, force free wake.

In section 2.4 it was shown that the integral expression for ϕ and $\int_S \phi$ could be reduced to a numerical equation involving the summation of finite elemental surface contributions. On each of these elemental surfaces it was assumed that the local doublet strength was a constant.

Let us now relax the boundary condition expressed by equation (2.5.1) such that instead of requiring it to hold on the entire body region ($SCB' = 0$) we now require it to hold only at a finite number of body points. We will further take these control points to be located at say the centroid of the previously defined elemental

body areas. Because of the symmetry involved we need only require the normal velocity to be zero on one blade's control points in order to ensure a zero velocity on all other corresponding blade control points. In previous discussions for preciseness we identified the upper and lower surface elemental areas on a particular blade as element $(M, N)_{ijk}$. Let us now identify these same blade elements here using a single index say $I = 1, I_{\max}$. Thus the numerical form of the near boundary condition becomes a set of I_{\max} equations such that

$$\bar{\nabla}'\phi_I \cdot \bar{n}_I = -\bar{V}_{\infty I}' \cdot \bar{n}_I \quad (2.5.2)$$

for all $I = 1, I_{\max}$

where

$\bar{\nabla}'\phi_I$ represents the vector gradient of the potential on the centroid of element I.

$\bar{V}_{\infty I}'$ represents the free stream velocity on the centroid of element I

\bar{n}_I represents the outward unit normal of element I at its centroid.

Since $\bar{\nabla}'\phi_I \cdot \bar{n}_I$ is just the induced velocity along the normal direction of element I evaluated at the centroid of element I we may write that

$$\left(\frac{\partial \phi}{\partial n}\right)_I = \bar{\nabla}'\phi_I \cdot \bar{n}_I \quad (2.5.3)$$

Now using equation (2.4.9) we may evaluate $\left(\frac{\partial \phi}{\partial n}\right)_I$ such that we have

$$\begin{aligned} \left(\frac{\partial \phi}{\partial n}\right)_I &= -\frac{1}{4\pi} \sum_{j=1}^{I_{\max}} \mu_{0j} \sum_{l=1}^{L_{\max}} I_{H_{I,j,l}} + \int \\ &- \frac{1}{4\pi} \sum_{M=1}^{M_{\max}} [\mu_{0M1} - \mu_{0M1K}] \sum_{K=1}^{K_{\max}} \sum_{L=1}^{L_{\max}} I_{H_{I,j}(K,M)_L} \end{aligned} \quad (2.5.4)$$

where the first term represents the body surface induced normal velocity on control point I and the second term represents the wake induced normal velocity on control point I. Note that the normal influence coefficients are a function of the geometry of the problem only. Note further that singularities in the evaluation of particular influence coefficients will occur when we attempt to evaluate an elemental influence on itself. The actual evaluation of these influence coefficients and the resolution of the singularities will be presented in section 2.6.

If we now substitute this equation into equation (2.5.2) using equation (2.5.3) we may write the final form of the $I = 1, I_{\max}$ set of near surface boundary conditions to be satisfied as a numerical set of equations given by

In the preceding discussion we selected the control points at which the normal surface boundary conditions are to be satisfied as the centroids of the elemental surfaces. We actually chose the centroid location for two reasons. Firstly, the centroid of an elemental planar area is most logically the point which best represents the surface area and secondly, this point is the point on an elemental planar surface where the self induced doublet normal velocity magnitude is a minimum and, as such, the various elemental centroids represent consistent, comparable points.

2.6 Influence Coefficient Evaluation

Let us consider now the evaluation of the influence coefficients. More specifically we are concerned with analytically determining the potential ϕ and $\bar{\nabla}\phi$ at an arbitrary field point P induced by a finite planar doublet distribution. The actual evaluation is presented in Appendix C but we will present here the major results.

If we are given a planar n sided figure whose plane lies within the (x, y) plane of a (x, y, z) orthogonal coordinate system and whose positive surface unit normal lies along the positive z axis and given further this plane to be a surface doublet plane of constant strength μ whose axis everywhere is directed along the unit normal then the potential ϕ at an arbitrary field point P whose coordinates are

$$\begin{aligned} x &= x_p \\ y &= y_p \\ z &= z_p \end{aligned} \quad (2.6.1)$$

is given simply by

$$\phi(P) = -\frac{\mu}{4\pi} \iint_{\text{Surface}} \frac{z}{[(x-x')^2 + (y-y')^2 + z^2]^{3/2}} dS \quad (2.6.2)$$

The actual involved integration of this integral is presented in Appendix C. The resulting analytic expression for the potential is given as follows

$$f(P) = -\frac{\mu}{4\pi} I(P) \quad (2.6.3)$$

where

$$I(P) = \sum_{i=1}^n I_i(P) \quad (2.6.4)$$

$$I_i(P) = \tan^{-1} \left\{ \frac{1}{2} \frac{m_{ij} \alpha_i - B_i}{R_i} \right\} - \tan^{-1} \left\{ \frac{1}{2} \frac{m_{ij} \alpha_j - B_j}{R_j} \right\} \quad (2.6.5)$$

$$j = i+1 ; \text{ IF } j = n+1 \text{ THEN READ } j = 1 \quad (2.6.6)$$

$$m_{ij} = (a_j - a_i) / (s_j - s_i) \quad (2.6.7)$$

$$\alpha_i = (x - s_i)^2 + z^2 \quad (2.6.8)$$

$$B_i = (x - s_i) (y - a_i) \quad (2.6.9)$$

$$R_i = [(x - s_i)^2 + (y - a_i)^2 + z^2]^{1/2} \quad (2.6.10)$$

$(s_i, a_i, y)_{i=1, n}$ ARE CORNER POINT COORDINATES
DETERMINED BY CLOCKWISE
ROTATION AS VIEWED ALONG
THE NEGATIVE UNIT NORMAL.

$$\text{IF } s_i = s_j \text{ THEN } I_i(P) \equiv 0. \quad (2.6.11)$$

$$(2.6.12)$$

If the field point P lies on the plane of the surface doublet distribution, that is when $z = y_p = 0$, then the value of the integral taken as the limiting process as z approaches 0 positively results in

$$f(P) = -\frac{q}{r} \quad \text{For } P \text{ within doublet surface} \quad (2.6.13)$$

$$f(P) = 0 \quad \text{For } P \text{ outside doublet surface} \quad (2.6.14)$$

$$f(P) \sim \text{UNDEFINED} \quad \text{For } P \text{ on doublet surface edge.} \quad (2.6.15)$$

Given this expression for $f(P)$ we can now evaluate $\bar{\nabla} f(P)$

as

$$\bar{\nabla} f(P) = -\frac{q}{r^2} \bar{\nabla} r(P). \quad (2.6.16)$$

This operation is carried out in Appendix C. The results when referred to cartesian coordinates are

$$\int_S f(P) = -\frac{q}{r^2} \int_S r(P) \equiv -\frac{q}{r^2} I_S(P), \quad (2.6.17)$$

where S is a dummy independent variable standing for x, y or z and

$$I_S(P) = \sum_{i=1}^n I_{S_i}(P) \quad (2.6.18)$$

where

$$I_{S_i}(P) = \frac{2R_i [M_{iS} x_S - B_i] - [M_{iS} x_i - B_i] [2R_i + R_i z_S]}{(2R_i)^2 + (M_{iS} x_i - B_i)^2} + 2 \frac{2R_j [M_{iS} x_S - B_j] - [M_{iS} x_j - B_j] [2R_j + R_j z_S]}{(2R_j)^2 + (M_{iS} x_j - B_j)^2} \quad (2.6.19)$$

$$x_{iS} = \int_S x_i \quad B_{iS} = \int_S B_i \quad R_{iS} = \int_S R_i. \quad (2.6.20)$$

The symbols used here are the same as given following equation (2.6.3).

The value for \mathcal{I}_2 is to be taken as zero in the event $\mathcal{I}_1 = \mathcal{I}_2$

The relation for $\int_S R(P)$ is valid for all field points whether they lie on or off the plane of the doublet distribution except for the case where P lies on the edge, in which case, the integral is undefined. Note also that regardless of the size or shape of the planar doublet distribution equation (2.6.17) shows that

$$\frac{\partial \mathcal{A}(x, y, 0)}{\partial x} = 0 \quad (2.6.21)$$

$$\frac{\partial \mathcal{A}(x, y, 0)}{\partial y} = 0 \quad (2.6.22)$$

The normal derivative with respect to the doublet surface is well behaved everywhere except for the edge where it is undefined. It is continuous through the doublet surface. If one evaluates the normal derivative at the centroid of the doublet surface one finds that the magnitude decreases to zero in the limit as this finite area increases to include the entire (x, y) plane.

2.7 Pressure Coefficient Evaluation

Using the equations just derived for the influence coefficients it is possible given the geometry to define the necessary influence coefficients needed for the set of simultaneous equations which constitute the surface boundary conditions. Once the solution in terms of the doublet strength is known the local velocities may be determined essentially by back substitution. Given the velocities we may then determine the local pressures using the equation of motion given by equation (2.1.9), that is

$$\frac{D\vec{v}}{Dt} = -\frac{1}{\rho} \vec{\nabla} p, \quad (2.7.1)$$

After expanding this equation using vector identities and interchanging vector operations we find that the equation of motion may be written as

$$\vec{\nabla} \left\{ \frac{\partial \phi}{\partial t} + \frac{v^2}{2} + \frac{p}{\rho} \right\} = 0. \quad (2.7.2)$$

Since this relation must hold throughout the flow field it is necessary then that

$$\frac{\partial \phi}{\partial t} + \frac{v^2}{2} + \frac{p}{\rho} = \text{CONSTANT} = H. \quad (2.7.3)$$

If we now transform this equation to the non-inertial primed reference system we find that

$$\frac{P}{\rho} = H + \frac{1}{2} [\bar{\omega} \times \bar{R}' + \bar{V}_T] \cdot [\bar{\omega} \times \bar{R}' + \bar{V}_T] - \frac{1}{2} \bar{V}' \cdot \bar{V}' \quad (2.7.4)$$

Evaluation of the constant H for $\bar{V}'_{\text{mod}} = 0$ allows us to write

$$P = \frac{1}{2} \rho \bar{V}' \cdot \bar{V}' = P_{\infty} + \frac{1}{2} \rho \bar{V}'_{\infty} \cdot \bar{V}'_{\infty} \quad (2.7.5)$$

where

$$\bar{V}'_{\infty} = - [\bar{\omega} \times \bar{R}' + \bar{V}_T] \quad (2.7.6)$$

If we define a pressure coefficient such that

$$C_p = \frac{P - P_{\infty}}{\frac{1}{2} \rho (U_{\infty})^2} \quad (2.7.7)$$

we find then using equation (2.7.5) that

$$C_p = \frac{\bar{V}'_{\infty} \cdot \bar{V}'_{\infty}}{(U_{\infty})^2} - \frac{\bar{V}' \cdot \bar{V}'}{(U_{\infty})^2} \quad (2.7.8)$$

Thus given the velocities, the pressure coefficients may be determined.

CHAPTER 3. DISCUSSION OF THE SOLUTION SCHEME

3.1 Method of Presentation

In the discussion to follow in this section we will discuss more specifically the actual solution scheme employed beginning with the description of the rotor blades and carrying this through to the determination of rotor forces. The symbols used will in most cases correspond to those employed in the computer program. All lengths and velocities are taken to be nondimensionalized on the basis of the rotor radius (R) and tip speed (ωR) unless specified otherwise.

3.2 Rotor Planform Description

We have chosen to model the rotor geometry in terms of a blade fixed orthogonal coordinate system. In particular we have assumed that there are L_{max} identical rotor blades whose span axes are displaced from each other in the (x', y') plane of rotation by an angular measure, ΔT , given by

$$\Delta T = \frac{2\pi}{L_{max}} \quad (3.2.1)$$

We further assume that the blades are numbered consecutively in the direction of rotation such that blade one has its span axis projection coincident with the y' axis. It follows from this that only one blade need be defined as the other blades may be defined from the geometry of blade one by a simple axis rotation. Figure 2 visualizes the coordinate system convention indicating also the relation between the blade fixed coordinate systems and a fixed inertial reference system

(x, y, z) . In the description of blade one we have allowed for two approaches. The first approach to describing the rotor blade geometry is a completely general method. In essence we assume the rotor blade is positioned in space at some lifting attitude. We require only that it have some non zero hub radius and that its span axis projects along the y' reference axis. We assume then that the blade can be described by a set of grid point coordinates in the (x', y', z') system. If we let N_{max} represent the number of span stations and $N_{max U}$ and $N_{max L}$ represent the number of upper surface and lower surface chord stations per span station, then the blade one description involves a table of coordinates such that we specify

$$\begin{array}{ccccc} N & M & x_{1U, N, M} & y_{1U, N, M} & z_{1U, N, M} \\ N & M & x_{1L, N, M} & y_{1L, N, M} & z_{1L, N, M} \end{array}$$

for

$$M = 1, M_{max}$$

and

$$N = 1, N_{max U}$$

on the upper surface

$$N = 1, N_{max L}$$

on the lower surface

where

$$M = 1$$

is the root chord section

$$M = M_{max}$$

is the tip chord section

$$N = 1$$

is the leading edge span section

$$N = N_{max U} \text{ or } N_{max L}$$

is the trailing edge span section

on the upper or lower surface.

We will use x_{1U} etc. as distinct from x' etc. to clearly distinguish the blade one surface grid points from any other general

point. Note that the (x_1, y_1, z_1) system is coincident with the primed reference (x', y', z') system as shown in Figure 3.

A second method for describing the rotor planform which we have chosen to include in the programmed scheme involves the description of the grid points for a linearly twisted, constant chord, constant airfoil section type rotor blade.

In this method we assume the airfoil section is a NACA OXXX series airfoil where XX represents the percent thickness. In describing the blade we now specify our grid points as follows:

$$\begin{array}{l} M \quad SG \\ N \quad CGU \quad CGL \end{array}$$

for $M = 1, M_{max}$ and $N = 1, N_{maxU}$ or N_{maxL} where SG represents a span station expressed in terms of percent true span and CGU or CGL represents a chord station expressed in terms of percent chord on the upper or lower surface respectively. The remaining parameters necessary to define the rotor blade surface include the hub radius (Bl), the chord length (C) and the airfoil percent thickness ratio (TC). In applying the linear twist to the rotor blade the geometric pitch (THETA) at any span location is given by

$$THETA = T_0 + (TT)(SG) \quad (3.2.2)$$

where

- T₀ - geometric pitch at the root chord
- TT - amount of twist
- SG - true percent span station.

This twist is applied about the span axis which we assume to be located behind the leading edge intersecting the chord line at a chord station given by B3. The true span (B2) is taken to be the actual blade span length and is given by the difference between the rotor radius (R) and the hub radius. Figure 3 attempts to visualize these geometry parameters.

Given this information we can now calculate the grid point location in terms of our (X, Y, Z) reference system and express the results as

$$\begin{array}{rcc}
 N & M & X1U_{N,M} \quad Y1U_{N,M} \quad Z1U_{N,M} \\
 N & M & X1L_{N,M} \quad Y1L_{N,M} \quad Z1L_{N,M}
 \end{array}$$

which results in a surface grid point description compatible to the general description method described earlier. We have incorporated in this scheme as an option, a method to fair the tips by simply forcing the surface coordinate at the tip to lie along the chord line.

3.3 Elemental Planar Surface Description

In the description of the rotor blade surfaces and rotor blade wake surfaces we are given surface grid point locations. The surface defined within four control points is a warped surface ideally describing the blade or wake surface. Because of the numerical approximations applied to the integral boundary condition it is necessary to define a planar surface as our control surface element. In a manner similar to that found in Reference 14 we can define a planar element given the four grid point locations.

We assume that the four grid points whose given coordinates are $(x'_i, y'_i, z'_i)_{i=1,2,3,4}$ are numbered clockwise when looking down on the control surface from the external flow field. We can now construct two tangent plane vectors \bar{T}_1 and \bar{T}_2 such that their cross product will define a unit elemental surface normal direction. That is let

$$\bar{T}_k = T_{kx'} \hat{x}' + T_{ky'} \hat{y}' + T_{kz'} \hat{z}' \quad (3.3.1)$$

FOR $k = 1, 2$

where

$$\begin{aligned} \bar{T}_{1x'} &= x'_3 - x'_1 & \bar{T}_{2x'} &= x'_4 - x'_2 \\ \bar{T}_{1y'} &= y'_3 - y'_1 & \bar{T}_{2y'} &= y'_4 - y'_2 \\ \bar{T}_{1z'} &= z'_3 - z'_1 & \bar{T}_{2z'} &= z'_4 - z'_2 \end{aligned} \quad (3.3.2)$$

then $\bar{N} = \bar{T}_2 \times \bar{T}_1$ whose components are

$$\begin{aligned} N_x &= T_{2y}' T_{1z}' - T_{2z}' T_{1y}' \\ N_y &= T_{2z}' T_{1x}' - T_{2x}' T_{1z}' \\ N_z &= T_{2x}' T_{1y}' - T_{2y}' T_{1x}' \end{aligned} \quad (3.3.3)$$

The unit normal \bar{n} is just

$$\bar{n} = \frac{\bar{N}}{|\bar{N}|} = n_x \hat{x}' + n_y \hat{y}' + n_z \hat{z}' \quad (3.3.4)$$

The elemental surface plane can be specified using the known unit normal and a calculated average point $(x_i', y_i', z_i')_{avg}$ taken to be in the plane and calculated as the simple average of the corner point coordinates. In order now to project the given grid points into this elemental plane along the unit normal we first find the distance (H_i) that the i^{th} grid point is removed from the average point. This is given by

$$H_i = (x_{avg}' - x_i') n_x + (y_{avg}' - y_i') n_y + (z_{avg}' - z_i') n_z \quad (3.3.5)$$

Then the projection of the grid point into the plane along the unit normal results in a set of grid projected coordinates $(x_i', y_i', z_i')_{p_i}$ given by

$$\begin{aligned} x_{p_i}' &= x_i' + H_i n_x \\ y_{p_i}' &= y_i' + H_i n_y \\ z_{p_i}' &= z_i' + H_i n_z \end{aligned} \quad (3.3.6)$$

We can now construct an elemental fixed axis system $(\hat{x}, \hat{y}, \hat{z})$ such that the \hat{y} axis is directed along the unit normal (\bar{n}) , the \hat{x} axis is directed along the line joining projected corner point 1 with projected corner point 4 and the \hat{z} axis direction is given by $\hat{y} \times \hat{x}$.

Let vector \bar{T}_{P_2} be given by

$$\bar{T}_{P_2} = T_{P_{2x}} \hat{x}' + T_{P_{2y}} \hat{y}' + T_{P_{2z}} \hat{z}' \quad (3.3.7)$$

where

$$\begin{aligned} T_{P_{2x}} &= x'_{P_2} - x'_{P_1} \\ T_{P_{2y}} &= y'_{P_2} - y'_{P_1} \\ T_{P_{2z}} &= z'_{P_2} - z'_{P_1} \end{aligned} \quad (3.3.8)$$

Then the unit vector \bar{t}_{P_2} is given by

$$\bar{t}_{P_2} = \frac{\bar{T}_{P_2}}{|\bar{T}_{P_2}|} = t_{P_{2x}} \hat{x}' + t_{P_{2y}} \hat{y}' + t_{P_{2z}} \hat{z}' \quad (3.3.9)$$

Let \bar{t}_{P_2} be a unit vector along the \hat{z} axis, then

$$\bar{t}_{P_2} = t_{P_{2x}} \hat{x}' + t_{P_{2y}} \hat{y}' + t_{P_{2z}} \hat{z}' = \bar{n} \times \bar{t}_{P_1} \quad (3.3.10)$$

where

$$\begin{aligned} t_{P_{2x}} &= n_y' t_{P_{1z}} - n_z' t_{P_{1y}} \\ t_{P_{2y}} &= n_z' t_{P_{1x}} - n_x' t_{P_{1z}} \\ t_{P_{2z}} &= n_x' t_{P_{1y}} - n_y' t_{P_{1x}} \end{aligned} \quad (3.3.11)$$

If we now take the origin of the elemental (x', y', z') coordinate system to be at projected corner point (1) then the transformation equation relating the body fixed coordinate system to the elemental coordinate system is given by

$$\begin{pmatrix} x \\ y \\ z \end{pmatrix} = \begin{pmatrix} t_{px'} & t_{py'} & t_{pz'} \\ t_{px''} & t_{py''} & t_{pz''} \\ \eta_{x'} & \eta_{y'} & \eta_{z'} \end{pmatrix} \begin{pmatrix} x' - x_{1'} \\ y' - y_{1'} \\ z' - z_{1'} \end{pmatrix} \quad (3.3.12)$$

During the influence calculations which will be described later it will be necessary to designate one point on this elemental control surface at which the influence is to be calculated. We shall take as this control point the centroid of the elemental surface. It can be shown that the centroid location $(\bar{x}, \bar{y}, \bar{z})_{CG}$ is given by

$$\begin{aligned} \bar{x}_{CG} &= [A_1 \bar{x}_1 + A_2 \bar{x}_2 + A_3 \bar{x}_3 + A_4 \bar{x}_4] / A \\ \bar{y}_{CG} &= [A_1 \bar{y}_1 + A_2 \bar{y}_2 + A_3 \bar{y}_3 + A_4 \bar{y}_4] / A \\ \bar{z}_{CG} &= 0 \end{aligned} \quad (3.3.13)$$

where

$$\begin{aligned} \bar{x}_1 &= \frac{1}{3} x_2 \\ \bar{y}_1 &= \frac{2}{3} y_2 \\ A_1 &= -\frac{1}{2} x_2 y_2 \end{aligned} \quad (3.3.14)$$

$$\begin{aligned} \bar{x}_2 &= x_2 + \frac{1}{3} [x_3 - x_2] \\ \bar{y}_2 &= y_2 + \frac{1}{3} [y_3 - y_2] \\ A_2 &= \frac{1}{2} [x_3 - x_2] [y_3 - y_2] \end{aligned} \quad (3.3.15)$$

$$\bar{f}_3 = f_3 + \frac{1}{3} [f_4 - f_3]$$

$$\bar{g}_3 = \frac{1}{3} g_3 \quad (3.3.16)$$

$$A_3 = \frac{1}{3} g_3 [f_4 - f_3]$$

$$\bar{f}_4 = \frac{1}{3} f_3$$

$$\bar{g}_4 = \frac{1}{3} g_2 \quad (3.3.17)$$

$$A_4 = f_3 g_3$$

$$A = A_1 + A_2 + A_3 + A_4 \quad (3.3.18)$$

3.4 Blade Influence Calculations

We have to this point in the discussion essentially described the geometry of blade one as a set of upper and lower surface grid points. Furthermore, we have presented a method to specify an elemental planar control surface in terms of its location in space with respect to a blade fixed reference system and with respect to its own elemental coordinate system. Therefore, we have the information necessary to compute the influence coefficient of one blade element on another blade element.

In order to make the problem more easily tractable we shall first define a new indexing system for identifying the particular elemental surface. Recall that in the description of blade one we have specified M_{max} span stations, $N_{max U}$ and $N_{max L}$ upper and lower chord stations where grid point $M=1$, $N=1$ corresponds to the root chord at the leading edge of the upper or lower surface, and grid point

$M = M_{max}$, $N = N_{max U}$ corresponds to the tip chord at the trailing edge on the upper surface. If we index the elemental control surface with the indices taken to be the index of the most immediate inboard span station and forward chord station then essentially we can describe the particular elemental control surface as (element) $_{M,N}$. If we define

$$1919 = M_{max} - 1 \quad (3.4.1)$$

$$NN_U = N_{max U} - 1 \quad (3.4.2)$$

$$NN_L = N_{max L} - 1 \quad (3.4.3)$$

then we can state that there are $MM \times NN_U$ elemental control surfaces on the upper blade one surface and likewise, there are $MM \times NN_L$ elemental control surfaces on the lower blade one surface. Because we will be specifying the influence of one element on another element it behooves us to index the elements with a single index. We will identify the elements as $I = 1, I_{max}$ where the elements are numbered consecutively beginning on the upper surface at the root leading edge element and proceeding first chordwise and then spanwise. If $I = I_{max_U}$ is the last element on the upper surface then $I = I_{max_U} + 1$ is taken to be the root leading edge lower surface element and the indexing proceeds to I_{max} in a similar manner to the upper surface. It follows then that for a particular control element specified as (M, N) then in terms of index I we have,

$$I = (M-1)NN_U + N \quad \text{on the upper surface} \quad (3.4.4)$$

$$I = (M-1)NN_L + N + I_{max_U} \quad \text{on the lower surface} \quad (3.4.5)$$

where

$$I_{max_U} = MM \times NN_U \quad (3.4.6)$$

The computation of the blade influence coefficients now proceeds in a straight forward fashion. That is suppose we first define once and for all the I_{max} elemental control surfaces of blade one. Beginning on the upper surface, say elemental surface (M, N) , we can immediately using equation (3.4.4) index this element as elemental

surface I. Now proceeding in a clockwise fashion around the element we define the corner point coordinates as

$$\begin{aligned} X_1' &= X1U_{N,M} \\ Y_1' &= Y1U_{N,M} \\ Z_1' &= Z1U_{N,M} \end{aligned} \quad (3.4.7)$$

$$\begin{aligned} X_2' &= X1U_{N,M+1} \\ Y_2' &= Y1U_{N,M+1} \\ Z_2' &= Z1U_{N,M+1} \end{aligned} \quad (3.4.8)$$

$$\begin{aligned} X_3' &= X1U_{N+1,M+1} \\ Y_3' &= Y1U_{N+1,M+1} \\ Z_3' &= Z1U_{N+1,M+1} \end{aligned} \quad (3.4.9)$$

$$\begin{aligned} X_4' &= X1U_{N+1,M} \\ Y_4' &= Y1U_{N+1,M} \\ Z_4' &= Z1U_{N+1,M} \end{aligned} \quad (3.4.10)$$

Note for the lower surface element we would define the corner point coordinates in a clockwise fashion as

$$\begin{aligned} X_1' &= X1L_{N,M} \\ Y_1' &= Y1L_{N,M} \\ Z_1' &= Z1L_{N,M} \end{aligned} \quad (3.4.11)$$

$$\begin{aligned} X_2' &= X1L_{N+1,M} \\ Y_2' &= Y1L_{N+1,M} \\ Z_2' &= Z1L_{N+1,M} \end{aligned} \quad (3.4.12)$$

$$\begin{aligned}
 X_3' &= X1L_{N+1, M+1} \\
 Y_3' &= Y1L_{N+1, M+1} \\
 Z_3' &= Z1L_{N+1, M+1}
 \end{aligned}
 \tag{3.4.13}$$

$$\begin{aligned}
 X_4' &= X1L_{N, M+1} \\
 Y_4' &= Y1L_{N, M+1} \\
 Z_4' &= Z1L_{N, M+1} .
 \end{aligned}
 \tag{3.4.14}$$

Now using the equations developed in the discussion of the elemental planar surface (section 3.3) we can define all the geometric relations needed for later influence calculations. That is, we develop and save the following parameters for all elements I of blade one:

- A) Transformation matrix relating the primed reference system to the elemental reference system.
- B) Origin of the elemental coordinate system with respect to the primed reference system.
- C) Elemental corner point coordinates with respect to the elemental reference system.
- D) Elemental centroid coordinates with respect to the elemental reference system and with respect to the primed reference system.
- E) Elemental area.

Given now the element I of blade 1 on which we wish to find the influence of element J of blade 1 we would proceed as follows:

- A) Recall the location of the centroid of element I with respect to the (X', Y', Z') reference system, ie $(X', Y', Z')_{CGI}$.

- B) Using the transformation matrix relating the primed reference system to the Jth elemental $(x, y, z)_J$ coordinate system, transform the location of the coordinates $(x', y', z')_{1,1}$ to coordinates $(x, y, z)_{1,1}$.
- C) Given now the corner point coordinates of element J with respect to its coordinate system, ie $(x, y, z)_{1,1}$, calculate using equation (2.6.18) the velocity influence coefficients in the \hat{x} , \hat{y} and \hat{z} direction at point $(x, y, z)_{1,1}$, that is, define $I_{x,J}$, $I_{y,J}$ and $I_{z,J}$.
- D) Since these are the influence coefficients expressed with respect to the Jth elemental coordinate system, transform these coefficients to the (x', y', z') system using the inverse of the transformation matrix of B above such that the final result is in the form of velocity influence coefficients expressed with respect to the primed reference system, that is, $I_{x',J}$, $I_{y',J}$, and $I_{z',J}$.

Since the boundary condition requires us to define the influence coefficients on all I_{max} blade one elements of all elements of all blades $L=1, L_{max}$ we would simply repeat the procedure outlined above for all J elements of blade one, and for exactness, we should replace the Jth subscript above with J_1 to indicate that this represents the influence of the Jth element of blade one on the Ith element of blade one.

In order now to compute the elemental influence coefficients of blades $L \neq 1$ on the elements I of blade one we have to alter the procedure outlined earlier. Note first that we have assumed all rotor

blades are identically described. Thus the J elemental surface of blade $\angle \neq 1$ are similar to the J elemental surfaces of blade $\angle = 1$. Thus, since we are given the geometric parameters defining blade one elements, all that we need to do in order to define the parameters of the J elements of blade $\angle \neq 1$ is to apply a simple transformation involving a rotation of axis about the Z' or $Z1$ axis. The rotation angle is of course the angle between the blade $\angle = 1$ span axis and the blade $\angle \neq 1$ span axis. Once this transformation is accomplished the outlined procedure above may be followed. The final result is then a set of influence coefficients relating the influence of blade L, elemental surface J on the blade one Ith elemental surface centroid. The total influence then of all blade J elements on all I elements can be written with respect to the primed reference system as

$$I_{X'_{I,J}} = \sum_{L=1}^{L_{max}} I_{X'_{I,J_L}} \quad (3.4.15)$$

$$I_{Y'_{I,J}} = \sum_{L=1}^{L_{max}} I_{Y'_{I,J_L}} \quad (3.4.16)$$

$$I_{Z'_{I,J}} = \sum_{L=1}^{L_{max}} I_{Z'_{I,J_L}} \quad (3.4.17)$$

Thus the blade influence coefficients are determined.

3.5 Wake Influence Coefficients

The problem concerned with calculating the wake influence coefficients once the wake geometry is established is essentially the same problem encountered with calculating the blade influence coefficients. For the wake influence, we are concerned with calculating the influence on blade one element I , of a wake element as it leaves the trailing edge and spirals down in a streamwise direction. Since we have shown that the doublet strength remains constant in the wake along a streamline, then we may numerically integrate the influence of streamline segments and sum the results to present the net effect of a particular wake streamline on an element I .

In this problem, because of the numerical approach, we are concerned not with a single wake streamline but rather with a series of adjacent streamlines which leave the rotor blade in finite segments on each of which the doublet strength is a constant given by the difference in upper and lower blade surface trailing edge element doublet strengths. As such we wish now to calculate the influence of spiraling finite width wake segments on blade elements $I=1, I_{max}$.

We will choose to represent the wake as MM spiral segments, each of which trails from one of the J blade trailing edge surface elements previously discussed. In order to demonstrate the feasibility of a lifting rotor surface analysis and to begin the free wake analysis we will choose to model the wake in terms of a prescribed classic wake model. The description of this wake is relatively simple and is used here because of that fact. In no way is this theory limited to such a wake.

From the rotor blade one description we know the M_{\max} trailing edge span station coordinates. These may be expressed in terms of a primed cylindrical coordinate system (r', θ', z') such that the dimensional coordinates are given by

$$(r'_{TEM}, \theta'_{TEM}, z'_{TEM}) \quad \text{FOR } M=1, M_{\max}. \quad (3.5.1)$$

It follows then that the streamline leaving the trailing edge at any of these span stations will follow a helical path, the equation of which is expressed in terms of a parameter z' as follows,

$$\begin{aligned} r'(z') &= r'_{TEM} = \text{constant} \\ \theta'(z') &= \theta'_{TEM} - \omega_z'(z' - z'_0) \\ z'(z') &= z'_{TEM} - v_z'(z' - z'_0) \end{aligned} \quad (3.5.2)$$

where ω_z' is a constant rotational rate taken as positive in the usual sense about the z' axis, and v_z' is a constant velocity taken as positive along the z' axis. If the distances are nondimensionalized in the usual sense using the blade radius (R), and the velocities are nondimensionalized using the rotor rotational tip speed $(\omega_z R)$, then the above set of equations becomes

$$\begin{aligned} r'(z') &= r'_{TEM} = \text{constant} \\ \theta'(z') &= \theta'_{TEM} - \Delta\theta' \\ z'(z') &= z'_{TEM} - v_z' \Delta\theta' \end{aligned} \quad (3.5.3)$$

where

$$\Delta\theta' = \omega_z'(z' - z'_0). \quad (3.5.4)$$

In this analysis we will take the velocity (v_z') to be the sum of the rotor climbing speed and a specified constant increment downwash such that the sum represents an average constant momentum downwash expressed with respect to the blade fixed reference system.

Having established these equations it is now a simple matter to describe the wake in terms of elemental surfaces just as was done for the blade surface. We will define the wake as consisting of MM spiral segments such that the Mth spiral wake segment has as its origin the trailing edge segment lying between trailing edge grid points M and M+1. Each spiral wake segment's influence then on blade one element I will be calculated as the sum of a finite number of trailing segments derived by incrementing the wake's displacement from the blade in terms of the parameter $\Delta\theta'$. The same procedure as outlined in the blade influence coefficients section 3.4 is followed with the result being expressed as a set of influence coefficients expressed in terms of the primed (x', y', z') reference system as $I_{x',I,M}$, $I_{y',I,M}$, $I_{z',I,M}$ where $I_{x',I,M}$ is the influence coefficient in the x' direction, derived from the influence on blade one element I of the wake M segments trailing the $L_{x,M}$ number of blades from the Mth trailing edge elemental surface.

In the actual computation scheme the wake influence calculations are terminated depending on one of the following constraints:

- A) After a finite number of wake turns are completed.
- B) After the influence coefficient on a specific blade element I has reached a value less than a specified percentage amount of a close blade wake element.

C) After a specified absolute number of wake influence

- calculations are performed.

The size of the wake elements are determined by the length of the trailing edge span station grid points and the angular measure $\Delta\theta'$. An option is included in the program to allow $\Delta\theta'$ to be specified as a certain value until a given number of wake turns are completed at which time $\Delta\theta'$ will take on a second specified value. This allows for finer wake elemental control surfaces to be specified in the wake region near blade one and coarser wake elemental control surfaces to be specified in the far wake region.

3.6 Generation of the Set of Surface Boundary Conditions and the Numerical Solution

To this point in the discussion the determination of the geometry of the blade and wake system and the analysis of the entire set of influence coefficients have been presented. We are concerned now with the actual formulation of the set of surface boundary conditions. Using the results of the previous two sections we may write the induced normal velocity on the centroid of a blade element I as

$$\bar{V}'_{ind I} \cdot \bar{n}_I = \sum_{J=1}^{J_{max}} -\frac{\mu_J}{4\pi} I_{N I, J} + \sum_{M=1}^{MM} -\frac{\mu_M}{4\pi} I_{N I, M} \quad (3.6.1)$$

where, except for the doublet strength, everything else is analytically determined. The first summation term represents the blade induced velocities and the second summation term represents the wake induced velocities. The element I unit normal \bar{n}_I expressed with respect to the primed coordinate system has been previously determined.

$I_{N I, M}$ represents the normal influence coefficient obtained by vectorially dotting the respective vector primed influence coefficient with the unit normal \bar{n}_I .

Once the doublet strengths have been calculated, the surface velocity potential is computed using equation (2.4.6). The induced surface velocity is then computed by

$$\bar{V}'_{ind} = \frac{\partial \phi}{\partial s} \hat{s}, \quad (3.6.2)$$

where $\frac{\partial}{\partial s}$ represents the tangential surface derivative.

It was shown earlier that the primed free stream velocity on the centroid of an element I can be written as

$$\bar{V}'_{\infty I} = - [\bar{\omega} \times \bar{R}'_{C_I} + \bar{V}_T] \quad (3.6.3)$$

where $\bar{\omega}$ is the rotor rotational rate ($\omega_z \hat{z}'$), \bar{V}_T is the rotor climb velocity ($V_T \hat{z}'$), and \bar{R}'_{C_I} is the primed vector to the centroid of element I. Now $\bar{\omega}$, \bar{V}_T and \bar{R}'_{C_I} are known, thus $\bar{V}'_{\infty I}$ is determined and it follows then that the primed free stream velocity normal to the surface element I given by

$$V'_{\infty N_I} = \bar{V}'_{\infty I} \cdot \bar{n}_I \quad (3.6.4)$$

is determined.

Substituting these results into equation (3.6.2) it follows then that the set of I_{mat} surface boundary conditions to be satisfied is given by

$$\sum_{J=1}^{I_{mat}} -\frac{\gamma_I}{4\pi} I_{N_I, J} + \sum_{M=1}^{MM} -\frac{\gamma_M}{4\pi} I_{N_I, M} = -V'_{\infty N_I} \quad (3.6.5)$$

For $I=1, I_{mat}$.

Since γ_M was shown in section 3.5 to be related to specific γ_I values the set of equations above are in fact in the form generally given by

$$[A] \times 1 = |B| \quad (3.6.6)$$

where the matrix A is an $I_{max} \times I_{max}$ square matrix, X is a I_{max} column matrix and B is an I_{max} column matrix. We have identified

$$X_J = - \frac{A_J}{A_I} \quad (3.6.7)$$

$$B_I = - V_{00}^I H_I \quad (3.6.8)$$

The solution to the I_{max} simultaneous set of linear algebraic equations is carried out numerically by either of two methods depending on the program option selected. One method employs the Gaussian elimination scheme with pivoting. This method, which is discussed completely in Reference 17, is an exact solution method whose scheme of operation is to successively convert the defined matrix into a matrix of one less row and column until in effect an upper triangular matrix results. The solution is obtained then by a back substitution scheme. Interchanging of rows is done in order to make the pivot diagonal terms dominate which is a condition necessary to ensure accuracy.

A second method chosen to obtain a solution to the set of equations is an iterative approximate method known as "The Method of Simultaneous Displacement for Linear Systems". A complete discussion of this method is presented in Reference 18. In essence, however, this scheme involves expressing the I_{max} linear equations in the form

$$IXI = [B]IXI + [C] \quad (3.6.9)$$

where B is an I_{max} square matrix and C is the given column matrix. An initial approximation vector is taken as

$$X_I^0 = 0 \quad \text{FOR ALL } I=1, I_{max}. \quad (3.6.10)$$

Successive approximations X_I^k are generated by the iteration

$$X_I^{k+1} = \sum_{J=1}^{I-1} U_{I,J} X_J^{k+1} + \sum_{J=I}^{I_{max}} U_{I,J} X_J^k + C_I. \quad (3.6.11)$$

This continues until the criterion

$$\frac{|X_I^{k+1} - X_I^k|}{|X_I^{k+1}|} < \epsilon \quad \text{FOR ALL } I=1, I_{max} \quad (3.6.12)$$

is satisfied.

In actual practice the iterative scheme is the solution of choice for large sets of simultaneous equations. This point will be discussed in a later discussion section.

3.7 Determination of the Velocities, Pressures, and Forces

Once the solution in terms of the doublet strengths are known it is a simple matter to determine the induced primed velocity on all blade one elements using equation (3.6.2). The pressure coefficient at the centroid of element I is then given by

$$C_{P_I} \equiv \frac{P_I - P_\infty}{\frac{1}{2} \rho (WR)^2} = \lambda^2 + \rho'_{CH_I} - \bar{v}'_{ind_I} \cdot \bar{v}'_{ind_I} \quad (3.7.1)$$

where λ is taken here to be the ratio of the rotor climb speed to the tip speed (WR) .

The non-dimensional force acting on any element I is given by

$$F_{S'_I} \equiv \frac{FORCE_I \hat{S}'_I}{\frac{1}{2} \rho (WR)^2 R^2} = - C_{P_I} \rho_I n_{S'_I} \hat{S}'_I \quad (3.7.2)$$

where \hat{S}'_I is any \hat{x}'_I , \hat{y}'_I or \hat{z}'_I direction.

The non-dimensional plane of rotation torque acting on any element I is given by

$$Q_I \equiv \frac{TORQUE_I}{\frac{1}{2} \rho (WR)^2 R^3} = - [F_{x'_I} y'_{CH_I} + F_{y'_I} x'_{CH_I}] \quad (3.7.3)$$

The total rotor axial thrust coefficient is given by

$$C_T \equiv \frac{TOTAL THRUST}{\rho (WR)^2 \pi R^2} = \frac{L_{max}}{2\pi} \sum_{J=1}^{I_{max}} F_{z'_I} \quad (3.7.4)$$

Similarly the total rotor torque coefficient is given

$$C_R \equiv \frac{\text{TOTAL TORQUE}}{\rho CWR^2 (\pi R^2) R} = \frac{L_{max}}{2\pi} \sum_{I=1}^{I_{max}} Q_I . \quad (3.7.5)$$

This concludes the step by step discussion of the solution scheme.

As a way of a short summary at this point we have shown how if we are given

- A) The rotor geometry including specific surface grid points.
- B) The rotor non-dimensional climb ratio, $\lambda = \underline{V_T} / \omega R$
- C) Some prescribed wake geometry specifically taken in the

previous discussion to be a simple classical helix shape then we can calculate the pressure, velocities, and forces acting on the blade.

CHAPTER 4. DISCUSSION OF THE COMPUTER PROGRAM

4.1 General Description

In order to demonstrate the feasibility of this lifting surface theory and its application to the prediction of rotor blade flow field analysis a computer program was written. The theory as described in the previous sections is a relatively straightforward theory, however, its application becomes rapidly complicated due to the geometry and large system of elemental control surfaces necessary for accurate results.

As a means of perceiving the extent of the problem we may consider at this point a reasonable end problem that we might wish the computer program and computer to handle.

Suppose we are given a two bladed rotor system whose geometry is specified along 16 span stations, 21 upper surface chord stations and 21 lower surface chord stations. This implies that we will eventually describe the three component vector velocities on 600 basic elemental surfaces. We have seen that the description of each elemental surface alone requires at least 25 parameters which for this posed problem means a total of 15,000 such parameters. The blade influence calculations alone total 720,000. If we describe the wake with a total of 1155 basic wake elements we require a total of 1,386,000 wake influence calculations to be performed. The simultaneous set of equations to be solved is a 600 x 600 system.

The computer program was run for this problem and will accommodate up to 2000 basic blade elements which is the critical size determining factor. It should be obvious that the constraints to this type of

computer solution will be the available size of the main core computer storage and the computational speed of the computer itself.

The program was designed to be run on West Virginia University's IBM 360 Model 75 computer. The greatest amount of computer core storage required at any one time is 240,000 bytes with 4 bytes being required for a word length. The program requires a minimum of three accessible external storage devices with at least two of these devices being a high speed storage device. At WVU this requirement was met by using the system disc files with two standard length nine track tapes being used for permanent storage. Seven track tape devices are incompatible with the program as written. The program itself is written in FORTRAN IV language and was compiled on the IBM FORTRAN G version compiler. The program is a research orientated program and does not necessarily reflect the most optimum design orientated program, that is, it contains various checks and options which are not absolutely necessary to the program solution. We recognize also that there exist areas in the program in which the exact analytic expressions may be approximated and advantage of these time saving methods have been used in this program. However, it is the intent of this program not to incorporate all these features at this time. The philosophy under which we have written this program is to make it as exact a numerical scheme as possible so that if an infinite number of control elements were taken the solution would be as exact as possible within the confines of any incompressible potential flow analysis.

The program is designed on a modular basis with each module being designed on the premise that given certain input information it is

the purpose of that module then to specifically calculate a certain aspect of the overall problem and to supply certain output information. The advantage here is that it allows for easy internal modification by simply replacing this module with another. The actual sharing of information is done for the most part through the use of common machine storage centers. In this way the amount of in core storage necessary is minimized as storage locations are used at different times for different parameters.

4.2 Specific Program Description

The overall program is subdivided into seven main programs identified as follows:

1. MAIN - INFLUENCE COEFFICIENTS
2. MAIN - CREATE SOLUTION FILE
3. MAIN - SOLVE BY ELIMINATION
4. MAIN - SOLVE BY ITERATION
5. MAIN - TRANSFER SOLUTION FILE
6. MAIN - VELOCITY CALCULATIONS
7. MAIN - PRINT

The purpose of each program is generally indicated by the assigned name. The Print program is actually an auxiliary program whose sole purpose is to retrieve additional non-essential information stored on the two permanent files. It was used during the program check procedures to study individual elemental influence coefficients.

The reason a series of main programs are used rather than one single main program is because the overall program logically divides itself into these areas and secondly we can minimize the amount of external storage devices and internal core storage required during any one series of computational steps thereby allowing for the computer to be run in a time sharing mode as is common procedure at most installations. A general computer program flow diagram is given in Figure 4 indicating the major steps in the program. The solid lines indicate continuation to the next step with the broken lines indicating continuation into another main program.

In Appendix D we have discussed the internal structure of the program at the level of the subroutine. Basically we have presented each subroutine as an entity and described its function and options. Except for the MAIN-INFLUENCE CALCULATIONS program, the actual program operation is straightforward. We have presented a detailed flow diagram for the MAIN-INFLUENCE CALCULATIONS program in order to serve as an aid in discussing this program operation in terms of its various options. We have also included in Appendix D a discussion of the input procedures and output information.

CHAPTER 5. RESULTS AND CONCLUSIONS

In this section we will present a summary of the results of two major case studies. These cases were chosen so as to verify the mathematical model and the computer program for the case of a prescribed wake model. Recall that the present work is not directly concerned with the force free wake analysis which, in fact, would require subsequent wake iterative computer runs to be made for each of the cases presented. The results presented here thus represent the starting or zeroth order solution to the overall rotor analysis. Subsequent solutions will, however, make use of the same program with the prescribed wake geometry having been predicted from the previous program solution.

In Table 1 we have presented a summary of the rotor description, elemental blade surface description, elemental wake surface description and free stream conditions as used in the first case study. This single bladed rotor system does not correspond to any real rotor system but was chosen because its analysis requires a relatively small number (160) of basic elemental surfaces for each blade description. Figure 5 attempts to visualize the density distribution of the elemental surfaces which describe the rotor blade surface. This plot is a planform projection of the symmetrically described 80 upper and 80 lower elemental surfaces. We have spaced the elemental surfaces more closely in those regions where we expect the pressure to vary most rapidly. The rotor hub radius of this two bladed system is taken to be 90% of the rotor radius, thus, the rotor blade occupies the outboard 10%. In Figures 6 through 9 we have presented a plot of the pressure coefficients vs.

chord station at each of the four span segments as identified on Figure 5. The pressure coefficient is defined on the basis of the rotor rotational tip speed squared and each point plotted represents an elemental centroid point at which the normal surface boundary condition was satisfied. These plots represent a realistic chordwise variation in pressure and show the three dimensional character of the flow near the rotor blade tips. In Table 2 we have summarized the computer time required for this case.

In order to more clearly show the three dimensional effects we studied the same two bladed rotor system as described above except that the geometric pitch angle at all span positions was now taken to be zero degrees. All other conditions remained the same as given in Table 1. This analysis thus corresponds to a three dimensional non-lifting potential flow thickness problem and as such no wake analysis was performed. Figure 10 is a plot of the surface velocity vs. chord station. The surface velocity here plotted is the velocity at each of the elemental centroid locations of the tip span segment (span segment 4 of Figure 5) divided by the local free stream velocity given by

$\bar{\omega} \times \bar{R}'$ where \bar{R}' is the position vector to the elemental centroid from the blade center of rotation. On this plot is also shown two-dimensional, zero angle of attack, NACA 0012 sectional, potential flow derived surface velocities non-dimensionalized by the free stream velocity as given in Reference 19. Only the upper surface velocities are plotted since the velocities are the same on the lower surface for this symmetric airfoil. Note that the three dimensional blade velocities are less in magnitude than the comparable sectional airfoil

velocities and the velocity curve defined by the rotor blade points has a near zero slope over much of the chord distance. These differences represent here the change in flow character between a three dimensional body executing a constant rotating motion compared to a two dimensional body executing a constant translatory motion. The fact that the rotor velocity ratio does not equal the two dimensional result is due to the three dimensional divergence effect on the flow over this small blade segment.

The second major case study is an analysis of an actual rotor system for which experimental surface pressure data is available (reference 20). In Table 3 we have presented a summary of the rotor description, elemental blade surface description, elemental wake surface description and free stream conditions as used in this second case study. The density distribution of the planform projected elemental surfaces is shown in Figure 11. Note that there are on each of the two blades 600 basic blade elemental surfaces symmetrically distributed on the upper and lower blade surfaces along the 15 identified span segments. The surface elements are more concentrated near the leading edge where we expect the surface pressure to vary most rapidly. In Figures 12 through 22 we have plotted the difference in the upper and lower surface pressure coefficient vs. the chord station at 11 selected span stations. Each point plotted represents the pressure coefficient difference obtained at two respective elemental centroid locations where the normal surface boundary condition was satisfied. The pressure coefficient is defined here on the basis of the rotor rotational tip speed squared. In order to better appreciate the chordwise and spanwise pressure variation

we have presented in Figure 23 a composite curve again showing the pressure difference vs. chord station at the same selected span stations in dimensional units. Figure 24 presents an experimentally determined plot of the absolute upper and lower surface pressure difference on the same rotor as a function of chord station at various span stations. This figure is a tracing of a figure presented in reference 20, in which the pressure difference was obtained experimentally at 6 chord stations at each of 8 span selected stations. Notice that the same scales have been used for both curves in order to facilitate comparison between the theoretical and experimental results. The span stations do not correspond however, so care should be taken when comparing specific values. There is a very close similarity in the distribution of the chordwise pressure between the experimentally measured and computed results. Since pressure taps were not located near the nose of the experimental rotor the authors of reference 20 rounded off their curves rather abruptly in these regions which probably contributed to their not checking as closely the integrated experimental force measurements with the test stand value. It is interesting to note that both the experimental and theoretical results show qualitatively similar losses in pressure near the tip.

The integrated results of Figures 23 and 24 are shown in Figure 25. This figure shows a comparison of the spanwise loading distribution between the experimental results and the theoretical calculations. The agreement is remarkably close in view of the fact that the classical prescribed wake was used for the theoretical lifting surface calculations. As shown in reference 21, the prescribed classic wake tends to predict higher thrust coefficients than the experiment shows. This reference also

points out that force free wakes reduce the spanwise loading over the classic wake prediction. The present results are therefore, in agreement and it is anticipated that the inclusion of a force free wake program will bring the theory into better agreement. The computed thrust coefficient for this case was $C_T = 0.0044$ compared to the experimental value of $C_T = 0.0038$. Therefore the classic rigid wake theoretical result was approximately 15% high. The corresponding theoretical torque coefficient was computed to be $C_Q = 0.00011$ for this case.

Figures 26 and 27 present plots of the predicted relative surface velocity direction on the upper and lower rotor surfaces respectively for case 2. In these plots we have forced the rotor surface to conform to the plane of the figure. The direction of the local surface velocities are shown drawn as a constant length vector from a series of surface control points which approximate selected elemental centroid locations. The plots are essentially comparable to what would result from an experimental flow visualization tuft study. The figures clearly show the three dimensional nature of the flow on the rotor blade surface. Note the circular nature of the flow which is evident at all span stations but which is most prominent at inboard span segments. This result is, of course, expected since the free stream component is truly circular ($V_{\infty}' = -\bar{\omega} \times \bar{R}'$). However, if one studies these results more clearly it becomes evident that the induced velocity component does alter the flow direction. If we restrict the following discussion to the induced spanwise surface velocity component the results show that beyond approximately the 50% span station the induced velocity is directed inboard. Inboard to the 50% span station the induced velocity is

directed outboard at surface points forward of the quarter chord approximately and inboard beyond the quarter chord. The flow deviation between the top and bottom surfaces near the tip trailing edge is of interest. The flow leaves the top surface trailing edge at approximately a 20 degree difference from the corresponding flow leaving the bottom surface. The directions indicate that the shed vortex sheet is already beginning to roll up. In Table 4 we have summarized the computer time required for each of the major steps in the execution of this 600 case study.

From the summary of results presented we conclude that the lifting surface theory as developed is applicable to rotor system analyses. Furthermore the application of this theory is feasible. The results, however, are highly dependent on the prescribed wake model used in the analysis and use of the classical wake model is insufficient to yield accurate results. It appears that the prescribed wake geometry must be similar to the actual free wake geometry in order to obtain accurate loading results.

There is a lack of experimental data or theoretical analyses which would help us confirm the theory developed here. To the authors' knowledge there exist very little available literature giving rotor blade surface velocities and directions and loading measurements on an rotating rotor system. The conclusions we have drawn above have as a necessarily assumed the present theory and application to be . The general potential theory certainly has been proven by past application on planar body motion analyses and we have systematically checked all application procedures in order to ensure accuracy.

CHAPTER 6. EXTENSIONS

The theory and formidable program presented in essence completes the basic approach to theoretically analysing a lifting rotor using potential lifting surface theory. Much work needs to be done, however, before the application of this theory can be used routinely for rotor design analysis. We recognize that extensions to this work should proceed along two major routes. One major route of study should be concerned with the wake. At present the program (not the theory) uses a classical helix wake washed away at some constant velocity from the rotor blades. As is noted by various authors (explicitly cited earlier in the report) the wake geometry plays a major role in determining blade surface velocities. Obviously a more accurate prescribed wake representation needs to be incorporated. At the present time we are extending this work in order to incorporate a theoretical force free wake analysis. This extension is to be accomplished by predicting a new wake geometry configuration based upon the solution obtained by this present work. In this manner successive solutions will be obtained by iteration on the wake geometry such that the force free wake solution will result.

A second major area where further extensions to this work is needed is in the area of reducing the required computer time. This may be practically accomplished in basically two ways, that is, first reduce the total number of influence calculations to be performed and, second, reduce the time required for each set of influence calculations. The former may best be accomplished by further studying

the individual wake elemental influence and optimizing, based on this study, the actual extent and elemental description of the wake itself. The latter above may best be accomplished by using approximate relations to describe the influence coefficients at a far removed surface point instead of using the exact relations which require perhaps twice as much computer time. The numerical results shown here have already incorporated this simplification in the program.

There are of course other means to reduce the required computer time. Linearizing the surface boundary condition would reduce the time required. Furthermore, incorporating an experimentally determined wake geometry would result in a substantial overall computer time reduction. This type of extension would make the present work suitable for studies on existing rotor systems but not necessarily applicable to new configuration rotor systems.

With the advances being made in computer technology, especially in the areas of increasing core storage coupled with the extensions above, it does appear that this rotor lifting surface theory will allow the aerodynamicist to perform a completely theoretical design analysis of any given rotor system.

The problem which remains to be analysed is the problem posed by a helicopter which is climbing as well as advancing perpendicular to its axial climb direction. The analysis of this rotor system requires an unsteady analysis as the blade loadings now become functions of the blade azimuth position thereby increasing the number of unknowns in the problem. The theory is simply an extension to the present problem, however, the actual solution scheme becomes rather complex.

REFERENCES

1. Multhopp, H., "Methods for Calculating the Lift Distribution of Wings (Subsonic Lifting Surface Theory)", ARC R&M 2884, 1955.
2. Verbaugh, P. J., "Unsteady Lifting Surface Theory for Ship Screws", Hydronautics - Europe, Technical Report No. 9, October 1965.
3. Hess, J. L. and Smith, A. M. O., "Calculation of Potential Flow about Arbitrary Bodies", Progress in Aeronautical Sciences, Vol. 8, Pergamon Press, New York, 1966.
4. Johnson, W., "Application of a Lifting-Surface Theory to the Calculation of Helicopter Airloads", AHS 27th Annual Forum, No. 510, May 1971.
5. Erickson, J. C., "A Continuous Vortex Sheet Representation of Deformed Wakes of Hovering Propellers", Proceedings of Third CAL/AVLABS Symposium on Aerodynamics of Rotary Wing and VTOL Aircraft, Vol. I, June 1969.
6. Landgrebe, A. J., "An Analytic Method for Predicting Rotor Wake Geometry", AIAA/AHS VTOL Research Design and Operations Meeting, AIAA Paper No. 69-196, February 1969.
7. Erickson, J. C. and Hough, G. R., "On the Fluctuating Flow Field of Propellers in Cruise and Static Operation", Submitted to AIAA J of Aircraft, January 1969.
8. Rorke, J. B. and Wells, C. D., "The Prescribed Wake-Momentum Analysis", Proceedings of Third CAL/AVLABS Symposium on Aerodynamics of Rotary Wing and VTOL Aircraft, Vol. I, June 1969.
9. Clark, D. R. and Leiper, A. C., "The Free Wake Analysis", AHS 25th Annual Forum, Paper No. 321, May 1969.
10. Ellis, C. W., "Recommendations for Future Aerodynamic Research", Proceedings of Third CAL/AVLABS Symposium on Aerodynamics of Rotary Wing and VTOL Aircraft, Vol. III; June 1969.
11. Carter, E. S., "Now is the Time for Aerodynamics to Come to the Aid of the Hardware", Proceedings of Third CAL/AVLABS Symposium on Aerodynamics of Rotary Wing and VTOL Aircraft, Vol. III, June 1969.
12. Djojodihardjo, R. H., "A Numerical Method for the Calculation of Nonlinear Unsteady Lifting Potential Flow Problems," Sc.D. Thesis, MIT, Dept. of Aeronautics and Astronautics, October 1968.

13. Djojodihardjo, R. H. and Widnall, S. E., "A Numerical Method for the Calculation of Nonlinear Unsteady Lifting Potential Flow Problems", AIAA 7th Aerospace Sciences Meeting, AIAA Paper No. 69-23, January 1969.
14. Hess, J. L. and Smith, A. M. O., "Calculation of Non-Lifting Potential Flow about Arbitrary Three-Dimensional Bodies", Douglas Aircraft Report No. ES 40622, pp. 66-73, March 1962.
15. Bois, G. Petit, Tables of Indefinite Integrals, p. 67 (6b), Dover Publications, Inc., New York, 1961.
16. Refer to Reference 14, above, p. 44.
17. Conte, S. D., Elementary Numerical Analysis, pp. 156-162, McGraw-Hill, New York, 1965.
18. Refer to Reference 17 above, pp. 191-197.
19. Abbott, I. H. and Doenhoff, A. E., Theory of Wing Sections, p. 321, Dover Publications, Inc., New York 1958.
20. Meyer, J. R. and Falabella, G., "An Investigation of the Experimental Aerodynamic Loading on a Model Helicopter Rotor Blade", NACA TN 2953, May 1953.
21. Bellinger, E. Dean, "Experimental Investigation of Effects of Blade Section Camber and Planform Taper on Rotor Hover Performance," United Aircraft Research Laboratories, Report No. K 911076-14, January 1972.

BIBLIOGRAPHY

1. Van de Vooren, A. I., Numerical Methods for Solving Fluid Flow Problems, Course given at WVU, Dept. of Aerospace Engineering, 1969-70.
2. van de Vooren, A. I., "Some Additions to Lifting Surface Theory", Mathemateich Instituut, Universiteit Groningen, Report TW-35.
3. Mil, M. L. et al.; "Helicopters - Calculation and Design, Volume I Aerodynamics", NASA TT F-494, September 1967.
4. Ashley, H., Windall, S., and Landahl, M., "New Directions in Lifting Surface Theory", AIAA J., Vol. 3, No. 1, January 1965.
5. Bradley, R. G. and Miller, B. D., "Lifting Surface Theory - Advances and Applications", AIAA 8th Aerospace Sciences Meeting, AIAA Paper No. 70-192, January 1970.
6. Jenney, D. S., Olson, J. R. and Landgrebe, A. J., "A Reassessment of Rotor Hovering Performance Prediction Methods", AHS 23rd Annual Forum, Paper No. 100, May 1967.
7. Sopher, R., "Three-Dimensional Potential Flow Past the Surface of a Rotor Blade", AHS 25th Annual Forum, May 1969.
8. Mandl, P., "Analytic Determination of the Axial Velocity through a Propeller Moving Perpendicular to its Axis", AGARD Conference Proceedings No. 22, September 1967.
9. Cummings, D. E. and Kerwin, J. E., "Propeller Wake Deformation Due to Instability of a Trailing Vortex Sheet", Proceedings of Third CAL/AVLABS Symposium on Aerodynamics of Rotary Wing and VTOL Aircraft, Vol. I, June 1969.
10. Sadler, S. G., "A Method for Predicting Helicopter Wake Geometry, Wake-Induced Flow and Wake Effects on Blade Airloads", AHS 27th Annual Forum, May 1971.
11. Landgrebe, A. J., "The Wake Geometry of a Hovering Helicopter Rotor and its Influence on Rotor Performance", AHS 28th Annual Forum, Paper No. 620, May 1972.
12. Gessow, A. and Myers, G. C., Aerodynamics of the Helicopter, Third Printing, Frederick Ungar Publishing Co., New York, 1967.
13. Gray, R. B., Series of Helicopter Courses given at Georgia Tech, 1966-67.

FIGURES

AXIS CONVENTION RELATING THE POTENTIAL AT
A FIELD POINT INDUCED BY A
DOUBLET SURFACE DISTRIBUTION

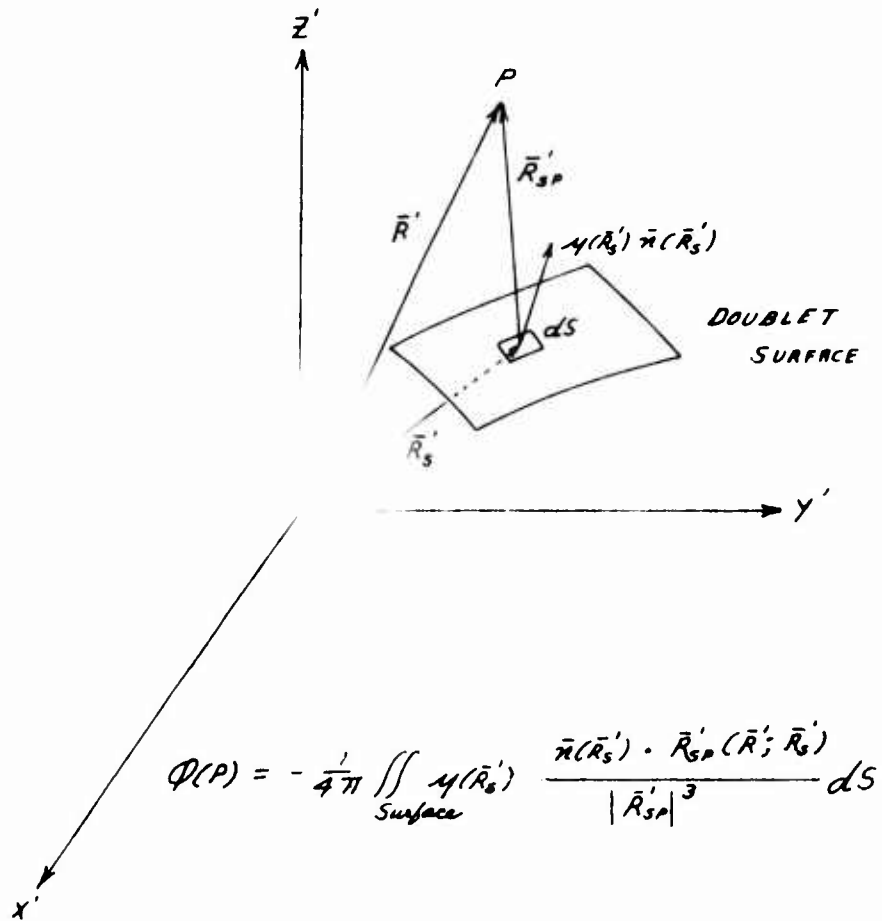


FIGURE 1

ROTOR SYSTEM AXIS CONVENTION

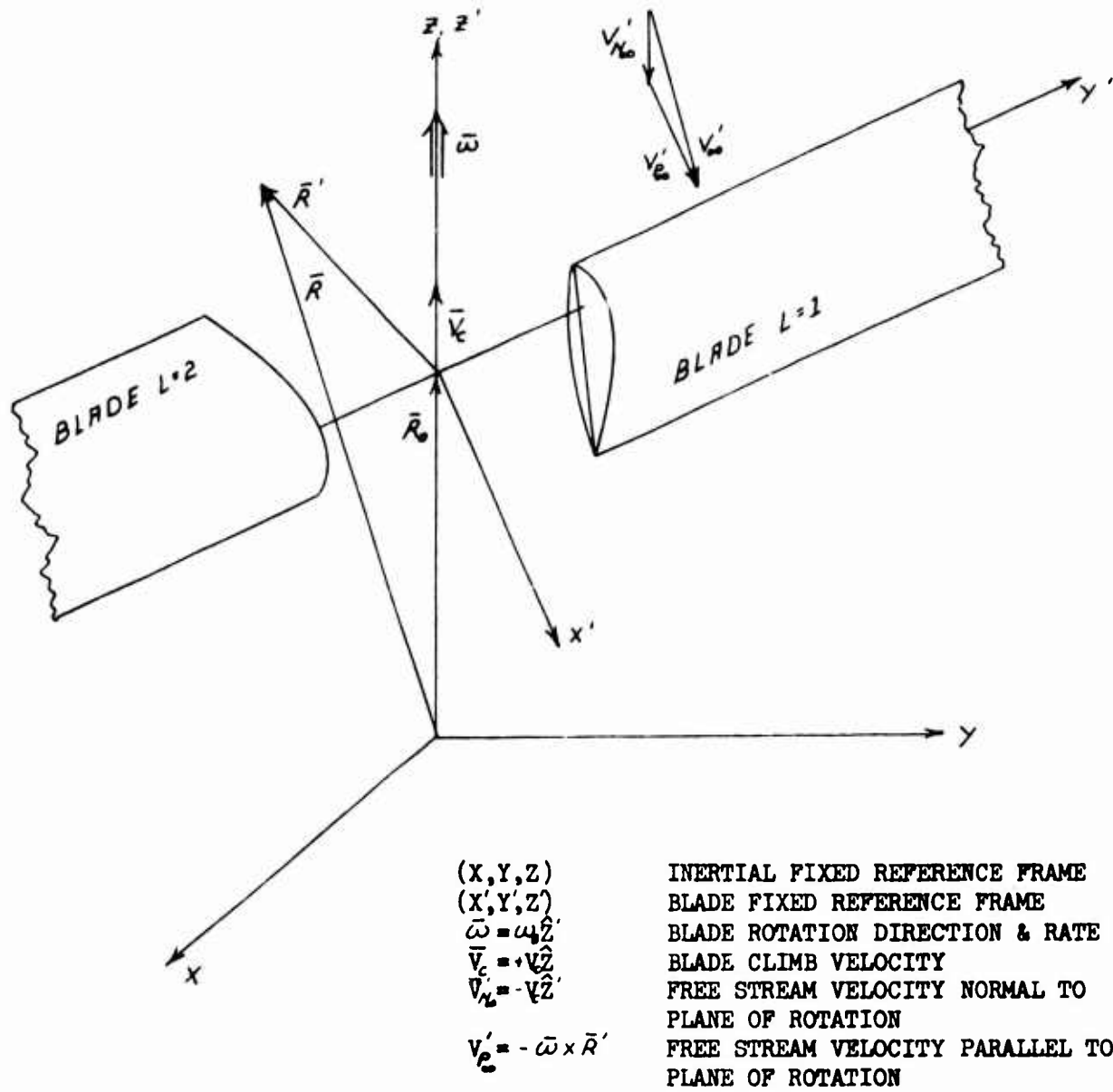


FIGURE 2

ROTOR BLADE AXIS CONVENTION

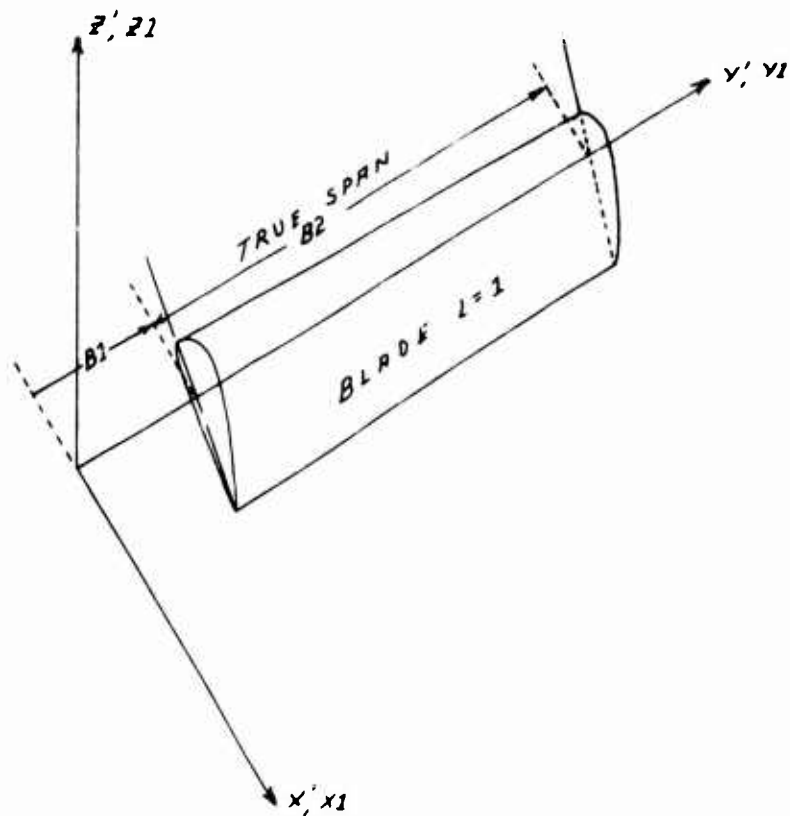


Figure 3a: Lifting Attitude of Blade

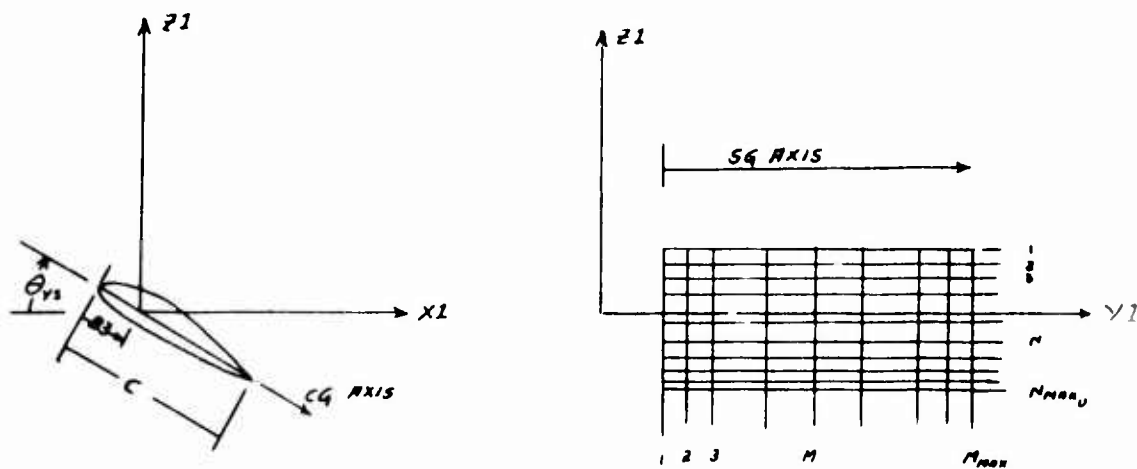
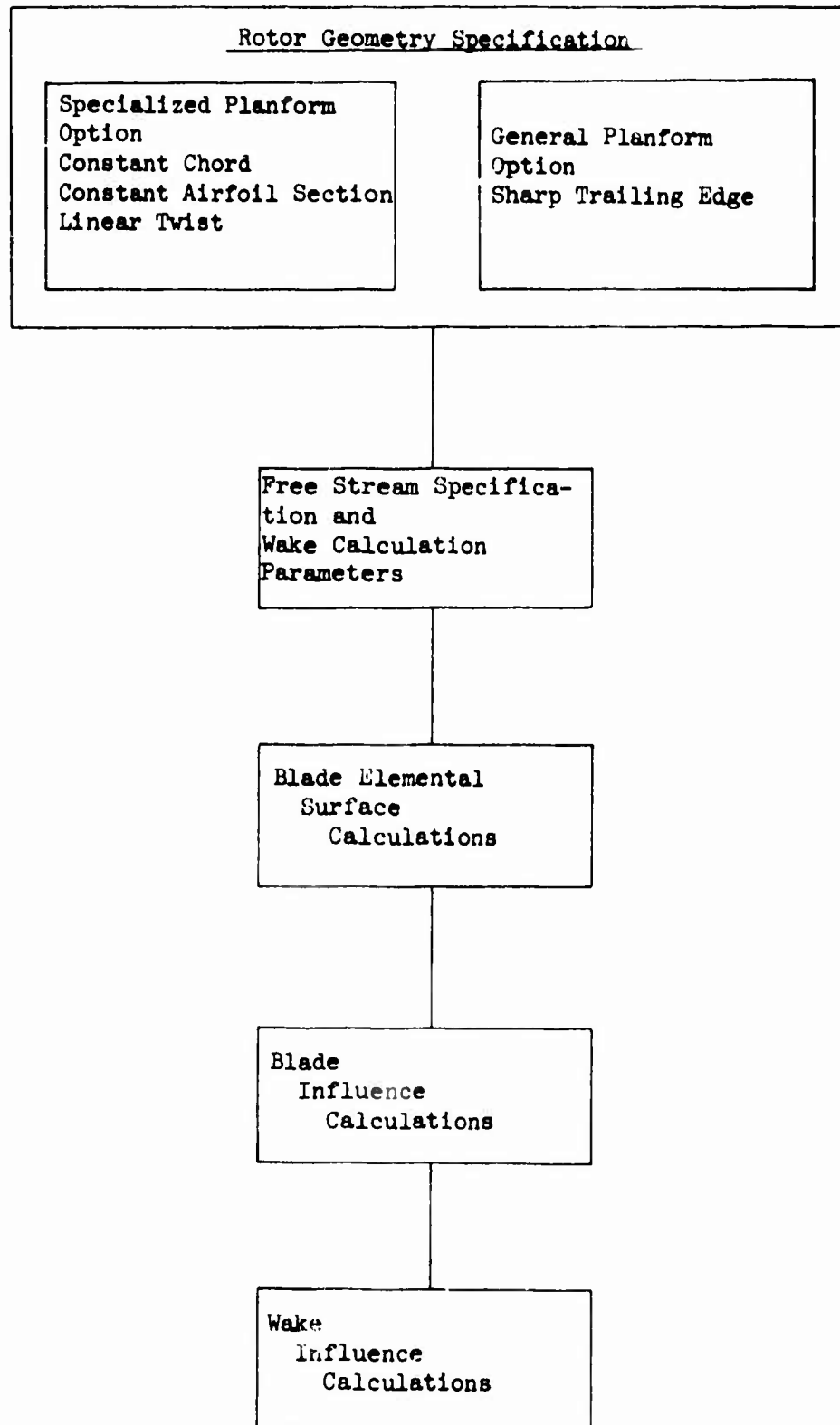


Figure 3b: Geometric Pitch & Grid Network

FIGURE 3

COMPUTER PROGRAM FLOW DIAGRAM



(Continued on next page)

FIGURE 4 (a)

COMPUTER PROGRAM FLOW DIAGRAM

(Continued from previous page)

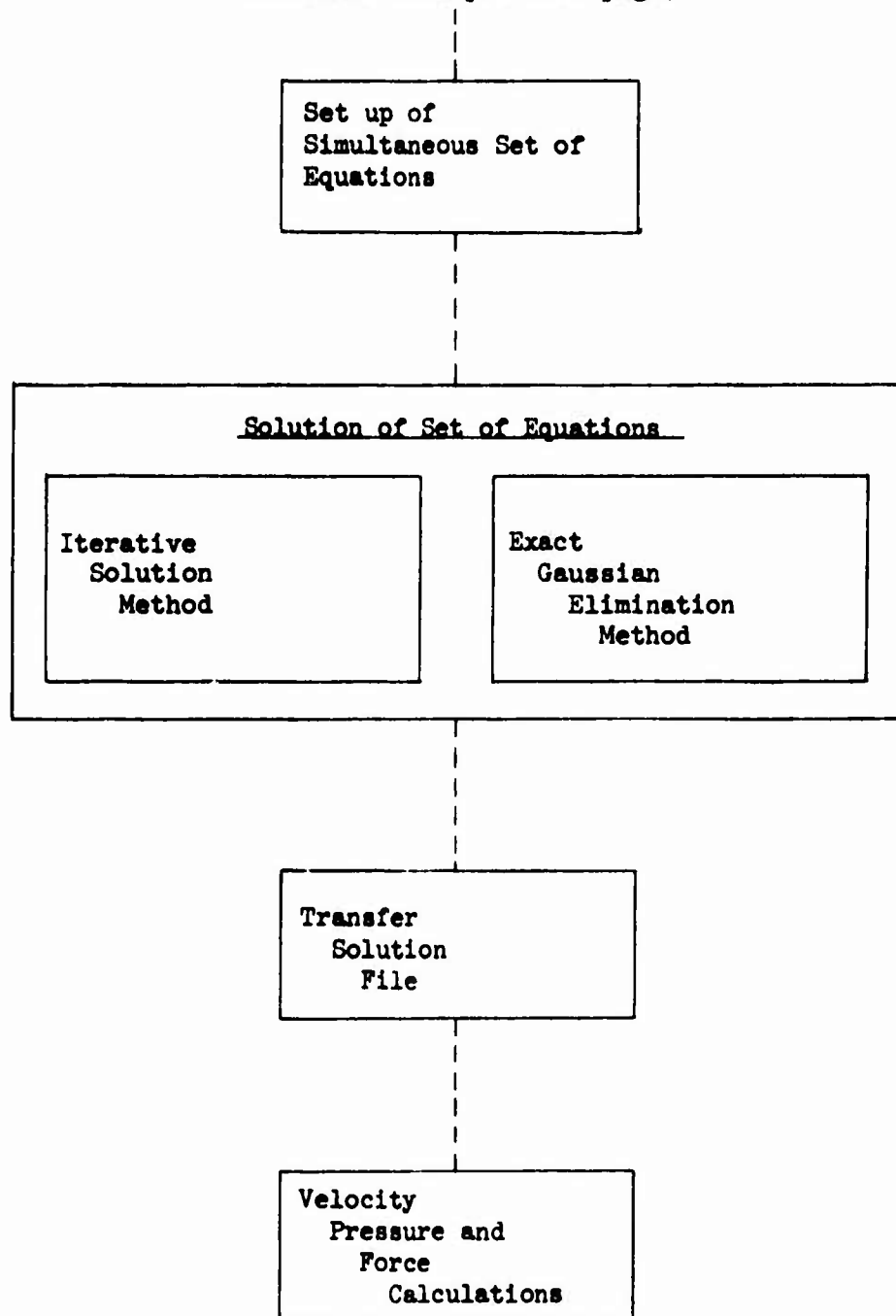
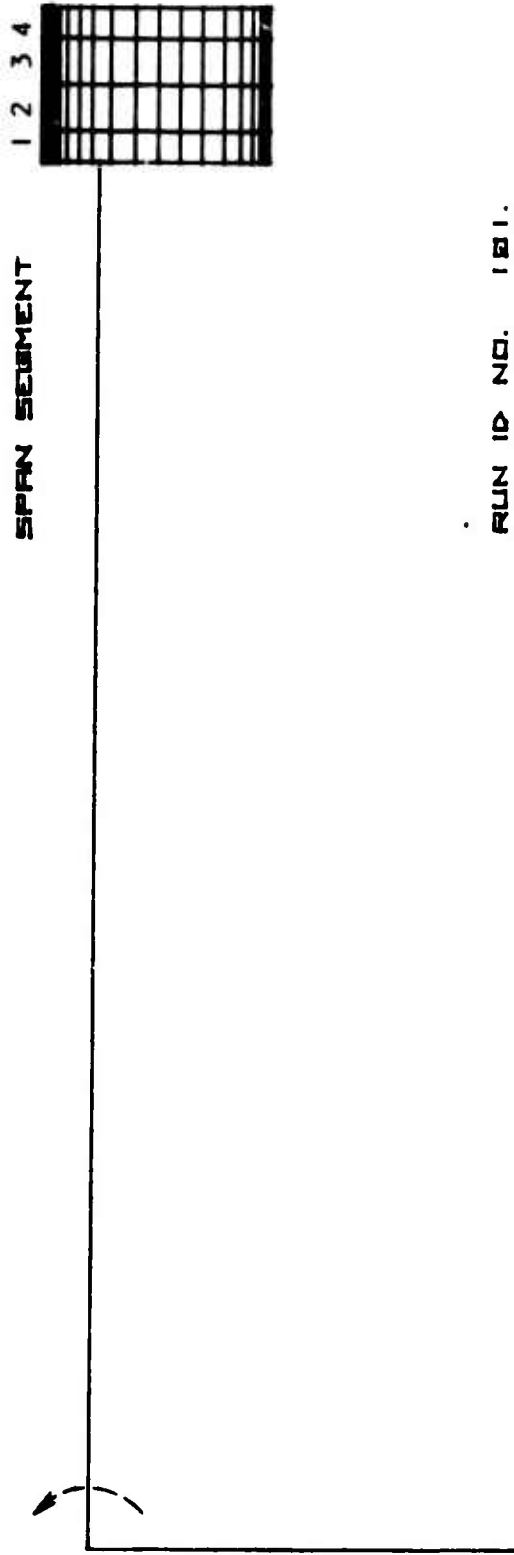


FIGURE 4 (b)

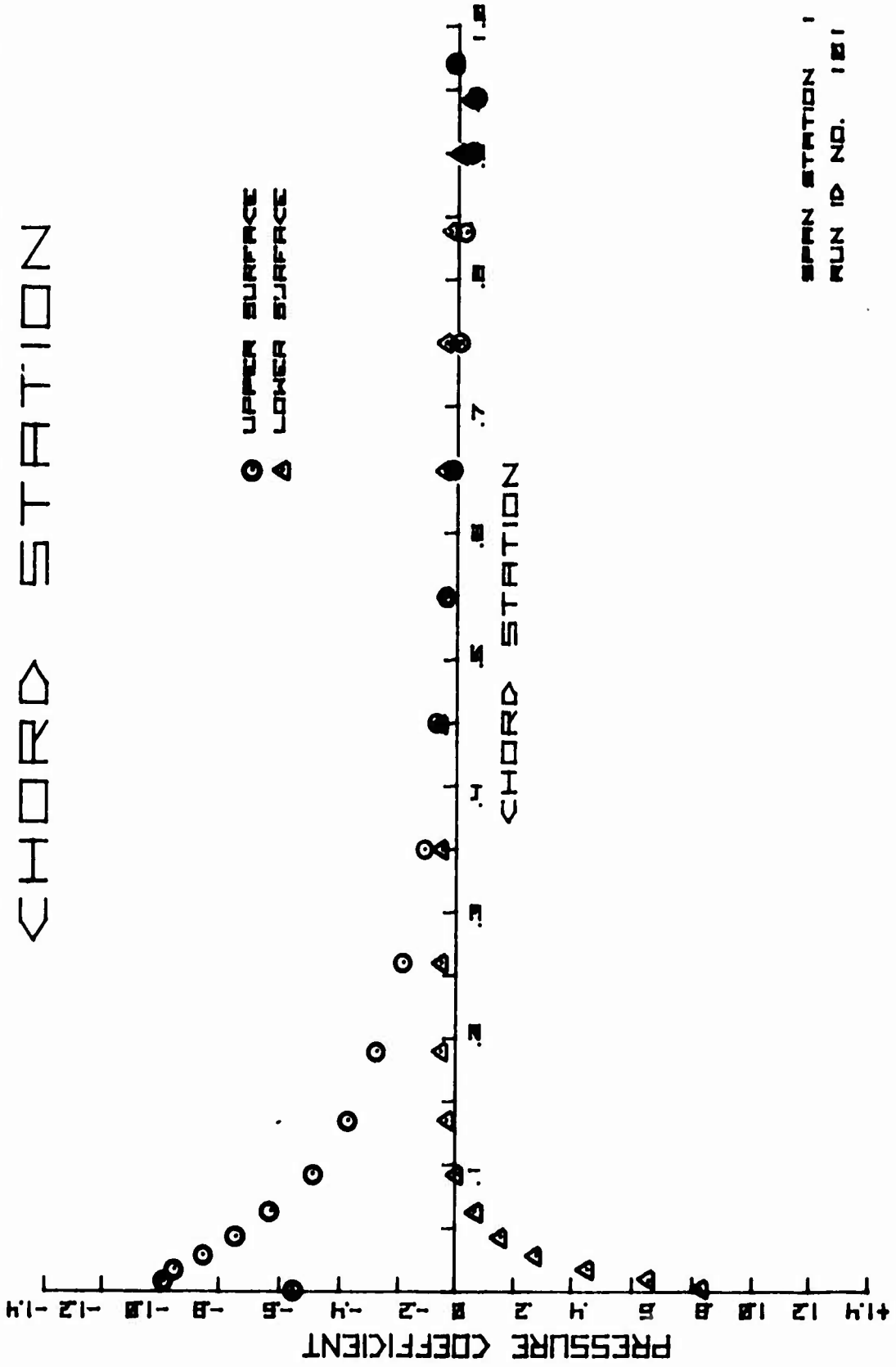
CONTROL SURFACE DENSITY PLOT



RUN ID NO. 181.

FIGURE 5

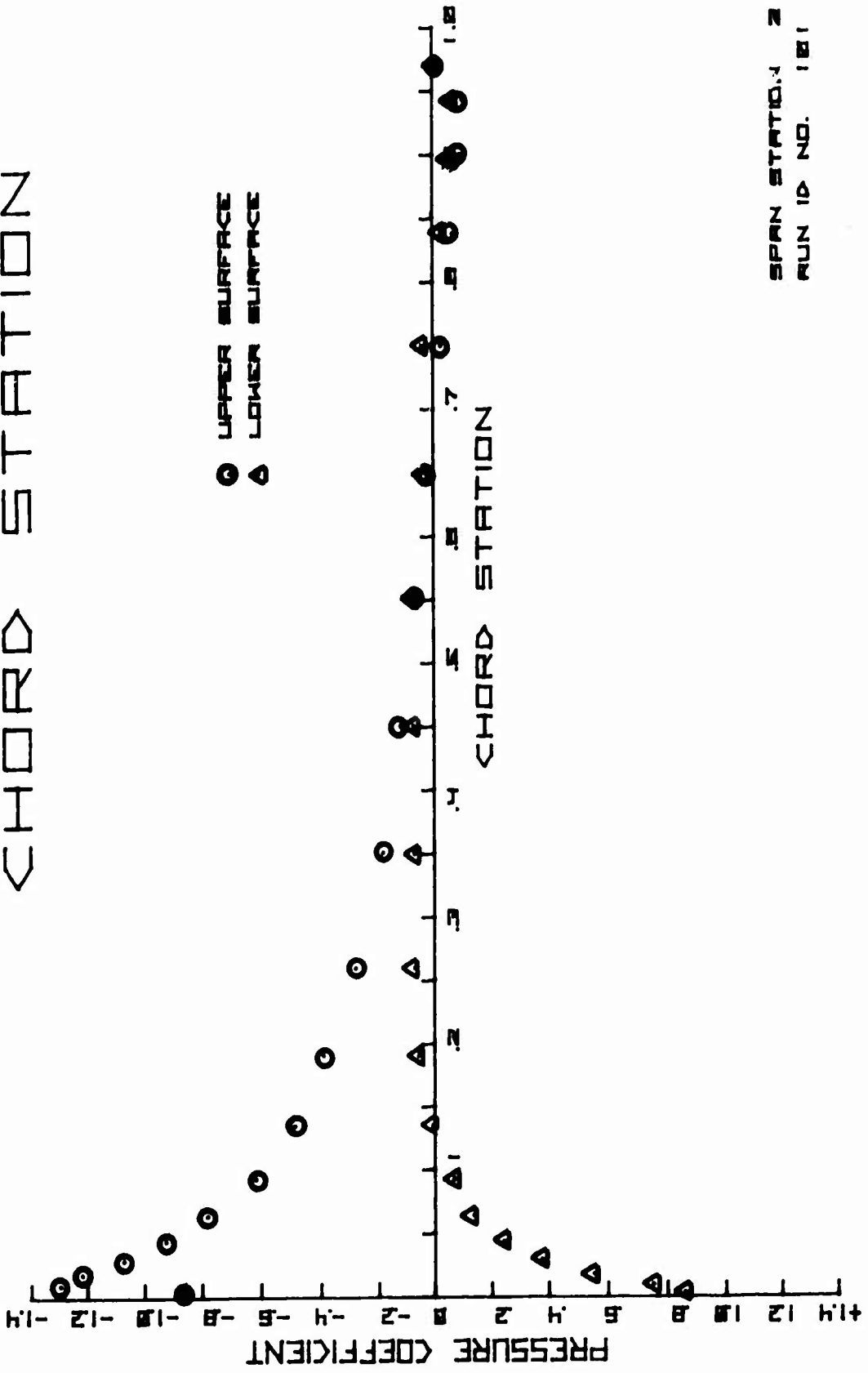
PRESSURE COEFFICIENT VS.
CHORD STATION



SPAN STATION 1
RUN ID NO. 101

FIGURE 6

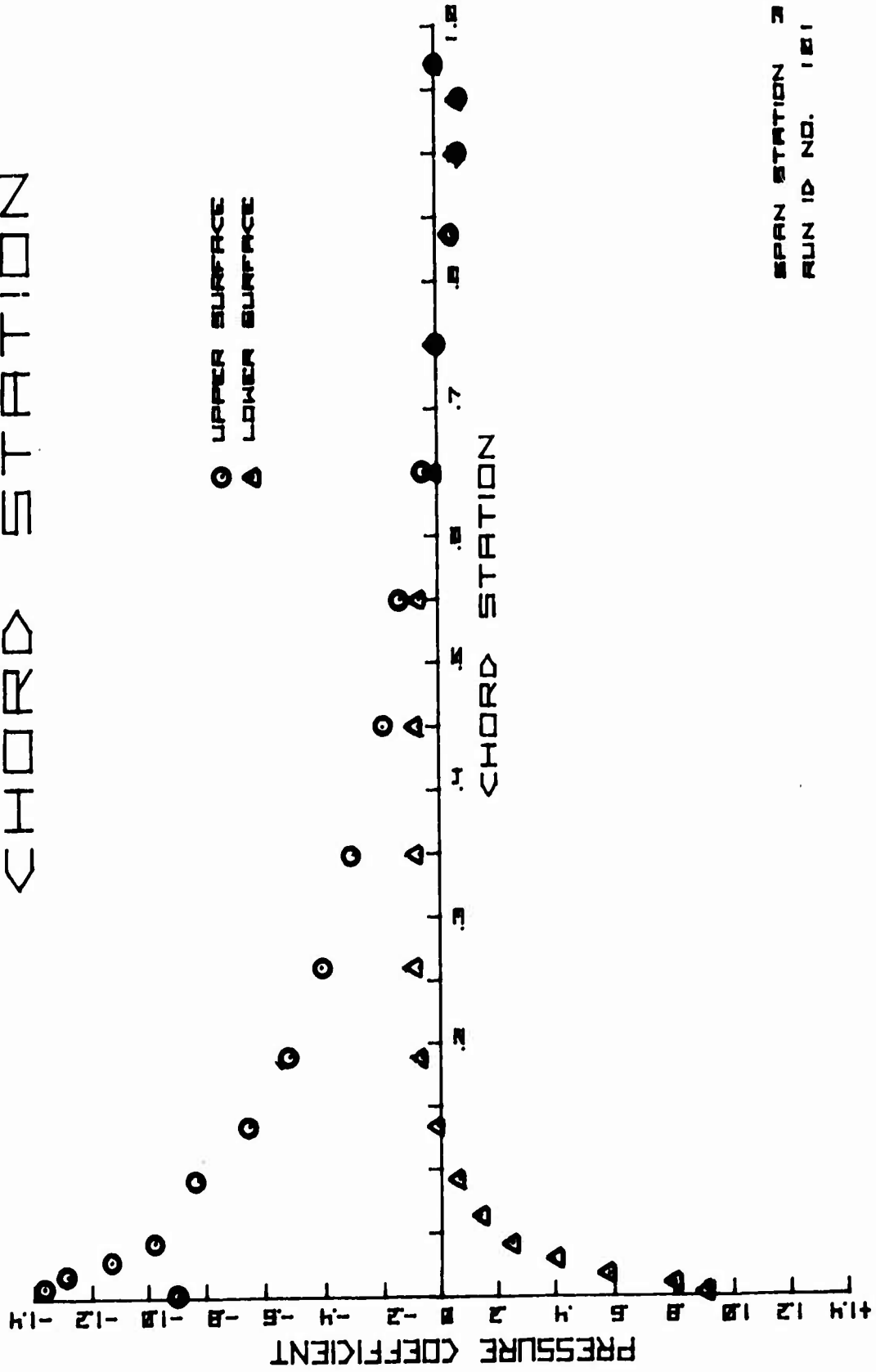
PRESSURE COEFFICIENT VS. CHORD STATION



SPAN STATION: 2
RUN ID NO. 181

FIGURE 7

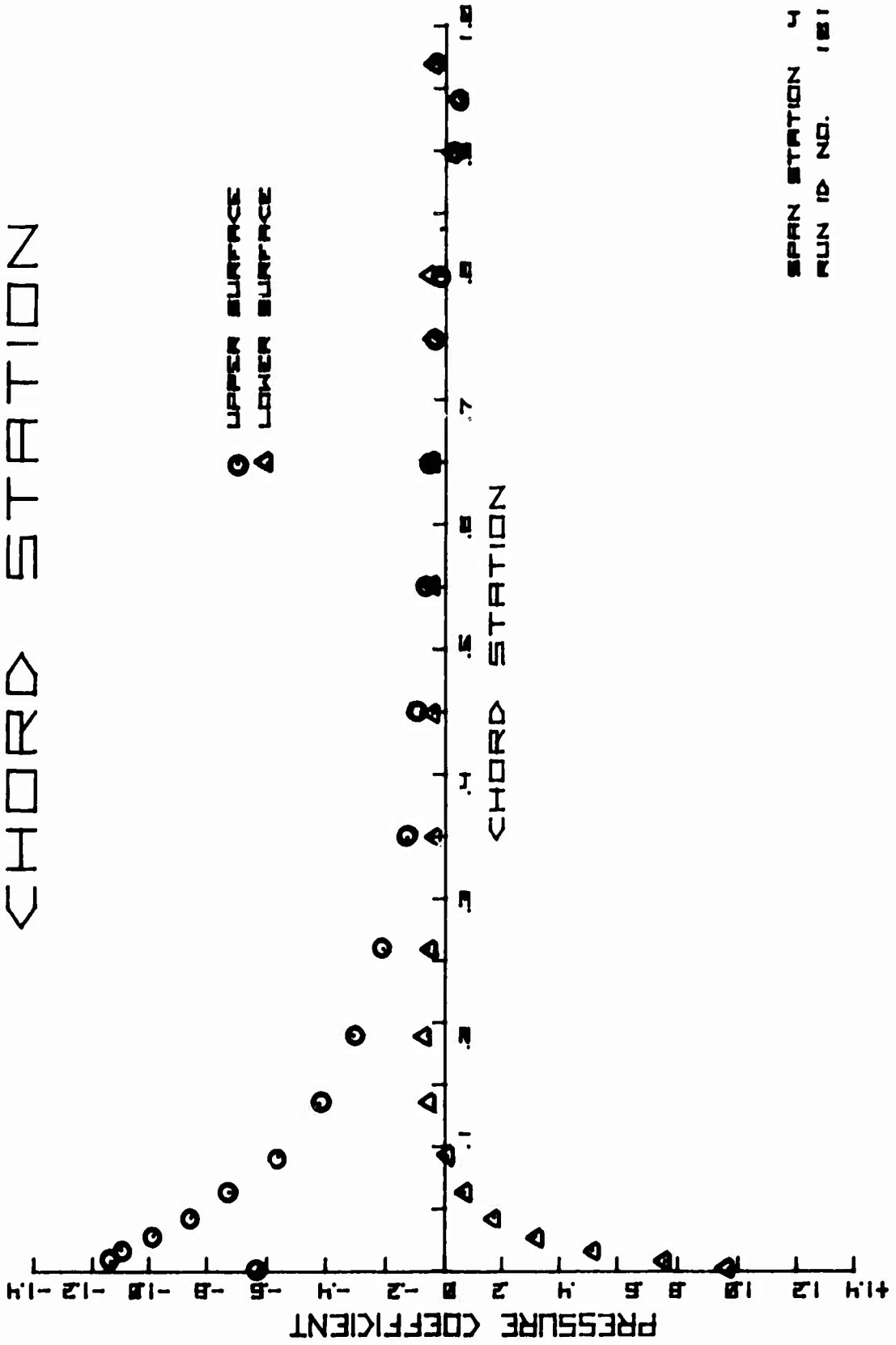
PRESSURE COEFFICIENT VS. CHORD STATION



SPAN STATION 3
RUN ID NO. 101

FIGURE 8

PRESSURE COEFFICIENT VS. CHORD STATION



SPAN STATION 4
RUN ID NO. 181

FIGURE 9

SURFACE VELOCITY VS. CHORD STATION

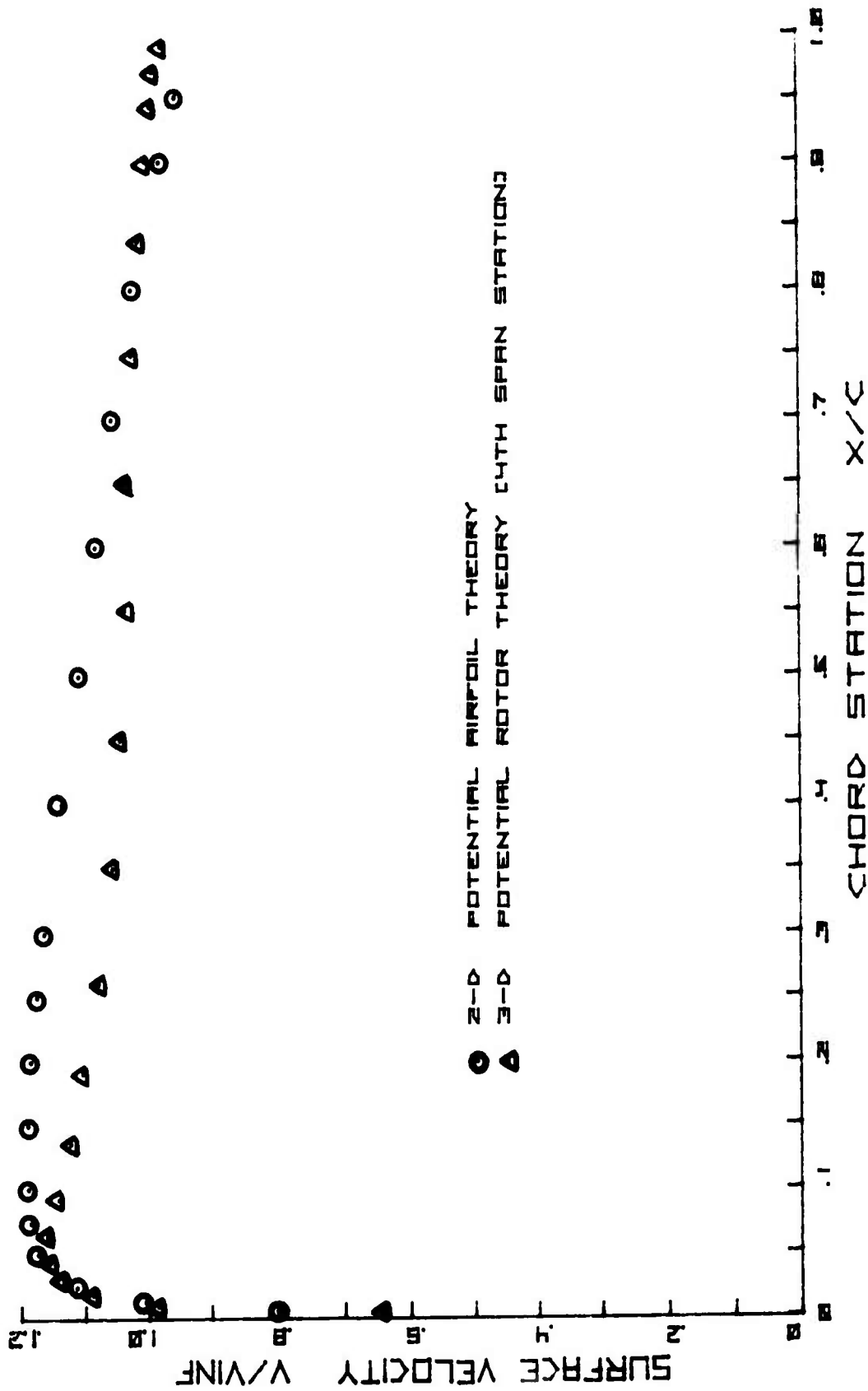
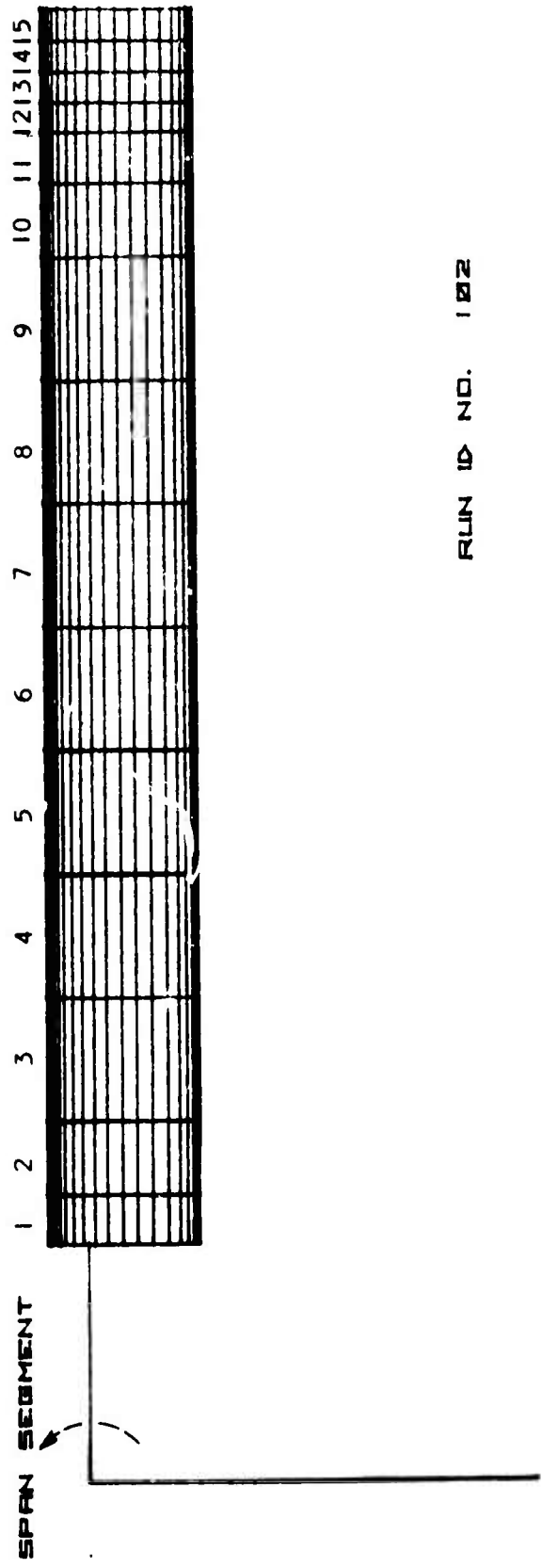


FIGURE 10

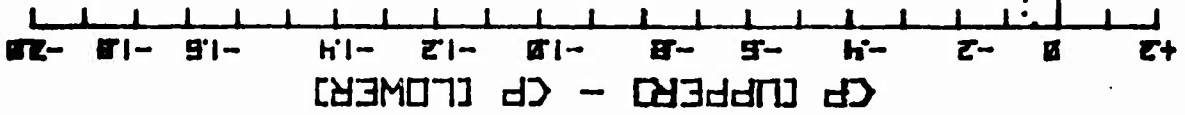
CONTROL SURFACE DENSITY PLOT



RUN ID NO. 102

FIGURE 11

CP UPPER] - CP LOWER] VS. CHORD STATION



SPAN STATION 1
RUN ID NO. 102

FIGURE 12

CP CUPPER] - CP CLOWER] VS. CHORD STATION

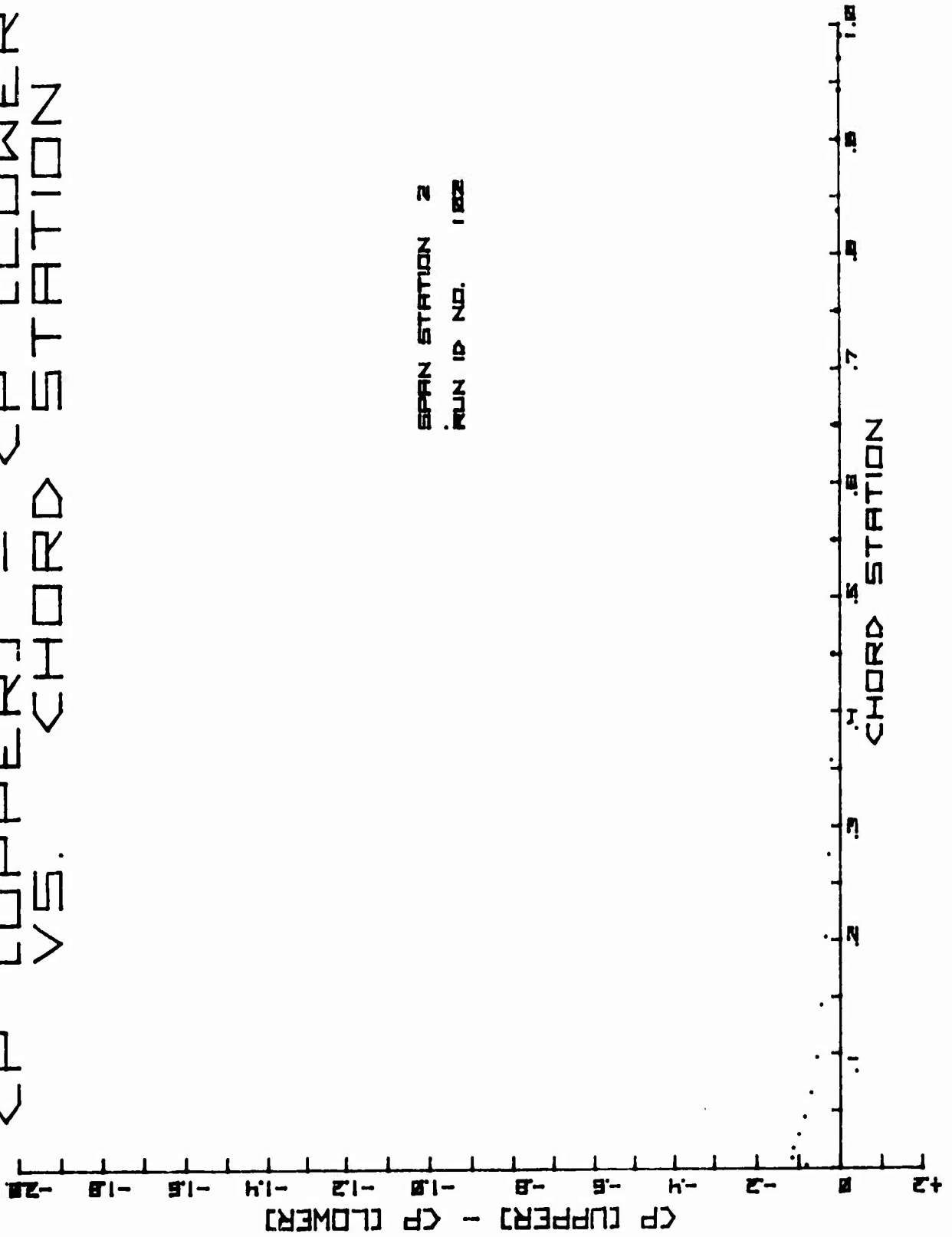
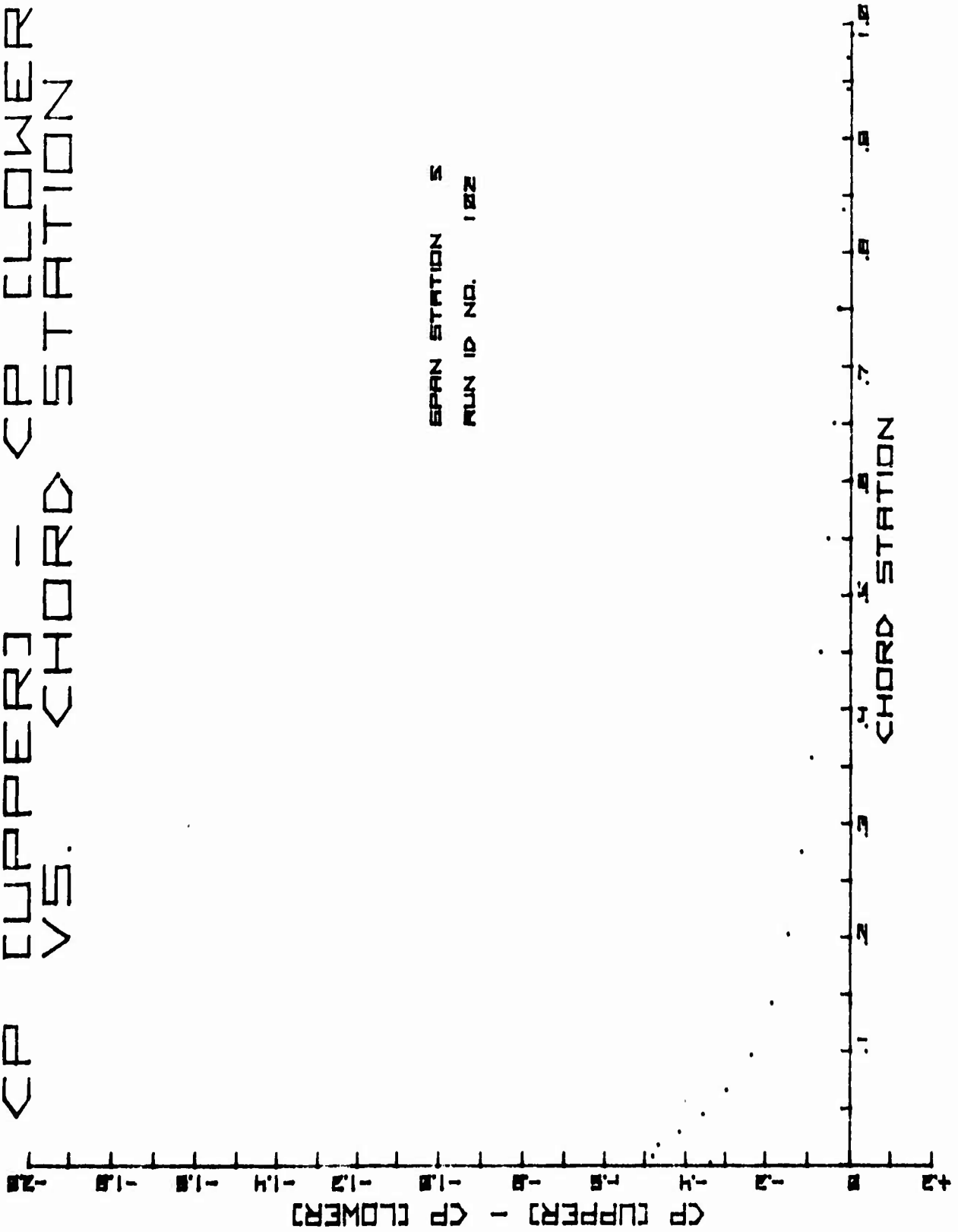


FIGURE 13

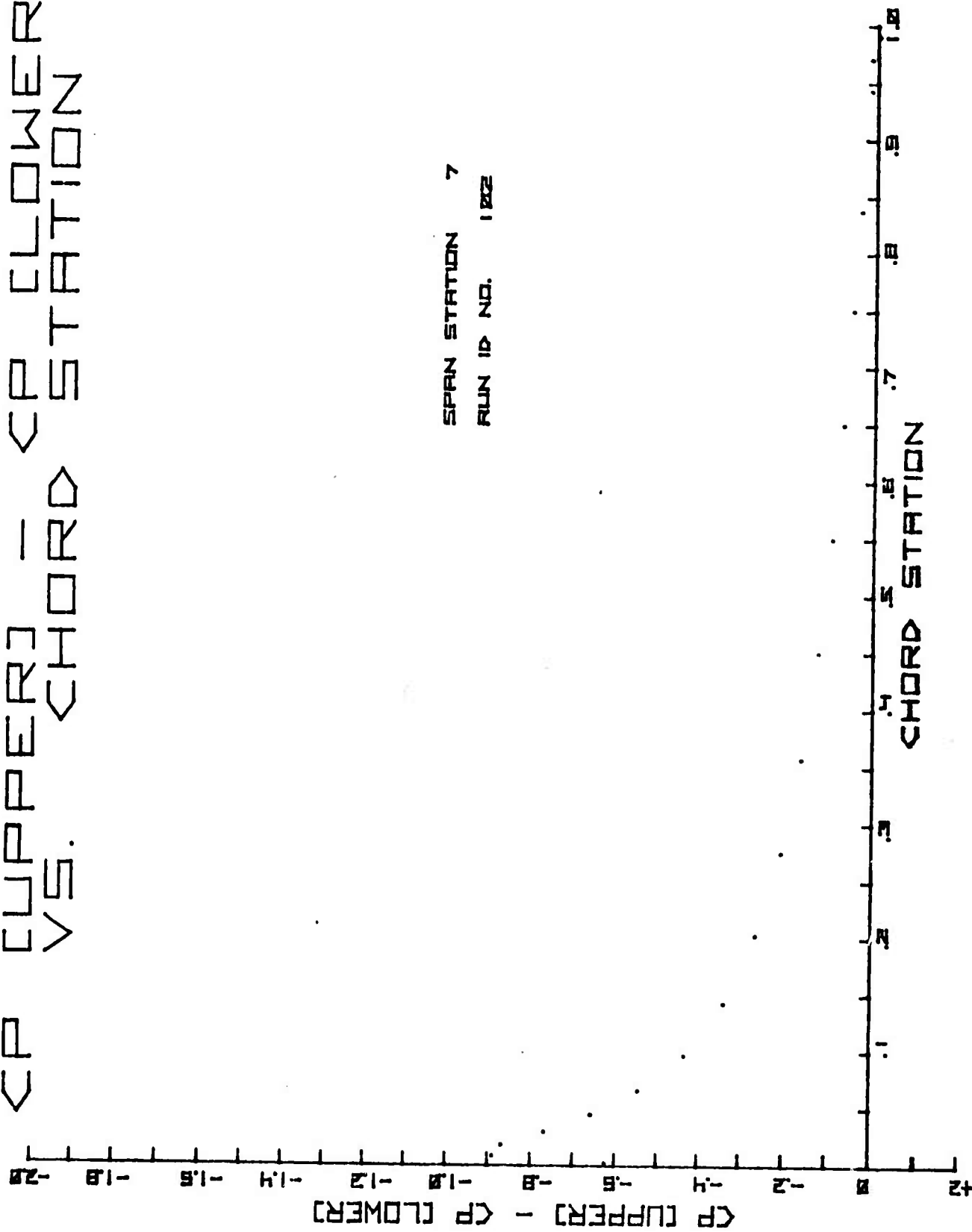
CP [UPPER] - CP [LOWER]
VS. CHORD STATION



SPAN STATION 5
RUN ID NO. 102

FIGURE 15

CP [UPPER] - CP [LOWER]
VS. CHORD STATION



SPAN STATION 7

RUN ID NO. 182

FIGURE 16

CUPPER VS. CUPPER
VS. CUPPER VS. CUPPER
VS. CUPPER VS. CUPPER
VS. CUPPER VS. CUPPER

SPAN STATION B
RUN ID NO. 182

(P CUPPER) - (P CUPPER)
-20 -18 -16 -14 -12 -10 -8 -6 -4 -2 0 2 4 6 8 10 12 14 16 18 20

FIGURE 17

VS. CUPPER VS. CUPPER
VS. CUPPER VS. CUPPER
VS. CUPPER VS. CUPPER
VS. CUPPER VS. CUPPER

CP UPPER] - CHORD STATION
VS. CHORD STATION
CP LOWER]

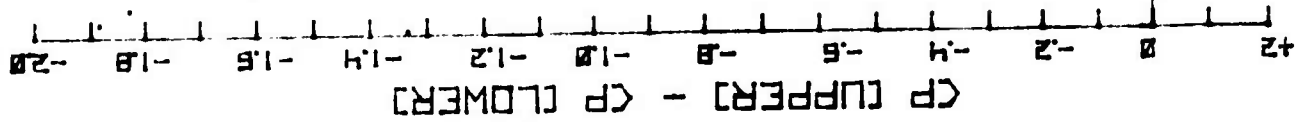
CP [UPPER] - CP [LOWER]
+2
-2
-4
-6
-8
-10
-12
-14
-16
-18
-20

SPAN STATION 8.
RUN ID NO. 102

CHORD STATION
1
2
3
4
5
6
7
8
9
10

FIGURE 18

CP [UPPER] - CP [LOWER]
VS. CHORD STATION



CP [UPPER] - CP [LOWER]

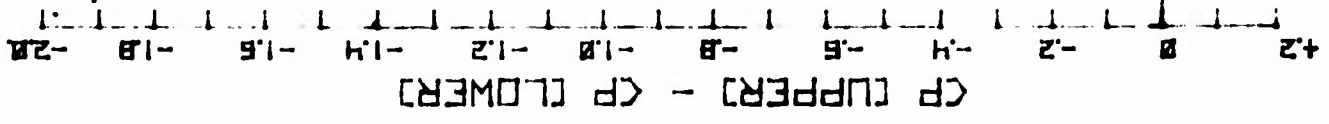
SPAN STATION 11
RUN ID NO. 102



CHORD STATION

FIGURE 19

CP CUPPER] - [CP CLOWER] - [CP CUPPER] - [CP CLOWER]
VS. CHORD] - [CP CLOWER] - [CP CUPPER] - [CP CLOWER]



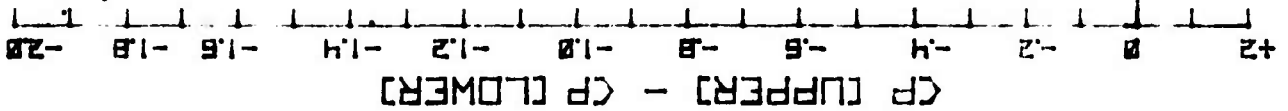
SPAN STATION 13
RUN ID NO. 102



CHORD STATION

FIGURE 20

CP UPPER] - CP LOWER] VS. CHORD STATION



CP UPPER] - CP LOWER]

SPAN STATION 14
RUN ID NO. 102

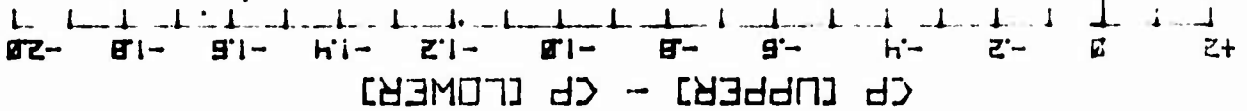


CHORD STATION

FIGURE 21

<P UPPER> vs. <P LOWER> CHORD STATION

SPAN STATION 15
RUN ID NO. 102



CHORD STATION
1.0
1.5
2.0
2.5
3.0
3.5
4.0
4.5
5.0
5.5
6.0
6.5
7.0
7.5
8.0
8.5
9.0
9.5
10.0

FIGURE 22

THE PRESENT RESULT OF
PRESSURE DIFFERENCE VS. CHORD STATION

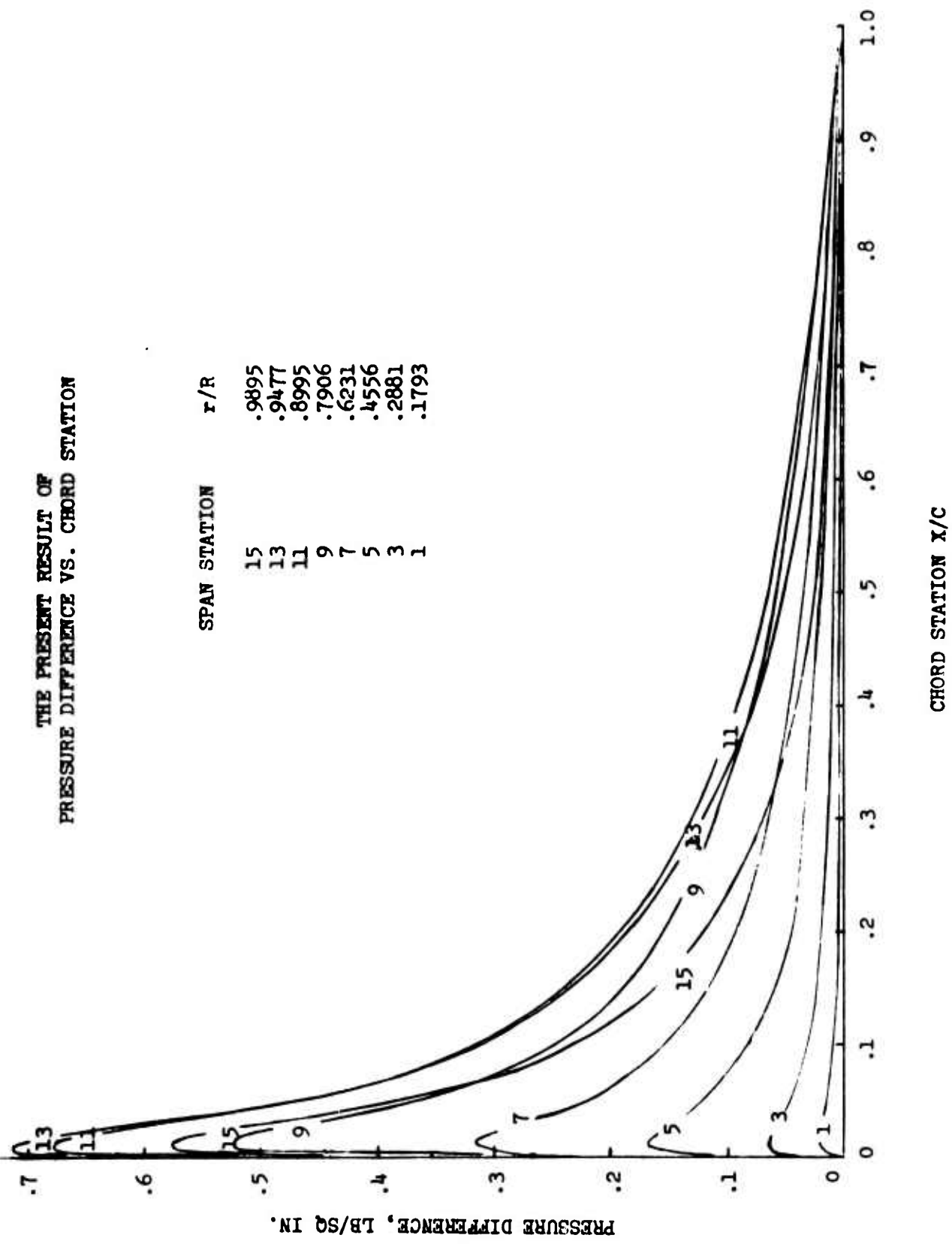


FIGURE 23

EXPERIMENTALLY DETERMINED
 PRESSURE DIFFERENCE VS CHORD STATION
 (REDRAWN FROM NACA TN 2953)

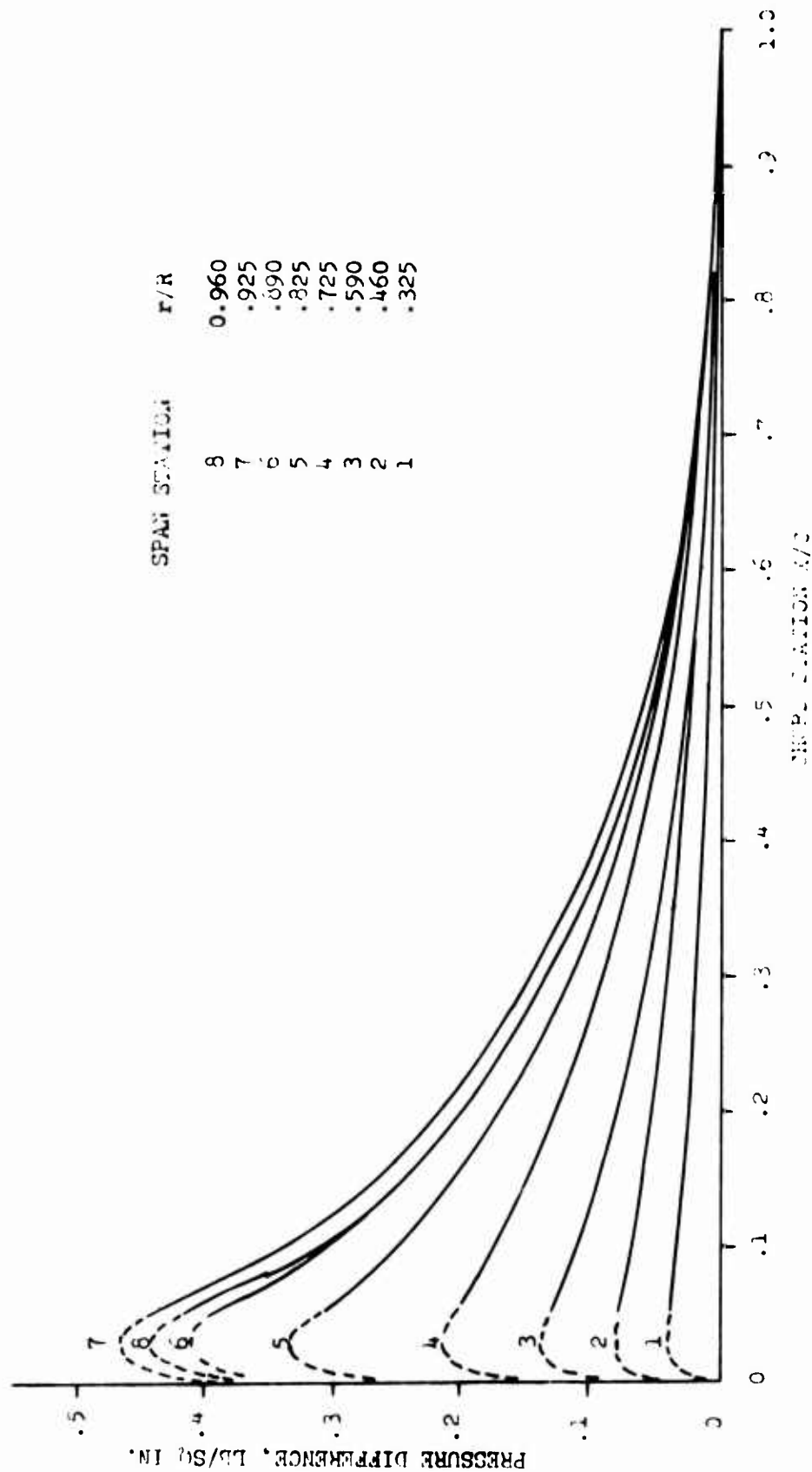


FIGURE 24

EXPERIMENTALLY DETERMINED
SECTION NORMAL FORCE
(REDRAWN FROM NACA TN 2953)
COMPARED WITH
THE PRESENT RESULT

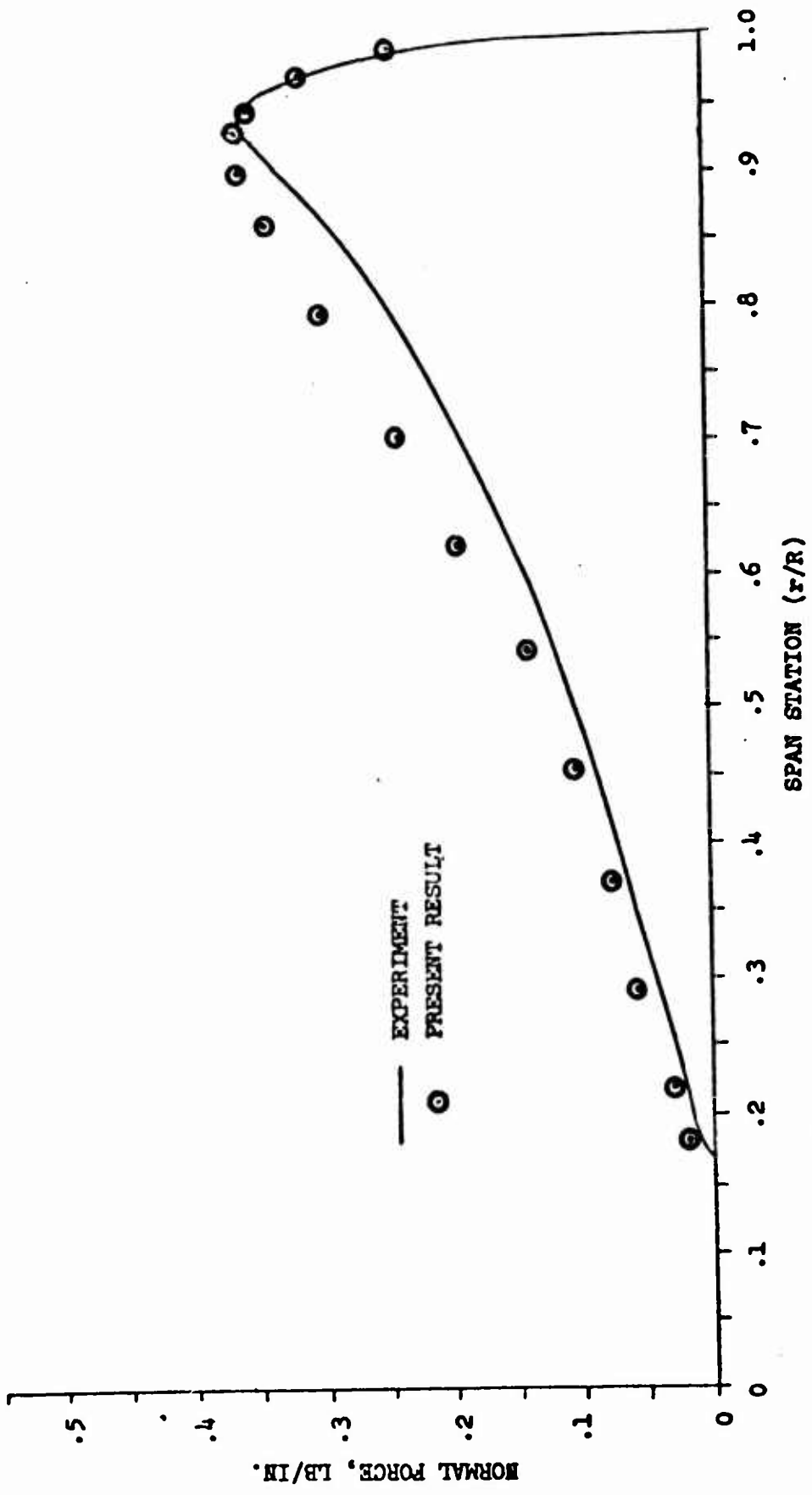


FIGURE 25

UPPER ROTOR SURFACE VELOCITY DIRECTION PLOT

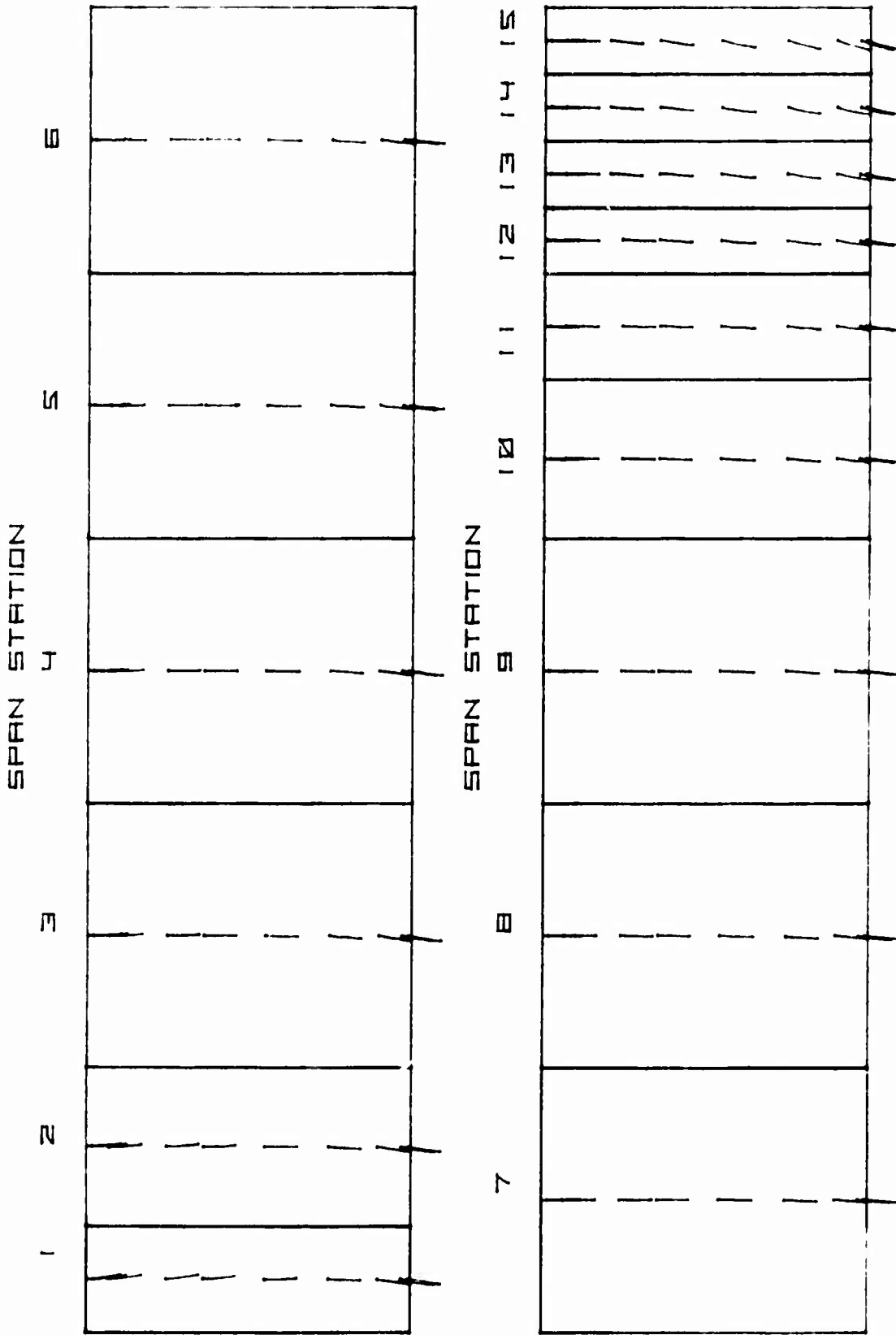


FIGURE 26

LOWER ROTOR SURFACE VELOCITY DIRECTION PLOT

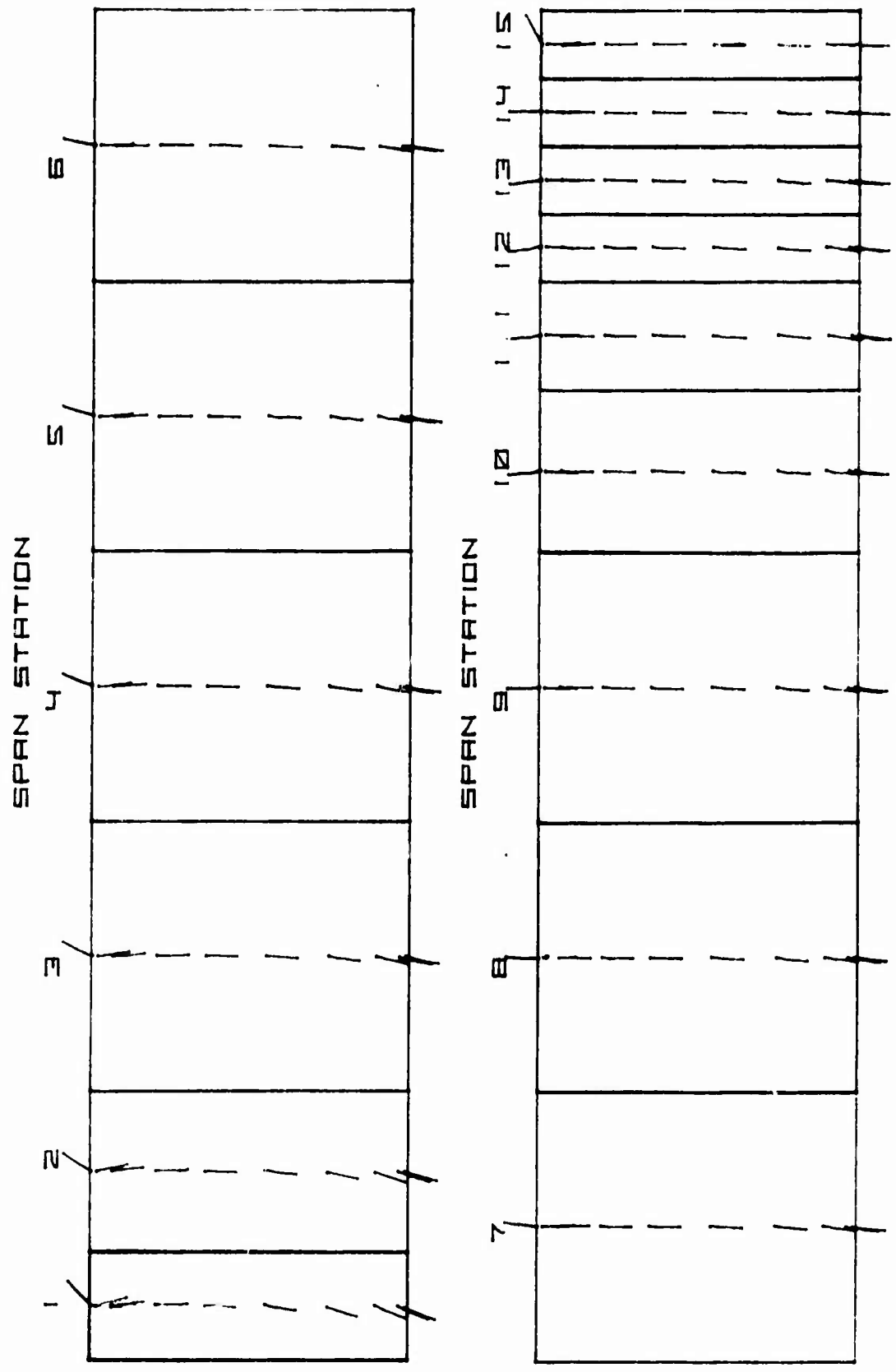


FIGURE 27

TABLES

ROTOR INPUT SUMMARY
FOR
CASE STUDY 1

ROTOR DESCRIPTION

NACA 0012 AIRFOIL SECTION	
ROTOR RADIUS	1.0
ROTOR HUB RADIUS	0.9
TRUE SPAN LENGTH	0.1
CONSTANT CHORD LENGTH	0.16
SPAN AXIS CHORD STATION	0.25
ROOT CHORD GEOMETRIC PITCH	10.0°
LINEAR TWIST ABOUT SPAN AXIS	0.0°
NUMBER OF ROTOR BLADES	1
NEITHER TIP IS PAIRED	

FREE STREAM CONDITIONS

HOVER MODE	$V_{\infty}/\omega R = 0$
ASSUMED CONSTANT WAKE DOWNWASH	$w/\omega R = 0.05$

ELEMENTAL BLADE SURFACE DESCRIPTION

NUMBER OF SPAN SEGMENTS	4
NUMBER OF CHORD SEGMENTS	40
a) UPPER SURFACE ONLY	20
b) LOWER SURFACE ONLY	20
ELEMENTAL AREAS ARE SYMMETRICALLY DESCRIBED WITH RESPECT TO CHORD PLANE	
TOTAL NUMBER OF BASIC BLADE ELEMENTS	160

ELEMENTAL WAKE SURFACE DESCRIPTION

PRESCRIBED CLASSIC WAKE MODEL	
NUMBER OF SPAN SEGMENTS	4
NUMBER OF STREAMWISE SEGMENTS	85
WAKE ELEMENT ANGULAR INCREMENT	
a) NEAR BLADE REGION	20°
b) FOR BLADE REGION (> 80° FROM BLADE)	30°
NUMBER OF WAKE TURNS COMPLETED	8.1
TOTAL NUMBER OF BASIC WAKE ELEMENTS	340

TABLE 1

COMPUTER EXECUTION TIME SUMMARY
FOR
CASE STUDY 1

EXECUTABLE SECTION	TIME (SECONDS)
I. INFLUENCE CALCULATIONS PROGRAM	
A. BLADE INFLUENCE CALCULATIONS (TOTAL NUMBER = 25,600)	97
B. WAKE INFLUENCE CALCULATIONS (TOTAL NUMBER = 54,400)	228
C. OTHER ROUTINES	6
II. CREATE SOLUTION FILE PROGRAM	11
III. SOLVE BY ELIMINATION PROGRAM (EXACT SOLUTION METHOD)	104
IV. TRANSFER SOLUTION FILE PROGRAM	1
V. VELOCITY CALCULATION PROGRAM	16
TOTAL ABOVE	457

TABLE 2

ROTOR INPUT SUMMARY
FOR
CASE STUDY 2

ROTOR DESCRIPTION

NACA 0015 AIRFOIL SECTION	
ROTOR RADIUS	1.0
ROTOR HUB RADIUS	0.1625
TRUE SPAN LENGTH	0.8375
CONSTANT CHORD LENGTH	0.1
SPAN AXIS CHORD STATION	0.2708
ROOT CHORD GEOMETRIC PITCH	3.0°
LINEAR TWIST ABOUT SPAN AXIS	0.0
NUMBER OF ROTOR BLADES	2
NEITHER TIP IS FAIRED	

FREE STREAM CONDITIONS

HOVER MODE	$V_T/\omega R = 0$
RESUMED CONSTANT WAKE DOWNWASH	$w/\omega R = 0.0444$

ELEMENTAL BLADE SURFACE DESCRIPTION

NUMBER OF SPAN SEGMENTS	15
NUMBER OF CHORD SEGMENTS	40
a) UPPER SURFACE ONLY	20
b) LOWER SURFACE ONLY	20
ELEMENTAL AREAS ARE SYMMETRICALLY DESCRIBED WITH RESPECT TO CHORD PLANE	
TOTAL NUMBER OF BASIC BLADE ELEMENTS	600

ELEMENTAL WAKE SURFACE DESCRIPTION

PRESCRIBED CLASSIC WAKE MODEL	
NUMBER OF SPAN SEGMENTS	15
NUMBER OF STREAMWISE SEGMENTS	77
WAKE ELEMENT ANGULAR INCREMENT	
a) NEAR BLADE REGION	20°
b) FAR BLADE REGION (> 90° FROM BLADE)	35°
NUMBER OF WAKE TURNS COMPLETED	7.3
TOTAL NUMBER OF BASIC WAKE ELEMENTS	1155

TABLE 3

COMPUTER EXECUTION TIME SUMMARY
FOR
CASE STUDY 2

EXECUTABLE SECTION	TIME (SECONDS)
I. INFLUENCE CALCULATIONS PROGRAM	
A. BLADE INFLUENCE CALCULATIONS (TOTAL NUMBER = 720,000)	2328
B. WAKE INFLUENCE CALCULATIONS (TOTAL NUMBER = 1,386,000)	5475
C. OTHER ROUTINES	20
II. CREATE SOLUTION FILE PROGRAM	137
III. SOLVE BY ITERATION PROGRAM (TOTAL NUMBER OF ITERATIONS = 281)	5970
IV. TRANSFER SOLUTION FILE PROGRAM	4
V. VELOCITY CALCULATION PROGRAM	130
TOTAL ABOVE	14334

TABLE 4

APPENDIX A
SUMMARY OF THE TRANSFORMATION EQUATIONS

Preceding page blank

We are concerned here with presenting in summary form the transformation equations which relate an inertial reference frame (x, y, z, t) to a body fixed reference frame (x', y', z', t') in which the body is translating with a constant velocity \bar{V}_T given by

$$\bar{V}_T = V_T \hat{z} \quad (\text{A.1})$$

and rotating about the z axis at a constant rotational rate given by

$$\bar{\omega} = \omega_z \hat{z} \quad (\text{A.2})$$

We assume that at time $t = t' = 0$ the axis systems were coincident.

It follows then that the coordinates of a point P in the inertial frame are related to the body fixed frame as follows:

$$x' = x \cos \omega_z t + y \sin \omega_z t \quad (\text{A.3})$$

$$y' = -x \sin \omega_z t + y \cos \omega_z t \quad (\text{A.4})$$

$$z' = z - V_T t \quad (\text{A.5})$$

where the inverse is given by

$$x = x' \cos \omega_z t' - y' \sin \omega_z t' \quad (\text{A.6})$$

$$y = x' \sin \omega_z t' + y' \cos \omega_z t' \quad (\text{A.7})$$

$$z = z' + V_T t' \quad (\text{A.8})$$

From these relations it follows then that

$$\frac{\partial}{\partial x} = \cos \omega_2 \frac{\partial}{\partial x'} - \sin \omega_2 \frac{\partial}{\partial y'} \quad (\text{A.9})$$

$$\frac{\partial}{\partial y} = \sin \omega_2 \frac{\partial}{\partial x'} + \cos \omega_2 \frac{\partial}{\partial y'} \quad (\text{A.10})$$

$$\frac{\partial}{\partial z} = \frac{\partial}{\partial z'} \quad (\text{A.11})$$

Furthermore, derivations with respect to t are given by

$$\frac{\partial}{\partial t} = -[\bar{\omega} \times \bar{r}' + \bar{v}_2] \cdot \bar{\nabla}' + \frac{\partial}{\partial t'} \quad (\text{A.12})$$

where

$$\bar{\nabla}' = \frac{\partial}{\partial x'} \hat{x}' + \frac{\partial}{\partial y'} \hat{y}' + \frac{\partial}{\partial z'} \hat{z}' \quad (\text{A.13})$$

$$\bar{r}' = x \hat{x}' + y \hat{y}' + z \hat{z}' \quad (\text{A.14})$$

It follows from the above that

$$\bar{\nabla} = \bar{\nabla}' \quad (\text{A.15})$$

and similarly

$$\bar{\nabla}^2 = \bar{\nabla}'^2 \quad (\text{A.16})$$

The substantial derivations are related as follows

$$\frac{D}{Dt} \equiv \frac{\partial}{\partial t} + \bar{V} \cdot \bar{\nabla} = \frac{\partial}{\partial t'} + \bar{V}' \cdot \bar{\nabla}' \equiv \frac{D'}{Dt'} \quad (\text{A.17})$$

where

$$\bar{V} = V_x \hat{x} + V_y \hat{y} + V_z \hat{z} \quad (\text{A.18})$$

$$\bar{V}' = V_x' \hat{x}' + V_y' \hat{y}' + V_z' \hat{z}' \quad (\text{A.19})$$

The velocities are related as follows

$$\bar{V} = \bar{V}' + \bar{\omega} \times \bar{R}' + \bar{V}' \quad (\text{A.20})$$

Furthermore, any scalar function H evaluated at some point

$\rho(x, y, z, t)$ must have the same value when evaluated at point

$\rho'(x', y', z', t')$ if point ρ is related to point ρ' using

the set of transformation equations given by equations (A.3), (A.4)

and (A.5). That is

$$\begin{aligned} H(x, y, z, t) &= H(x'(x, y, t), y'(x, y, t), z'(z, t), t') \equiv H \\ &= H(x', y', z', t') \end{aligned}$$

(A.21)

Using relation (A.12) we may note that for some scalar function F which is independent of z' that the above relation reduces to

$$F(x, y, z) = F(x', y', z'). \quad (\text{A.22})$$

APPENDIX B

RELATIONS BETWEEN DOUBLET'S AND VORTICITY AND EXTENSION
OF HELMHOLTZ CONDITION

We will discuss in this section the relations between doublets and vorticity. Having established the relationships it is then an easy matter to extend Helmholtz's theory which concerns vorticity to a corollary involving doublets in order to determine the strengths of the wake doublet surface distributions.

Let us assume that we have a surface doublet distribution whose potential at some point P is given by $\phi(P)$ and whose strength is given by $\gamma(x, y)$. The doublet axis is assumed to be directed everywhere along the positive local surface normal direction. We shall assume further that x and y are two orthogonal axes lying on the surface with the x axis directed along the unit normal as shown in Figure B.1. If doublets and vorticity are related we should be able to derive an expression relating the local doublet strength $\gamma(x, y)$ to the vorticity components $\omega(x, y)$ and $\zeta(x, y)$ whose assumed directions are as shown in Figure B.1. In order to derive this relationship we shall assume that U , V and W are the velocities along the x , y and z axis respectively. It can be shown now that

$$\omega(x, y) = U(x, y, z^+) - U(x, y, z^-) \quad (B.1)$$

where z^+ and z^- represent some small distance above and below the vortex location $(x, y, 0)$.

The velocity U , however, is related to the derivatives of the doublet potential with respect to x such that we may write,

SURFACE AXIS CONVENTION

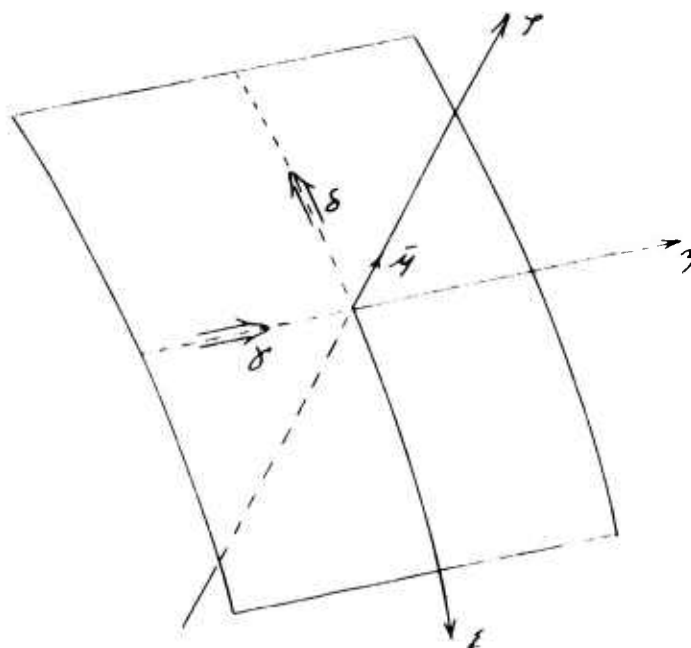


FIGURE B.1

$$\gamma(x, y) = \frac{\partial}{\partial x} \phi(x, y, z') - \frac{\partial}{\partial x} \phi(x, y, z) \quad (B.2)$$

If we now rewrite the derivative in terms of its definition as a limiting process we have

$$\begin{aligned} \gamma(x, y) &= \lim_{\Delta z \rightarrow 0} \frac{\phi(x+\Delta z, y, z') - \phi(x+\Delta z, y, z)}{\Delta z} \\ &= \lim_{\Delta z \rightarrow 0} \frac{\phi(x+\Delta z, y, z') - \phi(x, y, z')}{\Delta z} \\ &\quad - \lim_{\Delta z \rightarrow 0} \frac{\phi(x+\Delta z, y, z) - \phi(x, y, z)}{\Delta z} \end{aligned} \quad (B.3)$$

Rearranging the terms above we may further write γ as,

$$\begin{aligned} \gamma(x, y) &= \lim_{\Delta z \rightarrow 0} \left\{ \frac{\phi(x+\Delta z, y, z') - \phi(x+\Delta z, y, z)}{\Delta z} \right. \\ &\quad \left. - \frac{\phi(x, y, z') - \phi(x, y, z)}{\Delta z} \right\} \end{aligned} \quad (B.4)$$

It can be shown that the value of the doublet potential at a point just above or below the doublet itself approaches one half the negative or positive value of the local doublet strength itself. Thus we find that

$$\gamma'(x, y) = \lim_{\Delta x \rightarrow 0} \left\{ \frac{-\gamma(x + \Delta x, y) + \gamma(x, y)}{\Delta x} \right\} \quad (B.5)$$

But the limit term is just the definition of the derivative of the doublet strength with respect to x , therefore the relationship between the γ' vorticity and doublet strength at a point is given by

$$\gamma'(x, y) = - \frac{\partial}{\partial x} \gamma(x, y) \quad (B.6)$$

In a similar manner or by using the following vortex compatibility relation

$$\frac{\partial \gamma}{\partial y} = \frac{\partial \gamma'}{\partial x} \quad (B.7)$$

it follows that

$$\gamma(x, y) = - \int \gamma' dx \quad (B.8)$$

Now about a wing surface it can be shown that at a particular span station y the total circulation $\Gamma(y)$ is given by the line integral of the γ' vorticity from the point on the trailing edge lower surface Γ_{TL} , to the point on the trailing edge upper surface Γ_{TU} , that is referring to Figure B.2,

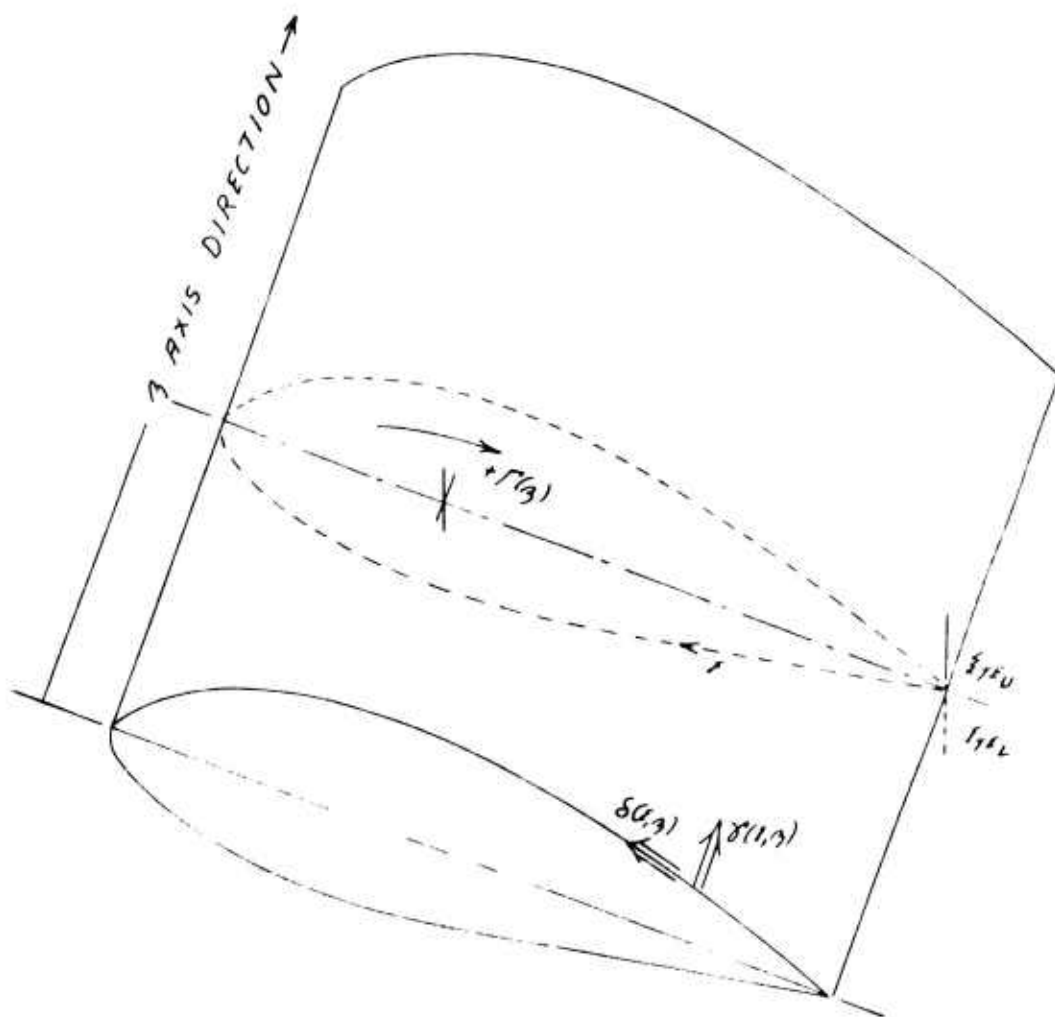
LINE INTEGRAL PATH FOR EVALUATION
OF THE CIRCULATION

FIGURE B.2

$$\Gamma(\beta) = \oint_{S_{\beta}}^{\beta_{\text{tip}}} \gamma(\beta, \beta) dS \quad (\text{B.9})$$

Using relation B.6 above it follows then that the circulation about a particular space station is given in terms of doublet strength by,

$$\Gamma(\beta) = - \left[\gamma(\beta_{\text{tip}}, \beta) - \gamma(\beta_{\text{root}}, \beta) \right] \quad (\text{B.10})$$

In the wake region the application of Helmholtz's theorem on the conservation of vorticity shows that

$$\frac{\partial \gamma_w}{\partial \beta} = \frac{\partial S_w}{\partial \beta} \quad (\text{B.11})$$

where now β and γ are orthogonal axes lying on the wake surface with the β axis directed along a local streamline and the γ axis being directed generally from root to tip across the wake. In order for a zero pressure discontinuity to exist across the wake in steady flows it can be shown that γ_w must be zero. Thus it follows using relation (B.6), where we now define γ_w as the local wake surface doublet strength whose axis is along the γ axis, that

$$\frac{\partial \gamma_w}{\partial \beta} = 0 \quad (\text{B.12})$$

everywhere in the wake surface. Since Kutta's hypothesis requires the fluid to leave the trailing edge smoothly and because the above relation implies that γ_w is a constant along a streamline we find following such a streamline that

$$\gamma_w(x, y) = \gamma_w(x_{TE}, y) . \quad (B.13)$$

Thus we find that along a wake streamline the value of the wake doublet strength is a constant and is given by its value at the trailing edge, that is

$$\gamma_w(x_{TE}, y) = \gamma(x_{TE_0}, y) - \gamma(x_{TE_1}, y)$$

along a wake streamline.

(B.14)

Note at this point that by properly integrating about the wake region one finds (as one should) that the circulation in the wake Γ_w about some constant γ to be

$$\Gamma_w(\gamma) = \gamma(x_{TE_0}, \gamma) - \gamma(x_{TE_1}, \gamma) \quad (B.15)$$

which is just the negative of the bound circulation given by equation (B.10).

APPENDIX C

ANALYTIC EXPRESSIONS FOR $A(p)$ AND $\bar{V}A(p)$

We will be concerned in this section with deriving an analytic algebraic expression for the doublet potential ϕ and its derivative $\bar{\nabla} \phi$ at some field point P given some arbitrary n sided planar doublet distribution of constant strength whose doublet axis is everywhere normal to the surface. Before we begin this derivation let us first define the doublet so as to make clear the axis convention used.

In a physical sense a doublet is derived as the sum of a source and a sink. Suppose we have a point source of strength q and a point sink of strength $-q$ located about the origin of an (x, y, z) rectangular coordinate system as shown in Figure C.1. It follows from this that the potential at some field point P is given by

$$\phi(P; \text{SOURCE} + \text{SINK}) = -\frac{q}{4\pi} \left[\frac{1}{R_1} - \frac{1}{R_2} \right] \quad (\text{C.1})$$

where the position vectors \bar{R}_1 and \bar{R}_2 are as shown in the figure. Let us now define the vector distance from the sink to the source as \bar{L} where

$$\bar{L} = L \bar{n} = \bar{R}_2 - \bar{R}_1 \quad (\text{C.2})$$

where \bar{n} is the unit vector along the line joining the sink to the source. It follows from this that the doublet potential at the field point P is obtained by taking the limit of the source plus sink potential at the point P as they each approach the origin assuming the product of the strength and vector distance \bar{L} remain constant

AXIS CONVENTION RELATING THE
POTENTIAL AT A POINT INDUCED
BY A SOURCE + SINK

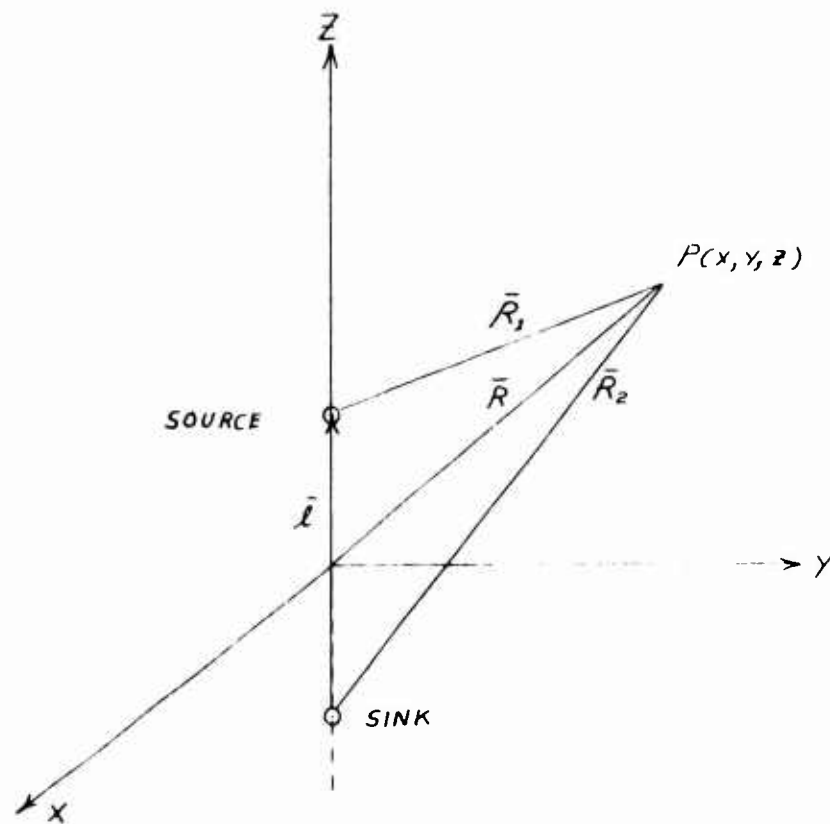


FIGURE C.1

and given by $\bar{\phi}$ where

$$\bar{\phi} = \gamma \bar{n} \cdot \bar{R} \quad (C.3)$$

Performing the limiting process we find that the potential at a field point P resulting from a doublet situated at the origin in Figure C.1 is given by

$$\phi(P) = -\frac{\gamma}{4\pi} \frac{\bar{n} \cdot \bar{R}}{|\bar{R}|^3} \quad (C.4)$$

where \bar{n} is the direction of the doublet axis directed along the positive r axis. Extending this result to a surface doublet distribution whose axis is everywhere directed normal to the local surface we find that the potential at a point P becomes

$$\phi(P) = -\frac{\gamma}{4\pi} \int_{\text{Surface}} \frac{\bar{n} \cdot \bar{R}_{SP}}{|\bar{R}_{SP}|^3} dS \quad (C.5)$$

where \bar{R}_{SP} is the vector distance from a point on the local doublet surface to the field point P and γ is now the doublet strength per unit area.

Given this expression for the potential what we now wish to do is to integrate this expression for an arbitrary n sided planar doublet surface distribution of constant strength. More specifically we may state the problem as follows:

Given: A planar n sided figure as shown in Figure C.2 (for $n = 4$) whose surface lies within the (x, y, z) plane and whose positive unit normal \vec{n} is along the positive z axis and, given this plane to be a surface doublet distribution plane of constant strength γ whose axis is everywhere directed along the unit normal then

- Determine: A. The potential ϕ at an arbitrary point P whose coordinates are (x, y, z) .
- B. The vector gradient of ϕ at some arbitrary point $P(x, y, z)$, that is, determine $\vec{\nabla}\phi(P)$ where

$$\vec{\nabla}\phi = \frac{\partial\phi}{\partial x}\hat{x} + \frac{\partial\phi}{\partial y}\hat{y} + \frac{\partial\phi}{\partial z}\hat{z}. \quad (C.6)$$

Note, in the analysis to follow the point P coordinates are given in terms of an (x, y, z) reference system which is coincident with the (x, y, z) system (refer to Figure C.2) in order to distinguish the coordinates of the fixed point P from the surface integration variables.

Now from Figure C.2 we may identify the following relationships:

$$\vec{n} = \hat{z} \quad (C.7)$$

$$|\vec{R}_{s,p}| = [(x-s)^2 + (y-y)^2 + (z)^2]^{1/2} \quad (C.8)$$

$$dS = ds dy \quad (C.9)$$

AXIS CONVENTION RELATING THE
PLANAR N=4 SIDED DOUBLET SURFACE
DISTRIBUTION TO SOME FIELD POINT

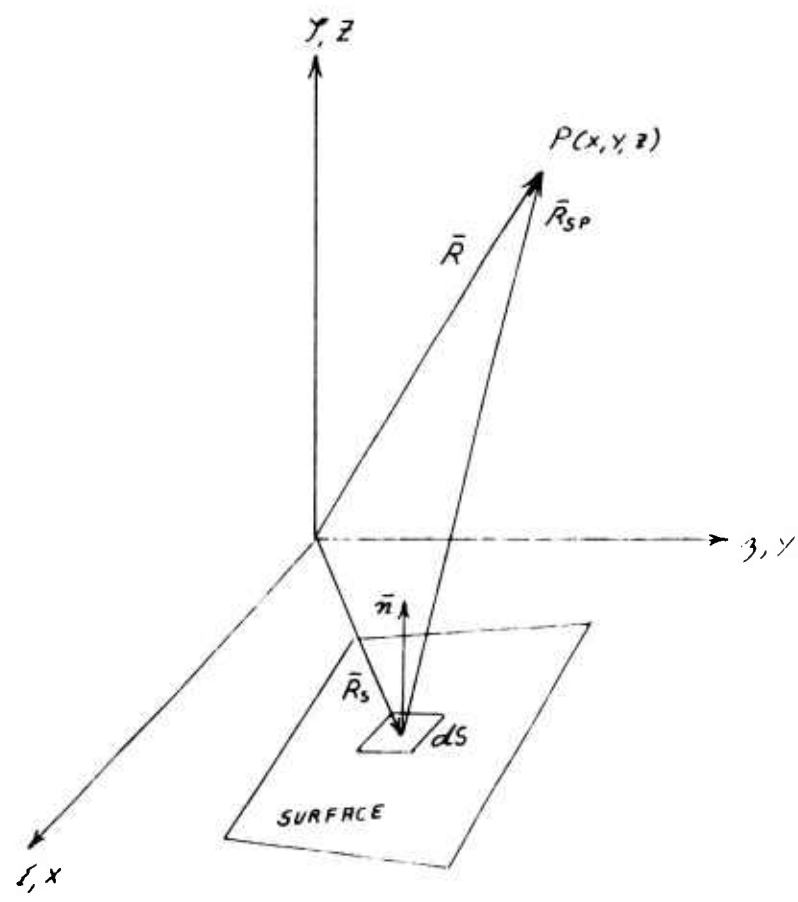


FIGURE C.2

Thus the expression for the doublet potential reduces to

$$A(P) = -\frac{\mu}{4\pi} \int_S \frac{z}{[(x-\xi)^2 + (y-\eta)^2 + z^2]^{3/2}} d\xi d\eta. \quad (C.10)$$

Identifying the integral above as $I(P)$ we may write

$$A(P) = -\frac{\mu}{4\pi} I(P) \quad (C.11)$$

$$\bar{\nabla} A(P) = -\frac{\mu}{4\pi} \bar{\nabla} I(P). \quad (C.12)$$

The problem now is the evaluation of the integral $I(P)$. Given the evaluation of $I(P)$ then the gradient may be obtained by straightforward differentiation. Note that the gradient may be taken inside the integral and then the resulting integrand may be integrated. We choose not to use this procedure as singularities of higher order than what already exist will result. Although these singularities may be evaluated in terms of the Cauchy principal values it does unnecessarily complicate the evaluation.

Let us consider now the evaluation of the integral given by

$$I(P) = \int_S \frac{z}{[(x-\xi)^2 + (y-\eta)^2 + z^2]^{3/2}} d\xi d\eta. \quad (C.13)$$

In Figure C.3a we have sketched the surface S for an $n = 4$ sided figure and have indexed the corner points in a manner such that

INDEXING CONVENTION FOR THE
PLANAR $N=4$ SIDED SURFACE

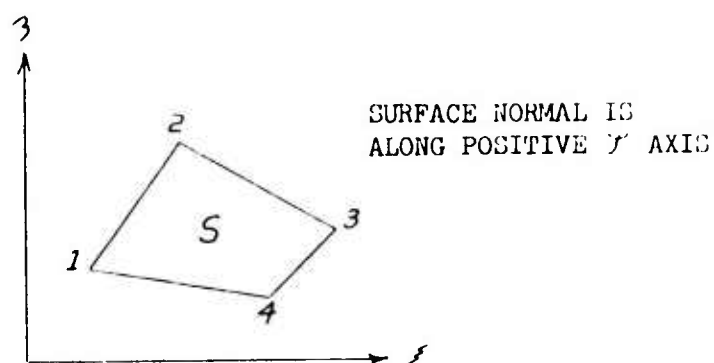


FIGURE C.3a

SUBDIVISION OF REGION S INTO REGIONS R_{ij}

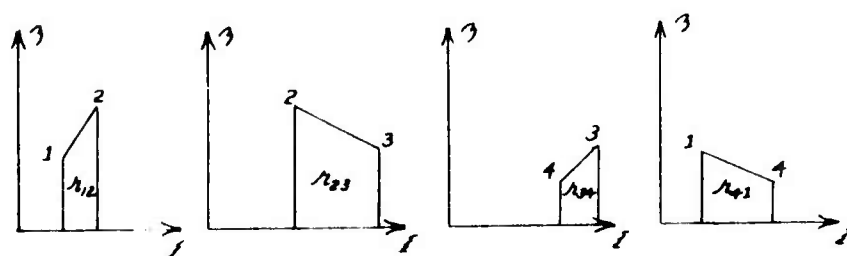


FIGURE C.3b

when viewing the surface along the negative surface normal direction the corner points are indexed consecutively $i = 1, n$ in a clockwise direction. Figure C.3b shows that the surface S may be subdivided into n regions such that the integral may be evaluated as the sum of n integrals each integrated about a specific region, $A_{i,j}$. We may define these regions more precisely if we first let the corner point coordinates be given by $(x, y)_{i,j}$ and define J as the indexed corner point located immediately clockwise (with respect to the negative surface normal direction) to the i indexed corner point. Now the equation of the straight line joining corners i and J is given by $y_{i,j} = m_{i,j}(x)$ where

$$y_{i,j} = m_{i,j}x + b_{i,j} \quad (C.14)$$

where

x lies between x_i and x_j

$$m_{i,j} = (y_j - y_i) / (x_j - x_i) \quad (C.15)$$

$$b_{i,j} = (y_i x_j - y_j x_i) / (x_j - x_i) \quad (C.16)$$

Note at this point that if the slope $m_{i,j}$ of the straight line is infinite a potential problem exists. However, in this case

$x_i = x_j$ and the surface area of the region $A_{i,j}$ is zero. Thus the integral contribution of this region is also zero.

It follows now that the integral $I(P)$ may be written as

$$I(P) = \sum_{i=1}^N \int_{\gamma_i}^{\gamma_{i+1}} \int_0^{\gamma_{i+1}} f(x,y) dz ds \quad (C.17)$$

where

$$f(x,y) = \frac{z}{[(x-y)^2 + (y-z)^2 + z^2]^{3/2}} \quad (C.18)$$

The integration with respect to z may however be rewritten as follows

$$\begin{aligned} \int_0^{\gamma_{i+1}} f(x,y) dz &= \frac{1}{2} \left\{ \int_0^{\infty} f(x,y) dz + \int_{\infty}^{\gamma_{i+1}} f(x,y) dz \right. \\ &\quad \left. + \int_0^{-\infty} f(x,y) dz + \int_{-\infty}^{\gamma_{i+1}} f(x,y) dz \right\} \end{aligned} \quad (C.19)$$

Thus we may write

$$\begin{aligned} I(P) &= \frac{1}{2} \sum_{i=1}^N \int_{\gamma_i}^{\gamma_{i+1}} \left[\int_{-\infty}^{\gamma_{i+1}} - \int_{\gamma_{i+1}}^{\infty} \right] f(x,y) dz ds + \\ &\quad + \frac{1}{2} \sum_{i=1}^N \int_{\gamma_i}^{\gamma_{i+1}} \left[\int_0^{\infty} - \int_{-\infty}^0 \right] f(x,y) dz ds \end{aligned} \quad (C.20)$$

The second summation term is zero, however, since after integrating with respect to β the integration with respect to γ effectively represents a line integral evaluation about a closed path. Thus the integration reduces to

$$J(P) = \sum_{i=1}^N J_i(P) \quad (C.21)$$

where we have defined

$$J_i(P) = \frac{1}{2} \int_{\gamma_i}^{\gamma_i} \left[\int_{-\gamma_{i,1}}^{\gamma_{i,2}} \right] f(\beta, \gamma) d\beta d\gamma. \quad (C.22)$$

The integration with respect to β may be carried out using Reference 15 such that the resulting expression for $J_i(P)$ becomes

$$J_i(P) = -2 \int_{\gamma_i}^{\gamma_i} \frac{(\gamma - \gamma_{i,1}) d\gamma}{[(x-\gamma)^2 + z^2][(x-\gamma)^2 + (\gamma - \gamma_{i,1})^2 + z^2]^{1/2}} \quad (C.23)$$

The evaluation of this remaining integral may be carried out using Reference 16 after substituting for γ, γ using relation (C.14). The resulting analytical algebraic relation for $J_i(P)$ is given by

$$\begin{aligned}
 I_i(P) &= \tan^{-1} \frac{1}{2} \frac{m_{ij} [(x-s_i)^2 + z^2] - (y-a_i)(x-s_i)}{[(x-s_i)^2 + (y-a_i)^2 + z^2]^{3/2}} + \sqrt{} \\
 &- \tan^{-1} \frac{1}{2} \frac{m_{ij} [(x-s_j)^2 + z^2] - (y-a_j)(x-s_j)}{[(x-s_j)^2 + (y-a_j)^2 + z^2]^{3/2}} \phantom{+ \sqrt{}}
 \end{aligned}
 \tag{C.24}$$

Summarizing what we have done to this point, we can write the analytic algebraic expression for the doublet surface potential at some field point P as

$$\phi(P) = - \frac{q}{4\pi} I(P) \tag{C.25}$$

where

$$I(P) = \sum_{i=1}^n I_i(P) \tag{C.26}$$

$$\begin{aligned}
 I_i(P) &= \tan^{-1} \left\{ \frac{1}{2} \frac{m_{ij} \alpha_i - B_i}{r_i} \right\} + \sqrt{} \\
 &- \tan^{-1} \left\{ \frac{1}{2} \frac{m_{ij} \alpha_j - B_j}{r_j} \right\}
 \end{aligned}
 \tag{C.27}$$

$$m_{ij} = (a_j - a_i) / (s_j - s_i) \tag{C.28}$$

$$\alpha_i = (x - s_i)^2 + z^2 \tag{C.29}$$

$$B_i = (x - s_i)(y - a_i) \tag{C.30}$$

$$r_i = [(x - s_i)^2 + (y - a_i)^2 + z^2]^{1/2} \tag{C.31}$$

$$\text{If } s_i = s_j \text{ THEN } I_i(P) = 0. \tag{C.32}$$

The cartesian gradient vector of the potential can now be determined by simply differentiating equation (C.25). The result may be written as

$$\vec{\nabla} A(P) = \frac{\partial A}{\partial x} \hat{x} + \frac{\partial A}{\partial y} \hat{y} + \frac{\partial A}{\partial z} \hat{z} \quad (C.32)$$

where for S a dummy variable of differentiation we find

$$\frac{\partial A}{\partial S} = - \frac{4}{\pi} I_S(P) \quad (C.34)$$

where

$$I_S(P) = \sum_{i=1}^N I_{S_i}(P) \quad (C.35)$$

$$I_{S_i}(P) = \frac{2\lambda_i [m_{iS} \alpha_{iS} - B_{iS}] - [m_{iS} \alpha_{iS} - B_{iS}] [2\lambda_{iS} + \lambda_i \rho_S]}{(2\lambda_i)^2 + (m_{iS} \alpha_{iS} - B_{iS})^2} + 2$$

$$- \frac{2\lambda_i [m_{iS} \alpha_{iS} - B_{iS}] - [m_{iS} \alpha_{iS} - B_{iS}] [2\lambda_{iS} + \lambda_i \rho_S]}{(2\lambda_i)^2 + (m_{iS} \alpha_{iS} - B_{iS})^2} \quad (C.36)$$

$$\alpha_{iS} = \frac{\partial \alpha_i}{\partial S} ; \quad \beta_{iS} = \frac{\partial \beta_i}{\partial S} ; \quad \lambda_{iS} = \frac{\partial \lambda_i}{\partial S} \quad (C.37)$$

$$\text{If } \xi_i = \xi_j \text{ THEN } I_{S_i}(P) = 0. \quad (C.38)$$

The remaining parameters are given by equation (C.28) through (C.31).

The expression for $\bar{\nabla} \phi(P)$ is valid for all $P(x, y, z)$ locations except for a point P lying on the edge of the surface where it is undefined. For a point P in the plane of the surface we find that $\frac{\partial \phi}{\partial x}$ and $\frac{\partial \phi}{\partial y}$ are zero.

The expression for $\phi(P)$ is valid for all $P(x, y, z)$ locations away from the doublet plane. For the point P lying in the plane of the doublet distribution we find that

A. For P within the doublet surface

$$\phi(x, y, 0) = \lim_{z \rightarrow 0^+} \phi(x, y, z) = \frac{\pi}{2} \quad (C.39)$$

B. For P outside the doublet surface

$$\phi(x, y, 0) = 0 \quad (C.40)$$

C. For P on the edge of the doublet surface

$$\phi(x, y, 0) = \text{UNDEFINED.} \quad (C.41)$$

We should note at this point that in the computer program all velocities and lengths are nondimensionalized based on the rotor tip speed (ωR) and the rotor radius (R) respectively. Since $\partial \phi / \partial s$ actually represents the velocity v_s along the \hat{s} direction at point P the form of the preceding equations as

programmed is as follows where the tilda (\sim) represents the nondimensional parameter:

$$\tilde{V}_S(\rho) = \tilde{M} \tilde{I}_S(\rho) \quad (C.42)$$

where

$$\tilde{V}_S = \frac{V_S}{\omega R} \quad (C.43)$$

$$\tilde{M} = -\frac{M}{4\pi \omega A R} \quad (C.44)$$

$$\tilde{I}_S = R I_S \quad (C.45)$$

The actual expression for \tilde{I}_S is the same as for I_S but now all lengths are to be first nondimensionalized by the radius R , for example instead of z read \tilde{z} where $\tilde{z} = z/R$. This completes the discussion of the analytic expressions for $f(\rho)$ and $\bar{V}_f(\rho)$.

APPENDIX D

DETAILED DISCUSSION OF THE COMPUTER PROGRAM

D.1 INTRODUCTION

In the following discussions we will consider the internal structure of the program at the level of the subroutines in terms of their function. Following this we will discuss the program operation and where necessary a specific flow diagram will be presented. The above discussion and flow diagram will then serve as an aid in describing the major program options and the input and output procedures.

In Section 4.0 we noted that the program is divided into seven major programs each of which is concerned with a particular aspect of the overall problem. In the discussions to follow we will consider these programs one at a time and discuss the programs as though they were independent of each other. It will be assumed here that the reader is familiar with the symbols and coordinate reference systems described earlier in Sections (2) and (3).

D.2 MAIN-INFLUENCE CALCULATIONS PROGRAM

In this section we will discuss the program MAIN - INFLUENCE CALCULATIONS. It is the function of this program to define the necessary geometry and to perform the calculations necessary to define the blade and wake influence coefficients. We shall present first a summary discussion of each subroutine found in this program.

D.2.1 Summary Discussion of the Subroutines

The subroutines used in the MAIN - INFLUENCE CALCULATIONS program are summarized here in the general order in which they are called upon by the main program.

Subroutine HEAD(K)

The function of this subroutine is to simply print a heading page indicating the main program title. This page is used as a cover page for the results printed out later.

Subroutine IN1

The function of this subroutine is to accept the card-input necessary to define the rotor blade for the specialized planform option described in section 3.2. The routine also checks certain input before allowing the program to continue to the next step. If an input error is found the program will abort after printing out the data as inputted and additional parameters determined on the basis of input supplied which would have been passed on to other routines.

Subroutine IN2

The function of this subroutine is to accept the card input necessary to define the rotor blade for the general planform option described in section 3.2. It also defines certain parameters based on the input supplied and passes these on to other routines.

Subroutine IN3

The function of this subroutine is to accept the card input necessary to define the rotor free stream conditions, the number of rotor blades and parameters necessary to define the method in which the wake influence calculations are to be performed.

Subroutine IN4

This is an auxiliary subroutine which is not used in the rotor problem. It is an input subroutine compatible with IN3 and is used to input card data comparable to IN3 when the program is selected to do a lifting surface theory analysis of a planar wing rather than of a rotor system.

Subroutine OUT1

The function of this subroutine is to print the input data of IN1. This output serves as a permanent record of the specialized planform geometry specified for the rotor system.

Subroutine OUT2

The function of this subroutine is to print the input data of IN2. This output serves as a permanent record of the general planform geometry specified for the rotor system.

Subroutine OUT3

The function of this subroutine is to print the input data of IN3. This output serves as a permanent record of the specified free stream condition and wake calculation mode selected.

Subroutine OUT4

The function of this subroutine is to print the input data of IN4. The output is comparable to OUT3 except that the output is for the planar wing rather than the rotor system.

Subroutine OUTA

The function of this subroutine is to print out a coordinate description of the airfoil chosen in the specialized planform option. This may be used to check the accuracy with which the airfoil is described in the program. This subroutine supports ROTORG and calls on AFOIL.

Subroutine AFOIL (X,ZU,ZL,DZUDX,DZL DX,BU,BL)

The function of this subroutine may be stated as follows:

Given: A chord station (X), where X represents the chord non-dimensionalized distance from the airfoil leading edge along the chord line,

Find: At the station X, the nondimensionalized upper and lower airfoil thickness (ZU and ZL), the upper and lower airfoil tangent slopes (DZUDX and DZL DX) and the angle the airfoil tangent lines make with the chord line in radians (BU and BL).

The subroutine defines the NACA OOX family of airfoils as a set of equations. The thickness ratio (TC), a parameter in this equation, is transferred to the subroutine implicitly. This subroutine supports ROTORG.

Subroutine ARCL (XI, XF, DARCLU, DARCLL)

The function of this subroutine is to calculate the upper and lower airfoil arc distances (DARCLU and DARCLL) lying between two lines drawn perpendicular to the two chord stations (XI, XF). This subroutine calls on AFOIL and is generally not used in the overall problem. It serves a part in checking the planform description when this option to be described later is chosen. This subroutine supports ROTORG.

Subroutine GEOMR1 (XC, YTS, ITIP)

The function of this subroutine may be stated as follows:

Given: A control point location in terms of a chord station (XC)
and a true span station (YTS).

Find: The actual upper and lower surface coordinates and the local surface tangent slopes in terms of the blade one coordinate system.

The information is transferred implicitly. The parameter ITIP is used to indicate whether the rotor tip or tips are to be faired. This subroutine supports ROTORG.

Subroutine ROTORG

The function of this subroutine is to serve as a control program in order to systematically define the actual control point locations in terms of the blade fixed coordinate system when the specialized planform description option is selected. Its main supporting subroutine is GEOMR1.

In addition to this function the subroutine has an option which serves the purpose of printing the surface grid point coordinates and/or card punching these coordinates in a form compatible with that required as input data by subroutine IN2.

Furthermore, this subroutine contains an option which will calculate mean control surface locations and slopes and print these results. This option may, however, not be selected during the running of the overall program. Independently this option serves as a reference check on the elemental control surface calculations done in a different manner later in the program.

Subroutine SURF

The function of this subroutine is to define an elemental planar four sided control surface in terms of its location, corner point coordinates and transformation matrix given initially four control point locations which do not necessarily lie in a plane. This subroutine supports CSURF and CWAKE.

Subroutine CG (CX,Y,XB,YB,ASUM, A)

The function of this subroutine is to calculate the centroid location $(X,Y)_B$, and area (ASUM) of a four sided planar figure whose corner point coordinates are given by $(X,Y)_{i=1,4}$ where $(X,Y)_1 = (0,0)$ and the corners are numbered in a clockwise direction. This subroutine supports SURF, and APPROX.

Subroutine ROTZ (THETA,X,Y,AJ)

The function of this subroutine may be stated as follows:

Given: A coordinate system (x, y, z) whose origin and transformation matrix are given with respect to an (XYZ) coordinate system by X, Y, Z and AJ .

Find: The origin and transformation matrix of the (x, y, z) system if it is simply rotated about the Z axis through a displacement $THETA$. $THETA$ being positive in the usual sense.

The results are transferred explicitly using X, Y and AJ . This subroutine supports $CWAKE$ and $CBLADE$.

Subroutine CALLOC

The function of this subroutine is to reallocate the main core storage registers.

Subroutine RENUM

The function of this subroutine is to renumber the blade elemental control surfaces in terms of an integer I . Prior to the use of this subroutine the upper and lower control surfaces were sequenced in terms of (N, M) .

Subroutine WT1 (IT1,IRW)

The function of this subroutine is to write or read off external file $IT1$ (depending on whether IRW equals 0 or is not equal to 0 respectively) the control parameters and data allocated in designated

common storage locations LINDA and BRENDA. Some parameters and data in these two locations are needed effectively in all of the major programs. Thus this subroutine and file IT1 serves as a continuity link among the programs.

Subroutine CSURF

The function of this subroutine is to serve as a control program in order to systematically define the geometry of all the blade one elemental control surfaces. The main supporting subroutine used for this task is SURF.

In addition this subroutine computes the free stream velocity conditions on each blade element and writes all the above results on external file IT1.

Subroutine INTEG (X,Y,Z,S,E,XI,XIS)

The function of this subroutine is to calculate the nondimensionalized doublet potential and velocity influence coefficients in a (x, y, z) reference system at a field point (x, y, z) resulting from an M sided planar doublet distribution whose direction is along the x axis and whose corner point locations are given clockwise in the (x, y) plane as $(S, E)_M$. The potential influence coefficient is given by XI, and the velocity influence coefficients in the x, y and z directions are given by XIS(1), XIS(2) and XIS(3) respectively. The subroutine tests to ensure that the field point does not lie on the edge of the planar surface. This subroutine supports CBLADE and CWAKE subroutines.

Subroutine CBLADE (ISTART,ISTOP)

The function of this subroutine is to serve as a control program in order to systematically define the total influence coefficients of all $J=1, JMAX$ blade elements on blade one elements I where I lies inclusively between control input specified elements $I=ISTART$ and $I=ISTOP$.

The blade influence coefficients are calculated with respect to the (X', Y', Z') blade fixed axis system and are written out on file IT2 immediately after all J elements of all blades influence on a blade one element I are known. They are written out as three sets of $JMAX$ influences corresponding to the X', Y' and Z' directional influences.

Subroutine PWAKE

The function of this subroutine is to serve as a preliminary subroutine to the wake subroutine when specific program options are selected. Basically it is used when the blade influence coefficients were defined during a previous execution run and entry is now made into the CWAKE subroutine directly. It serves the function of reading external file IT1 and positioning in main core storage the data necessary to execute the CWAKE routine.

Subroutine CWAKE

The function of this subroutine is to serve as a control program in order to systematically define the total wake influence coefficients of all $M=1, MM$ wake span stations on blade one elements $I=I, IMAX$.

The procedure is to begin at span station $M=1$ and to proceed streamline wise down the wakes calculating wake elements and their influence coefficients with respect to the (X',Y',Z') system on all $I=1, IMAX$ blade elements. At any single wake span station the influences are additive thus a single set of $IMAX$ total influence coefficients is kept. When the final streamwise wake element trailing $M=1$ wake span station is defined the set of three vectored $IMAX$ total wake influence coefficients are written out on external file $IT3$. The procedure is now repeated for span station $M=M+1$ through $M=MM$.

This subroutine also has a planar wake model to be used during the planar wing option.

Subroutine SETUP1

The function of this subroutine is to interchange the $IMAX$ column and three sets of MM rows of data written on external file $IT3$ during the $CWAKE$ routine and write this information on file $IT1$ behind the information already written on $IT1$.

Subroutine APPROX (X,Y,Z,S,E,XI,XIS)

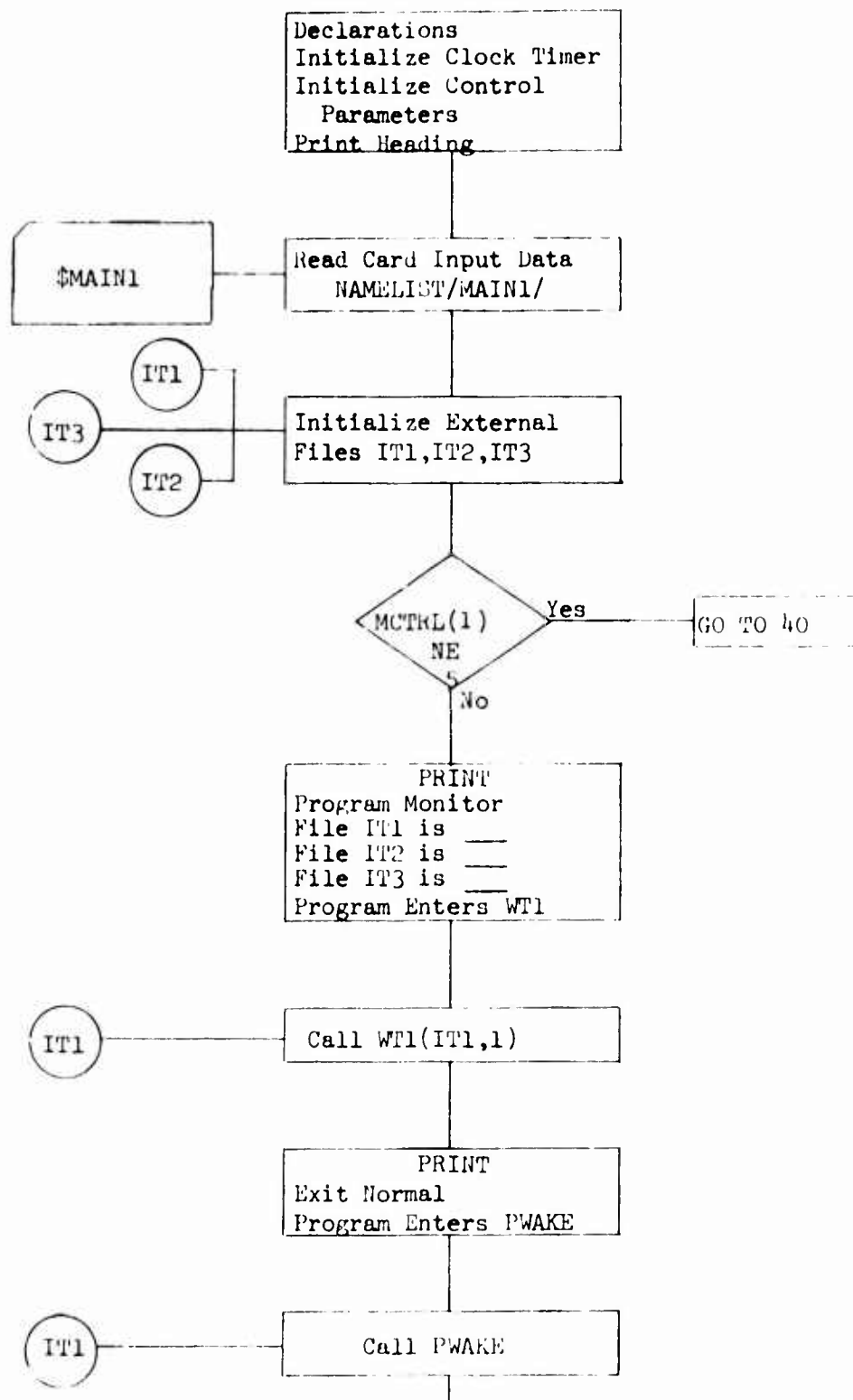
The function of this subroutine is to replace $INTEG$ to calculate the influence coefficients when the field point (X,Y,Z) is farther than a certain distance from the centroid of the doublet element. It uses multi-pole expansion, which is an approximation to the algorithm shown in Appendix C, and will save the time of calculation.

D.2.2 Program Operation in Terms of a Flow Diagram

Having completed now the discussion of the subroutines we may now describe the "Influence Calculation" program in terms of a flow diagram. In Figure D.1 is shown the detailed flow diagram. We have attempted to present this flow diagram at the level of the subroutines. We have indicated in the flow diagram the stages at which input is required and where output is effected. We have shown on the side of the flow diagram proper the supporting elements including external files and supporting subroutines required by each major subroutine called on by the major program.

Note in this diagram that the program has essentially 5 entry points and 5 exit points depending on the value of the parameters MCTRL(1) and MCTRL(2) respectively. Note further that the parameter MCTRL(3) determines whether IN3 (Rotor Analysis) or IN4 (Planar Wing Analysis) is selected. The external files are designated as IT1, IT2 and IT3. If the program is executed from beginning to end in one step three files are required. Note, however, that by executing the program in stages using the program option parameters MCTRL(1) and MCTRL(2) the maximum number of on line external files needed at any one time is two if the number of blade elements is 1000 or less. The third file in this case must be defined as a dummy file, say equal to one of the other two. Files IT1 and IT2 on program completion contain all the information needed in later main programs and are to be considered as permanent storage files. File IT3 on program completion contains wake influence coefficient data which has been rewritten in

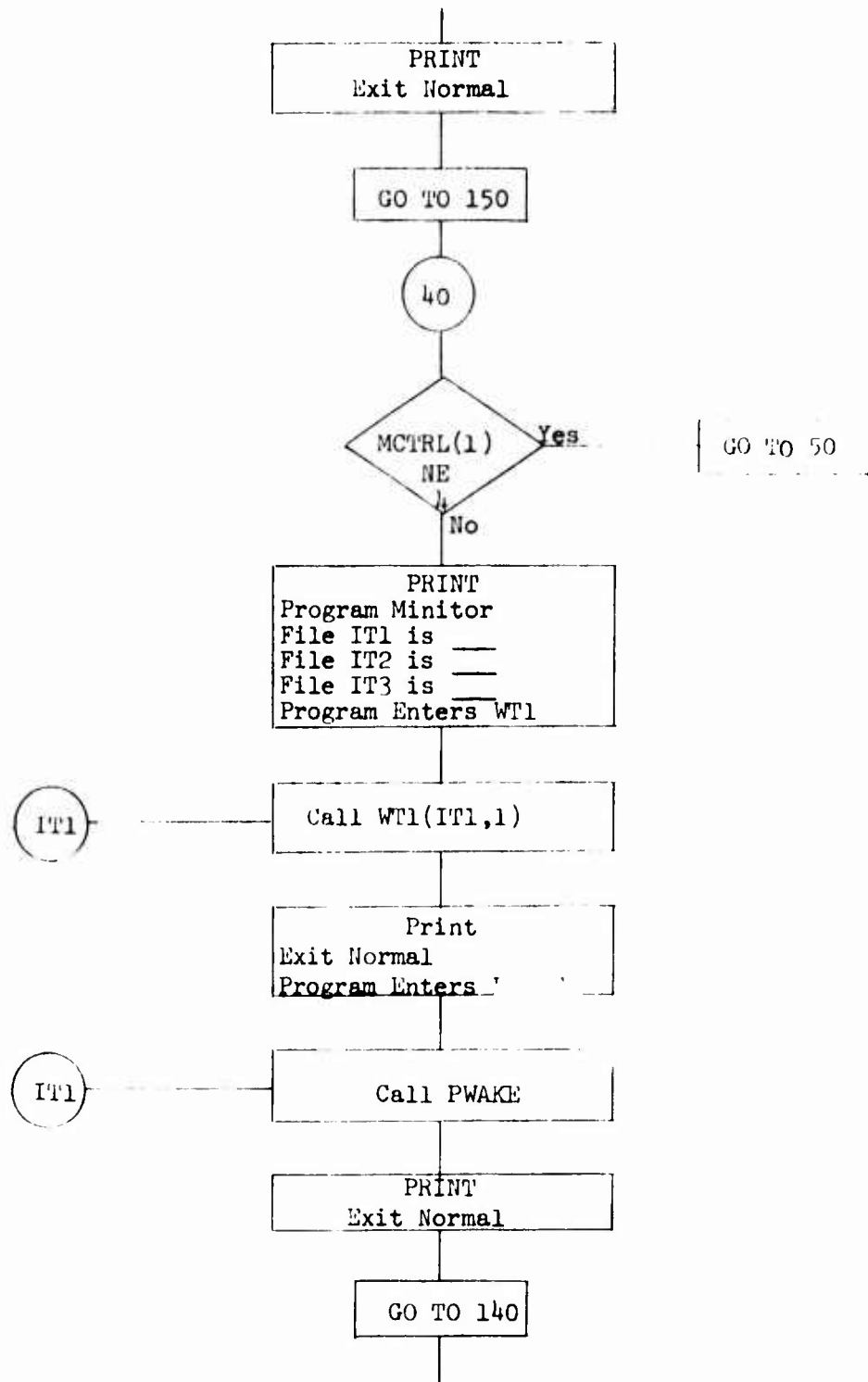
MAIN- INFLUENCE CALCULATIONS
DETAILED FLOW DIAGRAM



(Continued on next page)

FIGURE D.1 (a)

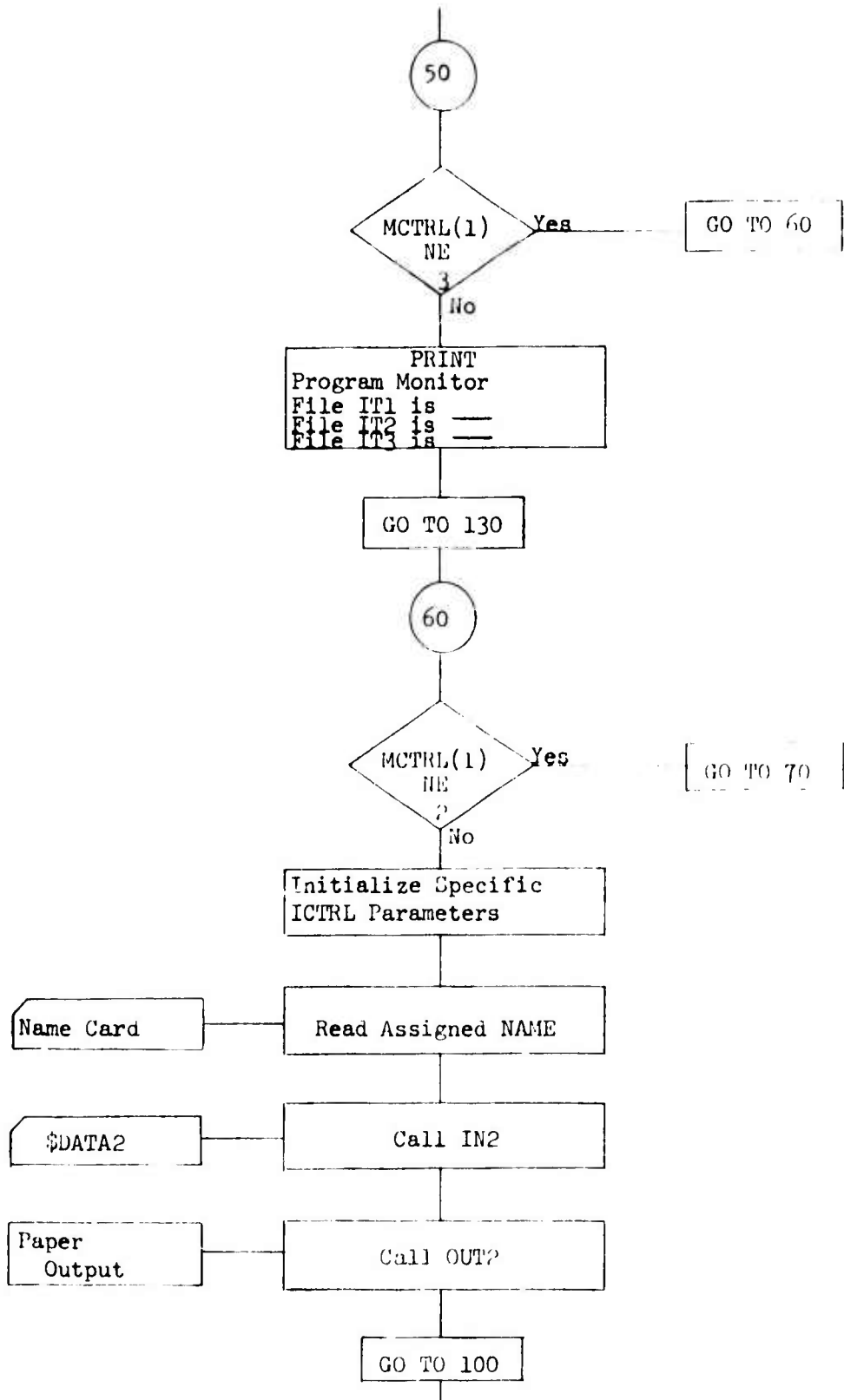
(Continued from previous page)



(Continued on next page)

FIGURE D.1 (b)

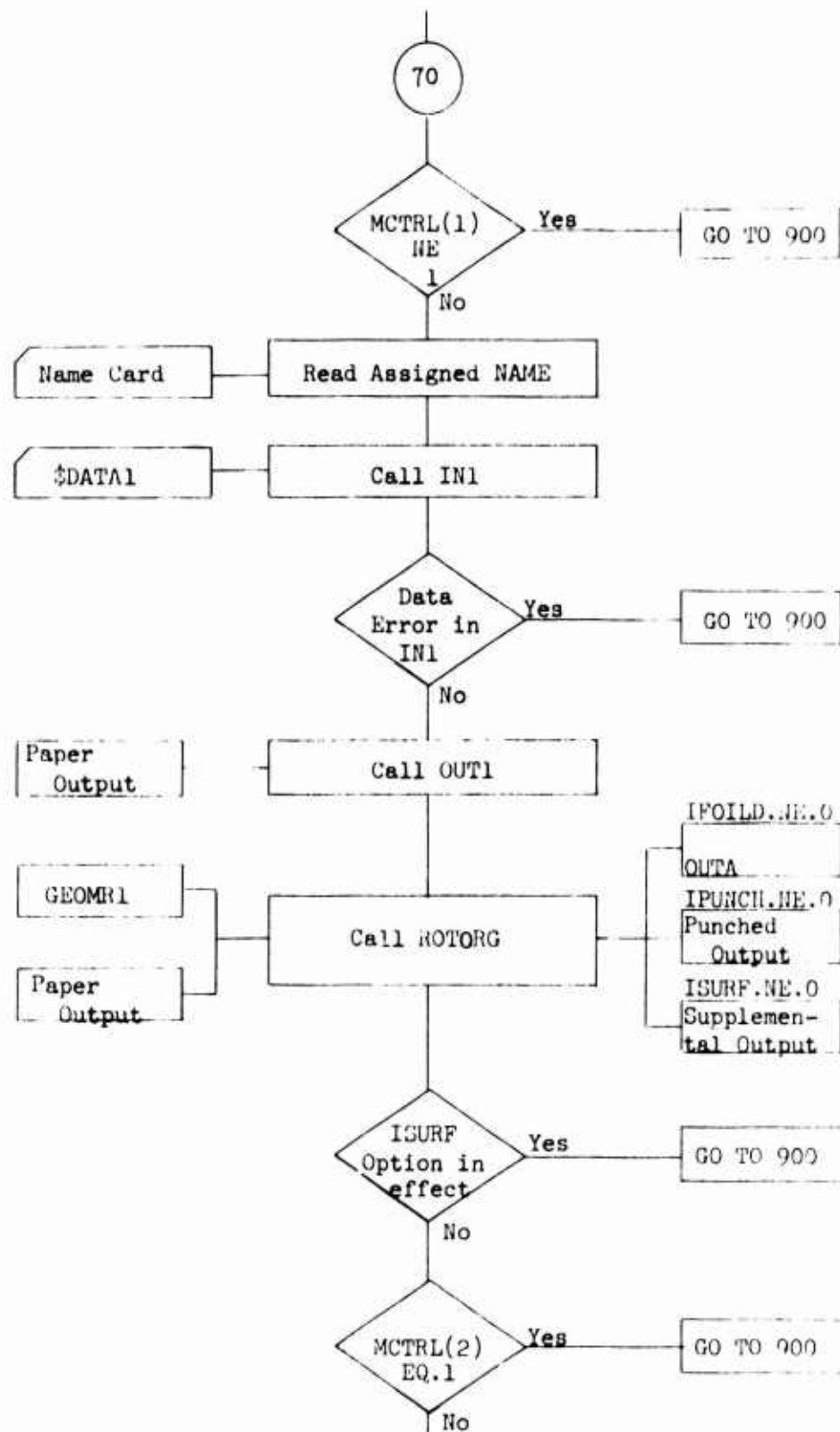
(Continued from previous page)



(Continued on next page)

FIGURE D.1 (c)

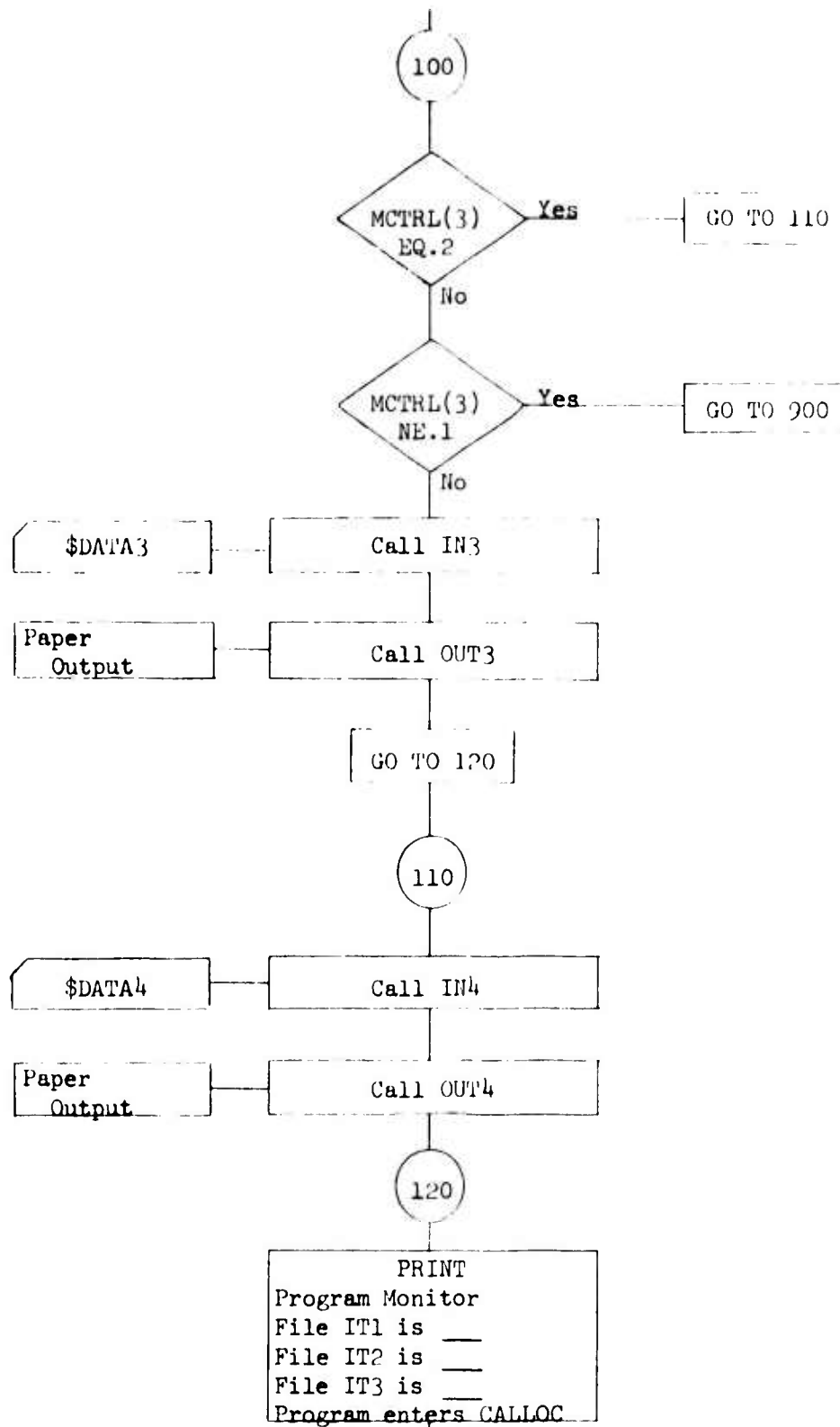
(Continued from previous page)



(Continued on next page)

FIGURE D.1 (d)

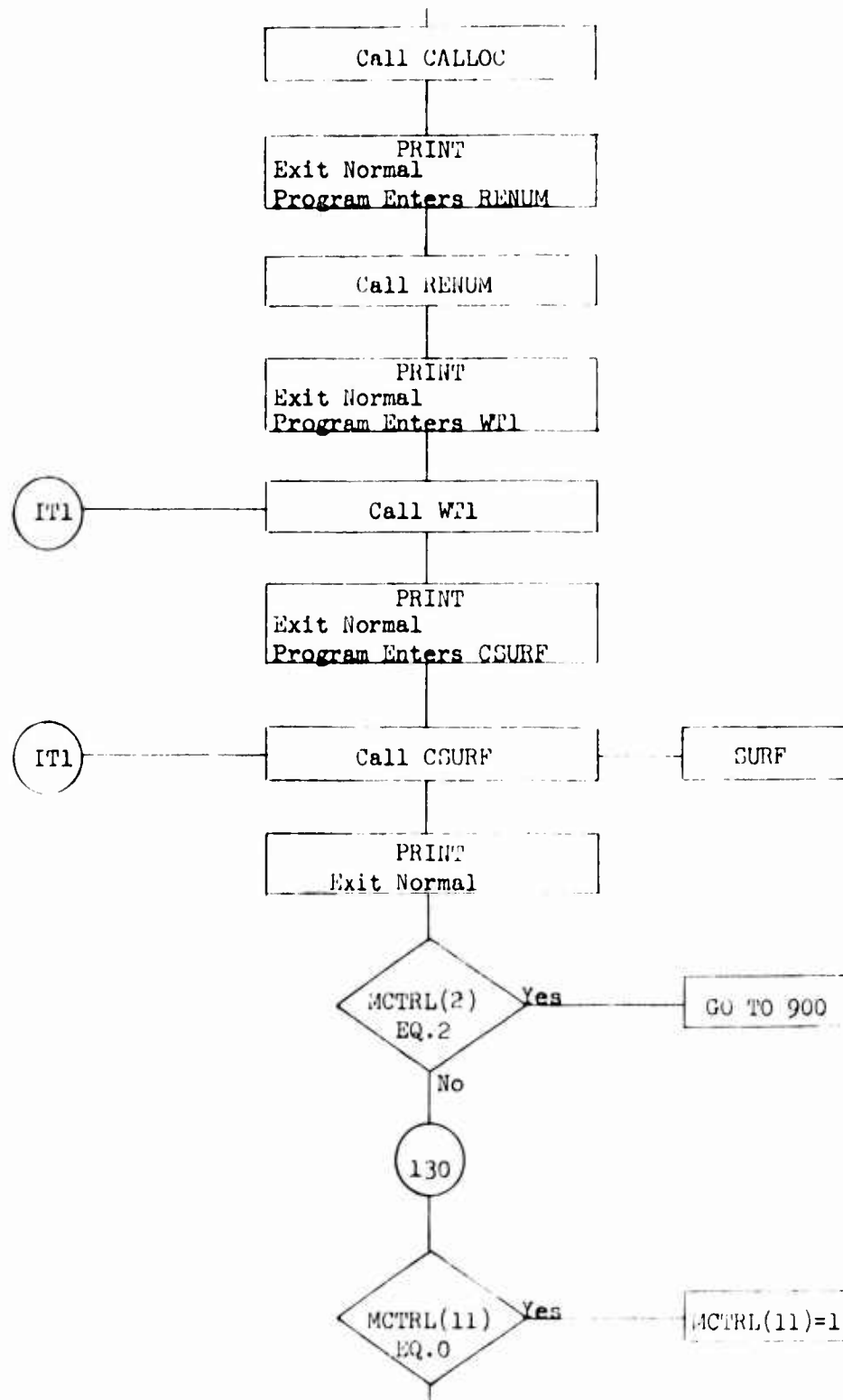
(Continued from previous page)



(Continued on next page)

FIGURE D.1 (e)

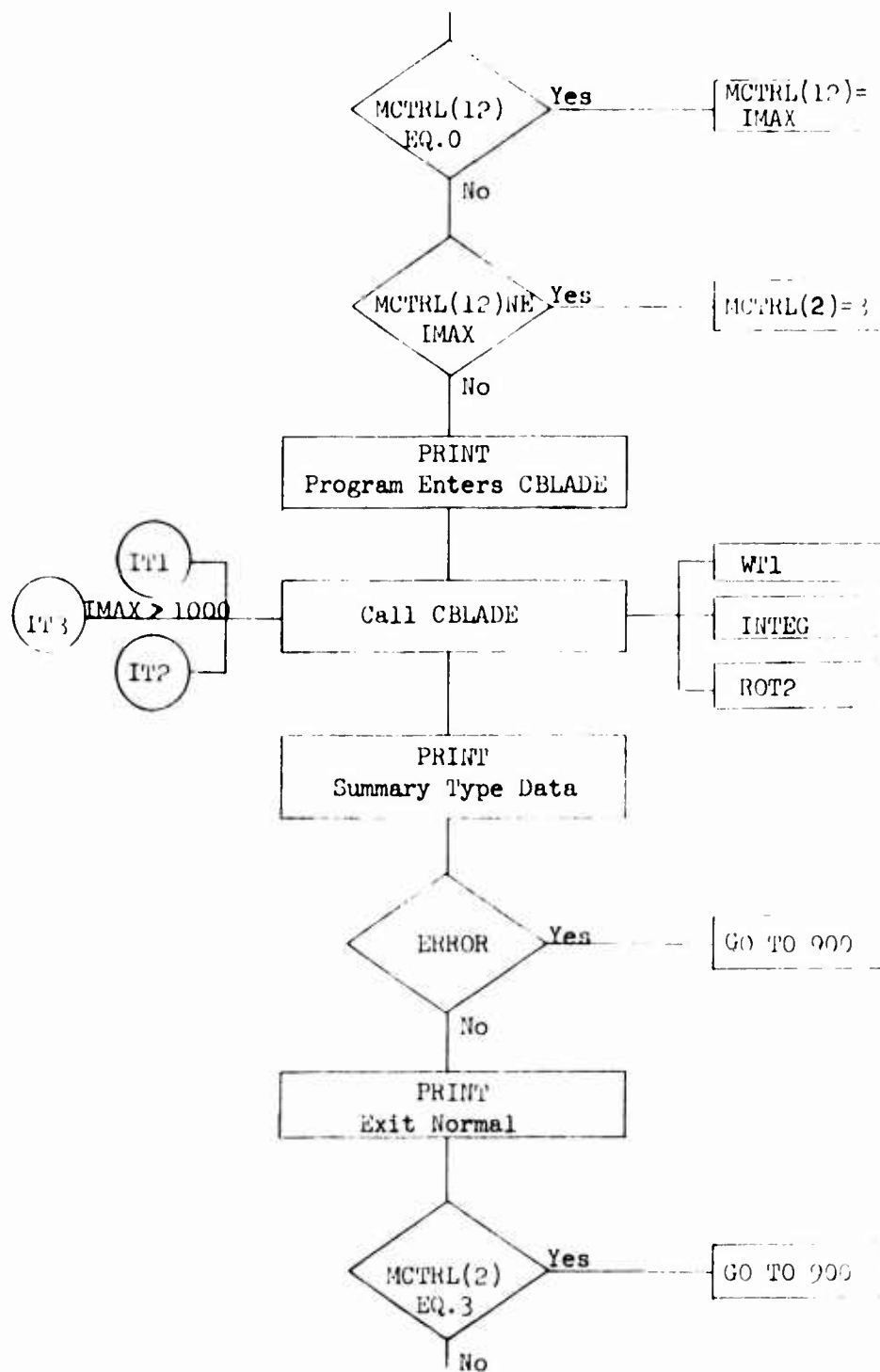
(Continued from previous page)



(Continued on next page)

FIGURE D.1 (f)

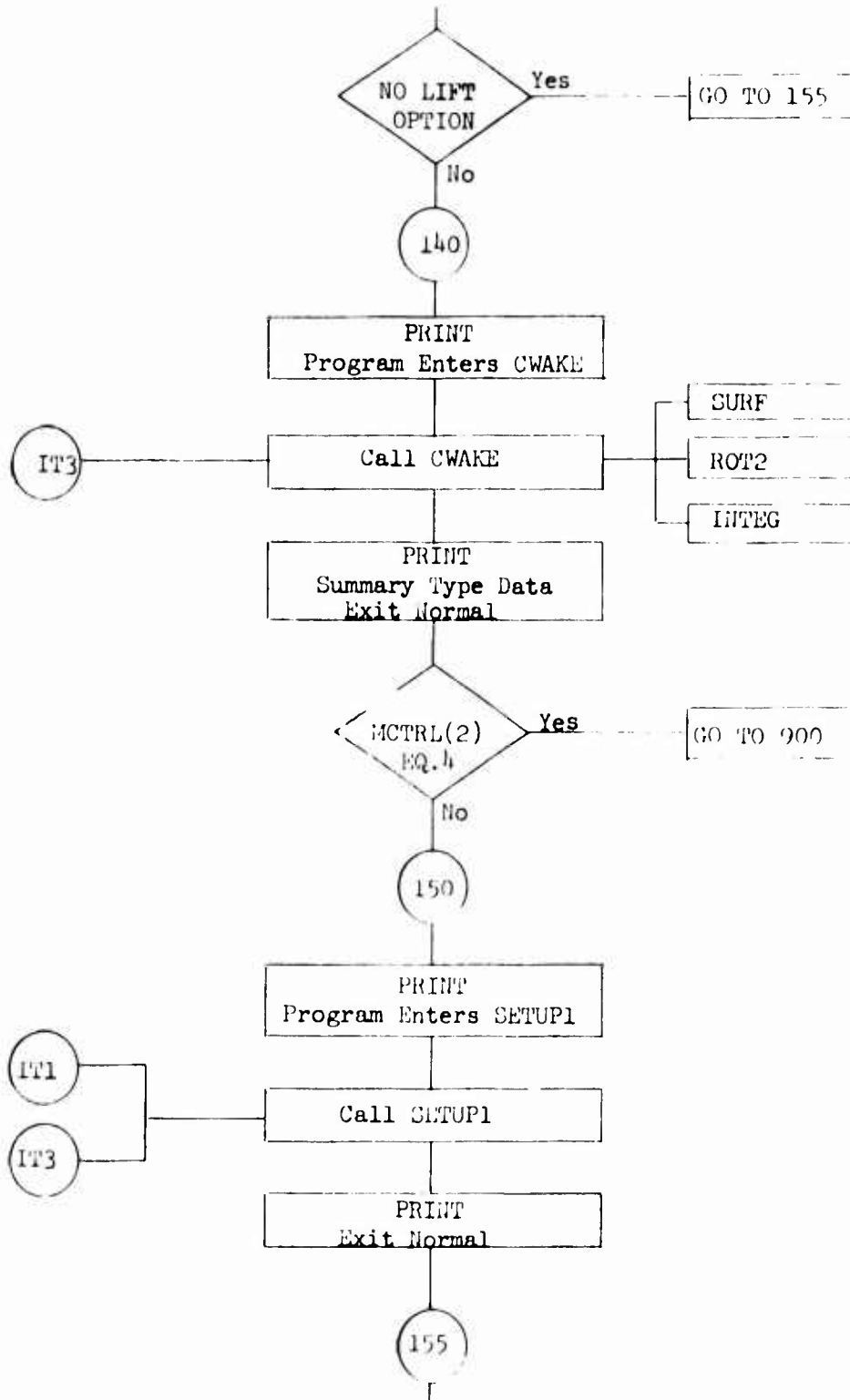
(Continued from previous page)



(Continued on next page)

FIGURE D.1 (g)

(Continued from previous page)



(Continued on next page)

FIGURE D.1 (h)

(Continued from previous page)

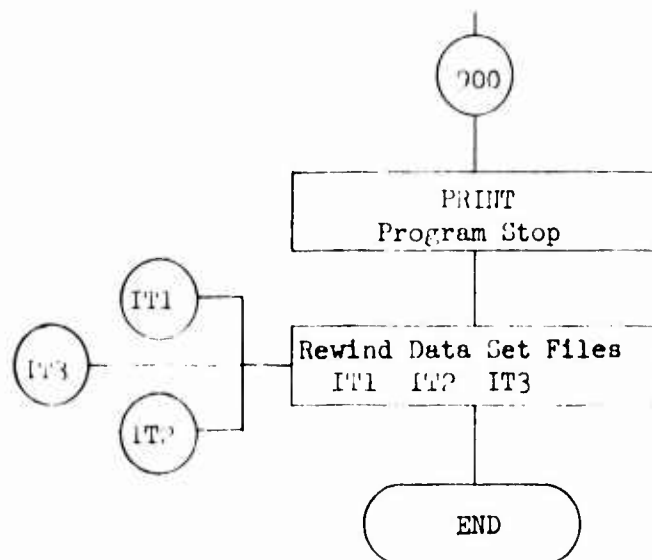


FIGURE D 1 (i)

an altered format on file IT1. As such File IT3 may be discarded on completion of the MAIN - INFLUENCE CALCULATIONS PROGRAM.

D.2.3 Program Input Procedures

The input required and input sequence can be determined from the flow diagram and this of course is a function of the MCTRL parameters which are inputted in the NAMELIST/MAIN1/ data group at the start of the program.

Except for the input read in subroutine IN2 and the identification name assigned to the run, the input is entered in a NAMELIST mode. This allows us to preset the input parameters and only input those parameters which we want to override in any particular run.

We shall consider now the details of inputting the data in the order in which they are executed in the overall program, that is

1. Main Program Control Parameters
NAMELIST/MAIN1/
2. Message Card
NAME
- 3.a Specialized Planform Geometry Description
NAMELIST/DATA2/
or
- 3.b General Planform Geometry Description
- 4.a Rotor Free Stream and Wake Analysis Parameters
NAMELIST/DATA3/
or
- 4.b Planar Free Stream and Wake Analysis Parameters
NAMELIST/DATA4/

1. Main Program Control Parameters

The following data is to be inputted in the NAMELIST/MAIN1/
data statement:

- MCTRL(1) = K (Default value is K = 1)
- K = 5 if the program is to effect execution at SETUP1.
 - K = 4 if the program is to effect execution at CWAKE.
 - K = 3 if the program is to effect execution at CBLADE.
 - K = 2 if the program is to effect execution at the initial
entry point and use the General Planform Option.
 - K = 1 if the program is to effect execution at the initial
entry point and use the Specialized Planform Option
- MCTRL(2) = K (Default value is K = 0)
- K = 4 if the program is to terminate execution after completion
of CWAKE.
 - K = 3 If the program is to terminate execution after completion
of CBLADE.
 - K = 2 if the program is to terminate execution after completion
of CSURF.
 - K = 1 if the program is to terminate execution after completion
of RORORG.
 - K = 0 if the program is to terminate execution after completion
of the entire program.
- MCTRL(3) = K (Default value is K = 1)
- K = 2 if the program is to execute the "Planar Wing Option".
 - K = 1 if the program is to execute the "Rotor Blade Option"
- MCTAL(11) = K (Default value is K = 1)
- K = I where I is an integer indicating the blade element I on
which the blade influence calculations of CBLADE are to
begin. ($1 \leq I \leq I_{\max}$)

MCTRL(12) = K (Default value is K = I_{max})

K = I where I is an integer indicating the blade element I on which the blade influence calculations of CBLADE are to end. (1 ≤ I ≤ I_{max})

IT1 = K (Default value is K = 1)

K = I where I is an integer indicating the external file assigned number on which the control parameters, selected geometry, blade element geometry and on program completion wake influence coefficients are to be written.

IT2 = K (Default value is K = 2)

K = I where I is an integer indicating the external file on which the Blade Influence Coefficients are to be written.

IT3 = K (Default value is K = 3)

K = I where I is an integer indicating the external file on which the Wake Influence Coefficients are initially to be written prior to entering SETUP1.

DUMMY = K

K = I where I is an integer. If the default values of the above parameters are to be selected simply input this parameter.

2. Message Card

Any message or title which is to be assigned to the run for identification is to be inputted here. The message must be on one card and may fill part or all of the 80 column card.

3.a Specialized Planform Description

The following parameters must be inputted as part of the NAMELIST/DATA1/ data statements:

CGU = 0.0, A.a B.b,1.0 (Default values are 0.0)

where SG is maximally dimensioned for 52 real numbers each indicating the true span station along which the upper and lower surface grid control points are to be defined. The first and last station must be 0.0 and 1.0 respectively, where SG = 0.0 is the root span station and SG = 1.0 is the tip span station. The list must be of increasing magnitude.

CGU = 0.0, A.a B.b,1.0 (Default values are 0.0)

where CGU is maximally dimensioned for 52 real numbers each indicating the chord station along which the upper surface grid control points are to be defined. The first and last station must be 0.0 and 1.0 respectively, where CGU = 0.0 is at the leading edge and CGU = 1.0 is at the trailing edge. The list must be of increasing magnitude.

CGL = 0.0, A.a B.b, 1.0 (Default values are CGU)

where CGL is the same as CGU except CGL refers to lower surface grid control points. If no CGL stations are included in the /DATA1/ list the program assumes the chord station grid points are to be symmetric with respect to upper and lower surface and thus sets CGL = CGU for all CGU input points.

TC = 0.a (Default value is 0.0)

where TC is the maximum airfoil thickness to chord ratio of the NACA O0XX family of airfoils.

C = A.a (Default value is 0.0)

where C is the chord length to rotor radius (R) ratio.

B1 = 0.a (Default value is 0.0)

where B1 is the distance the root chord is displaced from the axis of rotation as measured along the span axis and nondimensionalized by the rotor radius. This is the hub radius and must be greater than zero. The true span is defined from this parameter as $(1.0 - B1)$.

B3 = 0.a (Default value is 0.0)

where B3 is the distance the span axis is displaced from the leading edge as measured along the chord line and non-dimensionalized by the chord length.

T0 = A.a (Default value is 0.0)

where T0 is the root airfoil section geometric angle of attack in degrees. The angle is positive in the usual aerodynamic sense and is the angle measured from the plane of rotation to the chord line.

TT = A.a (Default value is 0.0)

where TT is the amount of linear twist in degrees which is to be applied to the rotor blade along the span axis. It is defined as the tip chord geometric pitch less the root chord geometric pitch.

ITIP = K (Default value is K = 0)

where ITIP is an option which allows for fairing of the rotor blade ends. Select K as follows:

K = 2 INBOARD TIP AND OUTBOARD TIP IS FAIRED
 K = 1 OUTBOARD TIP IS FAIRED
 K = 0 NEITHER TIP IS FAIRED

IPRINT = K (Default value is K = 0)

where IPRINT is an option which allows for printing of the computed surface grid point coordinates. Select K as follows:

K = 1 Coordinates are printed
 K = 0 Coordinates are not printed

IPUNCH = K (Default value is K = 0)

where IPUNCH is an option which allows for card punching of the computed surface grid point coordinates in a form compatible for input in the "General Planform Option". Select K as follows:

K = 1 Coordinates are punched
 K = 0 Coordinates are not punched

IFOILD = K (Default value is K = 0)

where IFOILD is an option which allows for computing and printing of the airfoil coordinates at every 1/100th chord station.

Select K as follows:

K = 1 Coordinates printed
K = 0 Coordinates not printed

ISURF = K (Default value is K = 0)

where ISURF is an option which allows for additional elemental surface parameters to be computed and printed. For each element an average location, average slope and calculated surface area are presented. If this option is selected the program will automatically terminate execution after completion of this step. Select K as follows:

K = 1 Additional surface data presented
K = 0 No additional surface data presented

Please note in addition to the above that the maximum number of elemental surfaces that may be defined may not exceed 2000. Thus if NMAXU and NMAXL, are the number of specified chord grid stations on the upper and lower surface and MMAX is the number of specified span grid stations then the following relation must hold

$$\sqrt{(NMAXU-1) + (NMAXL-1)} \sqrt{MMAX-1} \leq 2000.$$

3.b General Planform Geometry Description

In order to discuss the input procedure we must first define a reference system. Let us define a cartesian coordinate system (X_1, Y_1, Z_1) such that the rotor blade axis of rotation is the Z_1 axis. The projection of the blade span axis into the (X_1, Y_1) plane will lie along the Y_1 axis and the X_1 axis will generally be directed toward the pointed trailing edge. The blade must have a non zero hub radius. Now with the rotor blade in its lifting configuration within this reference system one must be able to define a system of surface grid point coordinates as follows:

- A. Inscribe a series of non intersecting lines (not necessarily straight lines) on the rotor blade upper surface joining a point on the root section to a point on the tip section. Two of these lines must lie along the leading edge and trailing edge. Index these lines consecutively as $N = 1, NMAXU$ where $N = 1$ is the line along the leading edge and $N = NMAXU$ is the line along the trailing edge. $NMAXU$ must be no greater than 51.
- B. Repeat (A) above for the lower surface where now $N = 1, NMAXL \leq 51$.
- C. Inscribe a series of non intersecting lines on the rotor blade upper and lower surface starting at a point on the leading edge going to the trailing edge along the upper surface and returning to the leading edge point along the lower surface. Identify these lines as $M = 1, MMAX \leq 49$ where $M = 1$ lies along the root and $M = MMAX$ lies along the tip.
- D. The intersection of a line of constant M with a line of constant N will now define a control grid point indexed as (N, M) . Four lines joining grid points $(N, M), (N, M+1), (N+1, M+1), (N+1, M)$ will define a control surface such that the sum of the control surface areas equals the wetted area of the blade. The number of control surface areas must not exceed 2000, that is $[(NMAXU-1) + (NMAXL-1)] \times (MMAX-1) \leq 2000$.
- E. Now for each grid point (N, M) the blade surface coordinates in terms of (X_1, Y_1, Z_1) must be defined. These lengths are to be non dimensionalized on the rotor radius.

Having determined this information, the data input is card punched and arranged as follows:

1. Punch on one card the value of NMAXU, NMAXL and MMAX according to the FORMAT (3I10).
2. Punch a set of cards such that the complete set of upper surface grid coordinates at all (N,M) grid points is given on these cards as N,M,X1U(N,M), Y1U(N,M), Z1U(N,M) according to the FORMAT (2I5,3E20.6).
3. Repeat (2) above for the complete set of lower surface grid coordinates.

4.a Rotor Free Stream and Wake Analysis Parameters

The following data is to be inputted in the NAMELIST/DATA3/ data statement:

LAMBDA = A.a (Default value is 0.0)

where LAMBDA is the free stream rotor inflow ratio and is given positively by the rotor climb speed divided by the rotor tip speed.

WAV = A.a (Default value is 0.0)

where WAV is the average induced downwash at the trailing edge which may be determined using actuator disk theory assuming a given thrust. This parameter along with LAMBDA is used to prescribe the wake geometry.

DWT1 = A.a (Default value is 20.0°)

where DWT1 is the angle increment in degrees which determines the initial wake elemental areas used for calculating near wake influences.

DWT2 = A.a (Default value is DWT1)

where DWT2 is the angle increment in degrees which determines the wake elemental areas used for calculating far wake influences.

ANGLE = A.a (Default value is 100.0°)

where ANGLE is the angular measure in degrees from the span axis beyond which point the wake calculations are to be done in increments of DWT2.

TURNS = A.a (Default value is 3.0)

where TURNS is the number of wake revolutions from the span axis beyond which the wake calculations are to cease.

INFLU = K (Default value is 0)

where INFLU is an option which allows the program to cease wake calculations at an angle comparable to TURNS above if the wake elemental influence coefficients becomes less than a prescribed amount described in AINFLU below. Select K as follows:

K = 1 to effect this option
K = 0 to negate this option

AINFLU = A.a (Default value is 0.01)

where AINFLU is a parameter defined as the absolute value ratio of the total influence at a point of one wake element to the total influence of another wake element. The point at which the influences are compared is the centroid of the first span station upper leading edge element. The program computes the influence for all elements of wake span station one comparing this always to the influence of the first wake element. When this ratio becomes less than AINFLU the parameter TURNS is redefined to effect the termination of calculations at this point for all span stations.

ISAFE = K (Default value is 250000)

where ISAFE is a parameter which indicates the total number of wake elemental influence calculations that are to be performed. Internally the program computes from this the maximum number of wake elements trailing any one blade at one span station that will approximate this ISAFE number of calculations thus it ensures all span wake segments have the same number of spiral wake elements.

NLIFT = K (Default value is 0)

where NLIFT is a parameter which indicates whether the program is to include a wake analysis (Lift Case) or is not to include a wake analysis (No Lift Case). Select K as follows:

K = 1 NO LIFT OPTION
K = 0 LIFT OPTION

LMAX = K (Default value is 2)

where LMAX is the number of equally spaced, identical rotor blades.

Note that in the above data there are three input parameters (TURNS, INFLU, ISAFE) which may be used to terminate the wake analysis calculations. They are in fact independent of each other.

4.b Planar Free Stream and Wake Analysis Parameter

The following data is to be inputted in the NAMELIST/DATA4/ data statement:

WAV = A.a (Default value is 0.0)

where WAV is the average induced downwash at the trailing edge nondimensionalized by the free stream velocity. This velocity is used to wash the wake below the plane of the free stream velocity.

NLIFT = K

where NLIFT is as defined in the preceding section.

Please note that the planar wing analysis option of this program has not at the present time been thoroughly checked. It is included here only to document the program. The planar wing analysis option

is obtained by altering the rotor blade analysis routine and we acknowledge the fact that this approach is very inefficient.

D.2.4 Program Output

The main output from this program is as follows:

- A. Printed output which essentially prints out the data that was read into the program.
- B. Printed output which essentially is a program monitor. This output indicates the cumulative time at which the major subroutines were entered and whether they terminated normally. Additional output indicating specific items are included in the CBLADE and CWAKE related monitor output statements. This output is self explanatory.
- C. Data output stored on external files IT1 and IT2. Unlike items (A) and (B) above this output is required for the continuation of the overall program. We will describe the detailed data on these two files when we discuss the "MAIN-PRINT" program whose function is to retrieve specific data from these files and print on paper this data.

In addition to the above listed output additional output may be selected. We have already discussed the nature of this output in the section describing the input procedures and program options available. The output as printed is self-explanatory.

D.3 MAIN - CREATE SOLUTION FILE PROGRAM

In this section we will discuss the program MAIN - CREATE SOLUTION FILE. This program is rather straightforward with its function being to operate on the coefficient data written on external files IT1 and IT2 by the MAIN - INFLUENCE CALCULATION program, in order to generate the set of normal influence coefficients and normal free stream velocities. This set of coefficients and velocities are then stored on external file IT3 or IT3 and IT4 in a form compatible for the solution programs which will be discussed in the next section.

D.3.1 Summary Discussion of the Subroutines

Subroutines SETUP2 (IT1, IT2, IT3)

The function of this subroutine is to generate from the data given on external files IT1 and IT2 the set of normal influence coefficients expressed as an IMAX square matrix [A] and to generate the set of IMAX normal free stream velocities expressed as the negative of the IMAX matrix |B| such that the linear set of IMAX algebraic equations to be solved is of the form

$$[A] |x| = |B|$$

This data is then written on external file IT3 in double precision as follows where each line represents a separate write statement:

IMAX

B(1), B(2), (B3) B(IMAX)
 A(1,1), A(1,2) A(1, IMAX)
 .
 .
 .
 .
 .
 A(IMAX,1) A(IMAX,IMAX)

This data file is compatible with the exact solution program discussed later.

Subroutine SETUP3 (IT1,IT2,IT3,IT4)

The function of this subroutine is the same as SETUP2 to the point where the algebraic equations are defined by

$$[A] |X| = |B|$$

This subroutine further operates on the coefficient such that the set of equations may be written as

$$x_I = -\frac{1}{a_{II}} [a_{I1} x_1 + a_{I2} x_2 + \dots + a_{I,I-1} x_{I-1}] + \frac{b_I}{a_{II}}$$

which in matrix form becomes

$$|X| = [C] |X| + |D|$$

where

$$[C] = \begin{vmatrix} 0 & -\frac{a_{21}}{a_{11}} & -\frac{a_{31}}{a_{11}} & \dots & -\frac{a_{i1}}{a_{11}} \\ \frac{a_{21}}{a_{21}} & 0 & \dots & \dots & -\frac{a_{21}}{a_{11}} \\ -\frac{a_{31}}{a_{33}} & \dots & \dots & \dots & \dots \\ \dots & \dots & \dots & \dots & \dots \\ -\frac{a_{i1}}{a_{i1}} & \dots & \dots & \dots & 0 \end{vmatrix}$$

$$D_i = \frac{v_i}{a_{i1}}$$

This subroutine then writes on external file IT3 the $[C]$ matrix as shown below where each line represents a separate write statement:

```

C1,1 C1,2 C1,3 . . . . . C1,IMAX
C2,1 C2,2 . . . . .
.
.
.
CIMAX,1 . . . . . CIMAX,IMAX

```

On external file IT4 is written the column matrix $|D|$.

This data as written on files IT3 and IT4 is compatible with the iteration program discussed later.

Subroutine WT1

See discussion in section D.2.1.

D.3.2 Program Operation

The program operation requires three or four external files depending on whether the solution will be obtained using the exact elimination or the iterative solution method respectively. If three files are required then the fourth file must be defined as a dummy file. Since the main program simply calls on either one of two sub-routines no flow diagram will be presented.

D.3.3 Program Input

The input required consists of the following parameters given as part of a NAMELIST/SOLUF/ data statement:

METH = K

where METH is a control parameter which indicates the proper solution file to be created. Select K as follows:

K = 1 Elimination Solution File
K = 2 Iterative Solution file

IT1 = K (Default value is 1)

where K is the reference number assigned to the comparable external file IT1 of the Main - Influence Coefficients program. No changes will be made to the file contents.

IT2 = K (Default value is 2)

where K is the reference number assigned to the comparable external file IT2 of the Main - Influence Coefficient program. No changes will be made to the file contents.

IT3 = K (Default value is 3)

where K is the reference number assigned to the input file created.

IT4 = K (Default value is 4)

where K is the reference number assigned to the additional solution file required if METH = 0 option is used. If METH = 1 option is chosen input the same reference number for IT4 as inputted for IT3.

D.3.4 Program Output

The output of this program consists of the following:

- 1) A printed statement indicating whether the elimination or iterative solution file was created.
- 2) Data written on external file IT3 if the elimination solution file was created or data written on external file IT3 and IT4 if the iterative solution file was created.

D.4 MAIN - SOLVE BY ELIMINATION PROGRAM

In this section we will discuss the program MAIN - SOLVE BY ELIMINATION. The function of this program is to solve a simultaneous set of equations using the Gaussian elimination method with pivotal condensation as described in Section 3.6. This program is not competitive with routines not requiring peripheral storage and it is suggested that this method be used only for simultaneous sets of equations having less than 350 unknowns because of time considerations.

D.4.1 Summary Discussion of the Subroutines

Subroutine SSIMQ

The function of this subroutine is to accept the coefficients as written on an external file in the manner described in the discussion of subroutine SETUP2 (Section D.3.1) and operate on this matrix of coefficients in order to reduce it to an effective diagonal matrix whose lower half is composed of zero elements. This is the pivot elimination part of the solution routine.

Subroutine BSUB

The function of this subroutine is to operate further on the diagonal matrix derived from SSIMQ and by the back substitution method obtain the unknowns to the simultaneous set of equations.

Subroutine HEAD

Refer to Section D.2.1.

D.4.2 Program Operation

The operation of this program is relatively straightforward. It does require four or three external data files depending on whether the initial coefficients are to be saved until the solution is completed or not saved respectively. The initial data must be given on file ITF and the final results are written on file ITF. Files labeled ITA, and ITC should be high speed data files as they are actively used in the elimination phase of the program. If the initial data is not to be kept, file ITF and file ITA may be the same file. File ITB is used to record the diagonal matrix and subsequently is used along with file ITF in the back substitution phase of the problem. The speed of transferring data from files ITB and ITF into and out of main core storage is not as critical as for ITA and ITC.

The program does contain a series of options which allow the solution to proceed in a series of executable runs or in one single executable run. These options are described in the next section but briefly we may list the options here as follows:

- A. The program may proceed from data entry through the elimination phase, through the back substitution phase to the recording of the solution value.
- B. The program may proceed from data entry into the elimination phase and terminate after a given amount of time has elapsed, or after the elimination phase is completed.
- C. The program may be restarted in the elimination phase and terminated as in (B).
- D. The program may initiate execution in the back substitution phase.

The solution values as written on file ITF are in a form compatible for input into the program MAIN - MOVE SOLUTION FILE which transfers the answers to one of the two permanent files.

D.4.3 Program Input

The following parameters are to be inputted as part of the NAMELIST/SELIM/ data statement:

IP = K

where IP is an option control parameter such that for:

- K = 0 The program will solve the system of equations in one execution step.
- K = 1 The program will begin execution in the back substitution routine assuming the elimination phase has been completed and the necessary data is on file ITB described later.
- K = 2 The program will begin execution as for K = 0 above but will terminate after the elimination phase is completed.
- K = 3 The program will restart in the elimination routine at elimination row (M) and pivot row (N) described later in the TMAX discussion.

TMAX = A.a

(Default value is 1200.0)

where TMAX is a parameter which is an input estimate of the time in seconds required for the elimination phase of the program. If the elimination phase has not been totally completed by this time the program will terminate the elimination phase after setting up files ITA and ITB in a manner compatible for the restart option selected by IP = 3 above. All restart information including the restart elimination row (M) and pivot row (N) are written for files ITA and ITB.

IMAX = K (Default value is 0)

where IMAX is a parameter indicating the number of unknowns in the system of equations.

DUMMY = K

where K must be inputted as 6926 if TMAX above is greater than or equal to 1200.

ITA = K (Default value is K = 1)

where K is the reference number assigned to external file ITA which is a data file active in the elimination routine and contains data necessary for the restart option.

ITB = K (Default value is K = 2)

where K is the reference number assigned to external file ITB which is a data file active in the elimination routine and contains data necessary for the restart option and the back substitution routine.

ITC = K (Default value is K = 3)

where K is the reference number assigned to external file ITC which is a temporary data file active in the elimination phase. The data written on it is not necessary for the restart option or back substitution routine.

ITF = K (Default value is ITA)

where K is the reference number assigned to external file ITF which is the initial data input file created by program "MAIN-CREATE SOLUTION FILE".. This is also the file on which the final solution values are written replacing the column input data record. File ITA may be taken to be the same as file ITF but in this case the data is destroyed before the program has obtained the solution values.

D.4.4 Program Output

The main output of this program consists of the following:

- A. A printed statement indicating whether a successful solution or singular solution resulted or a statement indicating where the solution was terminated.
- B. A printed listing of the solution values which are also written on File ITF in a form compatible for data-input into the program MAIN - TRANSFER SOLUTION FILE.

If the elimination phase is to be run in stages, files ITA and ITB should be considered as output both of which are needed as the data set input for the restart option.

If the program terminates after the elimination phase then file ITB should be considered as output which becomes the data set input for the back substitution phase.

D.5 MAIN - SOLVE BY ITERATION PROGRAM

In this section we will discuss the program MAIN - SOLVE BY ITERATION. The function of this program is to solve a simultaneous set of equations using the simultaneous displacement iterative method described in section 3.6.

D.5.1 Summary Discussion of the Subroutines

Subroutine ITER(FB,FC,IMAX,K,KMAX,DELTA,TMAX,IR)

The function of this subroutine is to perform the actual iterative procedure. The IMAX set of coefficients are given on external files labeled FB and FC which are described in section D.3.1 in the discussion of SETUP3. The parameter K indicates the iteration number. Delta is a test parameter which dictates the greatest difference that all present solution values may differ from their previous iterative values in order for the iteration scheme to be completed. KMAX and TMAX are parameters which may terminate the iterative scheme after KMAX iterations or after TMAX elapsed seconds. The parameter IR is a return code indicating on what basis the subroutine execution was terminated.

Subroutine DIFF (FB,FC,IMAX,K)

The function of this subroutine is to compute the value of the solution vector using the coefficients and compare this value to the K^{th} iterative solution vector and print out the results.

Subroutine HEAD(K)

Refer to section D.2.1.

D.5.2 Program Operation

The program operation requires two external data files. These files are the solution files created in the MAIN - CREATE SOLUTION FILE program and are discussed more specifically in the SETUP3 discussion of section D.3.1.

The program contains a number of options which permit the program to terminate when a certain convergence criteria is established, or when a given number of iterations have been performed or when a given amount of time has elapsed. The program prior to termination writes out on one of the external data files the latest iterative solution values thus allowing the program to be executed again using these last values as the initial iterative values for another series of iterations. The solution values are written on file FC immediately after the data records written on file FC by SETUP3 and they are written in a form compatible for input into the program MAIN - TRANSFER SOLUTION FILE which transfers the solutions to one of the two permanent files.

D.5.3 Program Input

The following parameters are to be inputted as part of the NAMELIST/SITER/ data statement:

FB = N (Default value is N = 1)

where N is the reference number indicating the external file on which the square coefficient matrix is written. This data file is data file IT3 created in the MAIN - CREATE SOLUTION FILE program if option METH=0 was executed. (Refer to section D.3)

FC = N (Default value is N = 2)

where N is the reference number indicating the external file on which the column matrix is written. This data file is data file IT4 created in the MAIN - CREATE SOLUTION FILE program if option METH=0 was executed. (Refer to section D.3). During execution the present iteration solution values are stored on this file immediately after the column matrix record destroying any other previously written iterative values.

IMAX = N (Default value is N = 0)

where N is the number of unknowns.

K = N (Default value is N = 0)

where the parameter K dictates whether previous iterative solution values are stored on file FC and are to be used as starting iterative values. Select N as follows

N = 1 Indicates previous solution values are stored on file FC and are to be used as starting iterative solution values.

N = 0 Indicates no previous solution values are stored on file FC and the program will assume the starting iterative solution values to be all zero.

KMAX = N (Default value is N=K+10)

where the value of N indicates the number of iterations to be performed subject to DELTA and TMAX constraints described below.

TMAX = A.a (Default value is 120.0)

where A.a is the cumulative time in seconds after which the program is to terminate the iteration scheme.

DELTA = A.a (Default value is 0.01)

where DELTA is a convergence criteria such that if all calculated values of the solution vector less the iterative solution vector values divided by the calculated solution vector values are less than DELTA in the absolute sense, then the iteration scheme is terminated.

D.5.4 Program Output

The printed output of the program consists of the following:

1. A printed line of output after each iteration which indicates the iteration number, the number of present solution values whose change from the previous solution values are less than the prescribed convergence parameter, the cumulative time and the actual value of the first number in the solution vector and its change from its previous value.
2. A printed line indicating on what basis the program terminated.
3. After the last iteration the entire solution vector and the difference vector (present solution less previous solution) are printed.

In addition to the above the solution vector is also written on file FC and this output should be considered as input for successive iteration program executions or for input to the MAIN - TRANSFER SOLUTION FILE program.

D.6 MAIN - TRANSFER SOLUTION FILE PROGRAM

The function of the MAIN - TRANSFER SOLUTION FILE program is to read the solution values written on an external file by either the elimination or iteration scheme program and to write these same answers on one of the two permanent files so that the two permanent files now have recorded on them all the information necessary to compute the various velocities, pressures and forces.

The program requires two files for its operation and is rather straightforward. The input required for this program includes the specification of the following two parameters as part of the NAMELIST/MOVEC/ data statement:

FA = K (Default value is K = 1)

where K is the reference number assigned to the permanent file FA which was initially created in the MAIN - INFLUENCE CALCULATIONS program and was there designated file IT1.

FC = K (Default value is K = 4)

where K is the reference number assigned to the file FC which has written on it the solution vector. If the solution was obtained using the elimination method then file FC is identical to the elimination file ITF. If the solution was obtained using the iterative scheme then file FC is identical to the iterative file FC.

The printed output of this program is simply a statement indicating successful completion of the program.

D.7 MAIN - VELOCITY CALCULATIONS PROGRAM

In this section we will discuss the MAIN - VELOCITY CALCULATIONS program. The function of this program is to compute on each blade element $I=1, I_{MAX}$, the various velocities, pressure coefficients and forces and to print these results as well as a summary of the geometry for each of these blade elements. The program also computes and prints the rotor thrust, torque and in plane force coefficients. The subroutines called are WT1 and HEAD. These have previously been discussed in section D.2.1 and will not be repeated here.

The program requires for its operation the two external permanent files initially created in the MAIN - INFLUENCE CALCULATIONS program and a temporary file to be used during the execution of this program.

D.7.1 Program Input

The program receives all of its data input from the permanent file. The card data input includes specification of the following parameters as part of the NAMELIST/DATAV/ data statement:

IT1 = K (Default value is K = 1)

where K is the reference number assigned to the permanent external file IT1. This file is to be identical to file IT1 created in the MAIN - INFLUENCE CALCULATIONS program.

IT2 = K (Default value is K = 2)

where K is the reference number assigned to the permanent external file IT2. This file is to be identical to file IT2 created in the MAIN - INFLUENCE CALCULATIONS program.

IT3 = K

where K is the reference number assigned to the temporary external file IT3. This file is used during execution of the program and upon completion contains no useful information.

D.7.2 Program Output

The program prints out the following summary results using the indicated symbols for each blade surface element $I=1, I_{MAX}$:

1. Element index location in terms of I and in terms of indices (N,M) where N is the chord station and M is the span station.
2. Centroid location in terms of the blade fixed coordinate system. The symbols used is RCG where $RCG = (XCG^2 + YCG^2)^{1/2}$.
3. The length of the curve connected by the centroids, starting from the leading edge, following the chordwise direction and ending at the trailing edge. The symbol used is CHODTL.
4. Nine components of the transformation matrix between the elemental surface coordinate system and the blade fixed coordinate system. The symbols used are TPLX, TPLY, TPLZ, TP2X, TP2Y, NX, NY, NZ.
5. The chordwise and spanwise surface velocities and their resultant at the centroid of the element with respect to the blade fixed coordinate system. The symbols used are VT1', VT2', and VT'.
6. The free stream velocity and its components at the centroid of the element with respect to the blade fixed coordinate system. The symbols used are respectively VINFX', VINFY', and VINFZ'.
7. The components of the free stream velocity in chordwise and spanwise directions at the centroid of the element with respect to the blade fixed coordinate system. The symbols used are VINFT1' and VINFT2'.
8. The derivatives of the velocity potential in both chordwise and spanwise directions. The symbols used are DPHIDC and DPHIDY.
9. The pressure coefficient, CP1, nondimensionalized on the basis of the tip speed velocity.
10. The pressure coefficient, CP2, nondimensionalized on the basis of the local free stream velocity.

11. The ratio of the surface velocity to the free stream velocity (V_T/V_{INF}).
12. The doublet strengths, MU .
13. The velocity potentials, PHI .
14. The angle that the surface velocity makes with the chordwise direction, $THETA$.
15. The elemental force components (F_{XE} , F_{YE} , and F_{ZE}) in terms of the blade fixed coordinate system.
16. The elemental torque (Q_{ZE}) about the axis of rotation.

All lengths and velocities above are nondimensionalized on the basis of the rotor radius and tip speed respectively.

In addition to the above a summary of the rotor aerodynamic coefficients are printed. This output is self explanatory. Also the differences between the pressure coefficients of upper and lower surfaces are calculated and printed.

D.8 MAIN - PRINT PROGRAM

In this section we will discuss the MAIN- PRINT program. The function of this program is to selectively read data stored on the two permanent data set files and print this data. This is an auxiliary program and is not used in the normal execution of the overall program. It was designed initially to be used in checking out the program operation. We will describe here how this program may be used for the purpose of printing out the net blade influence or wake influence coefficients on some blade control element I, and for printing out a complete description of the elemental control surfaces. The program does require for its operation the two permanent external files created in the MAIN - INFLUENCE CALCULATIONS program.

D.8.1 Program Input

The card input data consists of the following parameters inputted as part of the NAMELIST/DATAP/ data statement:

IT1 = K (Default value is K = 1)

where K is the reference number assigned to file IT1 which is identical to file IT1 created during the MAIN - INFLUENCE CALCULATIONS program.

IT2 = K (Default value is K = 2)

where K is the reference number assigned to file IT2 which is identical to file IT2 created during the MAIN - INFLUENCE CALCULATIONS program.

ISURF = K (Default value is K = 0)

where K is an integer indicating whether the control surface geometry data is to be printed. Select K as follows:

K = 1 Surface data printed
K = 0 Surface data not printed

M1 = K₁, K₂, . . . K_n, . . . K₂₀ (Default value is K_n = 0)

where K_n > K_{n-1} and K_n is the integer spanwise wake station for which the wake influence coefficients on all blade elements I=1, IMAX are to be printed. Select K as follows:

K₁ = 0 No wake influence coefficient printing.
K₁ = 9999 All spanwise wake influence coefficients are printed.
K_n = K The Kth spanwise wake influence coefficients are printed.

I1 = K₁, K₂, K₃, . . . K_n, . . . K₂₀ (Default value is K_n = 0)

where K_n > K_{n-1} and K_n is the integer blade control surface on which all blade elemental control surfaces influence coefficients are to be printed. Select K_n as follows:

K₁ = 0 No blade influence coefficients are printed.
K₁ = 9999 All blade influence coefficients are printed.
K_n = K All elemental blade influence coefficients on blade control surface K are printed.

D.8.2 Program Output

The program output may consist of the following depending on the options selected:

A. CONTROL SURFACE GEOMETRY DATA

This consists of the geometry data which describes each elemental control surface. It includes the following:

1. The transformation matrix [A] relating the blade fixed reference system to the elemental coordinate system. The symbols used are

$$[A] = \begin{vmatrix} TP1X & TP1Y & TP1Z \\ TP2X & TP2Y & TP2Z \\ TP3X & TP3Y & TP3Z \end{vmatrix}$$

2. The location of the origin of the elemental coordinate system with respect to the blade fixed coordinate system (X0, Y0, Z0).
3. The centroid location of the elemental surface with respect to both the blade fixed (XCG, YCG, ZCG) and elemental (XTCG, YTCG) reference systems.
4. The area of the element (ACS).
5. The corner point coordinates of the elemental surface with respect to the elemental reference system, $(XTP, YTP)_{i=1,4}$.
6. The negative of the free stream velocity components (VX, VY, VZ) at the elemental centroid location with respect to the blade fixed reference system. The negative of the normal free stream velocity (VN) is also given.

B. WAKE INFLUENCE COEFFICIENTS

For the selected spanwise wake station the influence coefficients (CXW, CYW, CZW) on all blade control surfaces $I=1, I_{MAX}$ are printed. These influence coefficients are referenced to the blade fixed coordinate system.

C. BLADE INFLUENCE COEFFICIENTS

For the selected control surface the influence coefficients (CXB, CYB, CZB) of all blade elements on this control surface are printed. These influence coefficients are referenced to the blade fixed coordinate system.

In addition to the above output those parameters of common statements LINDA and BRENDA which are essentially internal control parameters are also printed out. This information was written on file IT1 by subroutine

WT1 in the MAIN - INFLUENCE CALCULATIONS program. This information is shared by the various MAIN programs and serves as the continuity link among them.

D.9 CONCLUDING REMARKS

We have attempted in the previous sections to describe the series of computer programs and their operation in a manner more detailed than a typical "user's manual". We have chosen to describe it this way in order to document not only the program but the philosophy under which the program systematically performs the overall problem. With this as the basic program we hope to further modify the various routines in order to optimize the program in terms of reducing the computer time required.